

การประดิษฐ์ฟิล์มบางจากวัสดุประกอบคาร์บอนนาโนทิวบ์ – พอลิอะนิลีน  
ด้วยเทคนิคเลเยอร์-บาย-เลเยอร์ สำหรับประยุกต์ตัวรับรู้แก๊ส

นายเอกวิฐ์ เดชศรี

วิทยานิพนธ์นี้เป็นส่วนหนึ่งของการศึกษาตามหลักสูตรปริญญาวิทยาศาสตรดุษฎีบัณฑิต  
สาขาวิชาวิทยาศาสตร์นาโนและเทคโนโลยี (สหสาขาวิชา)  
บัณฑิตวิทยาลัย จุฬาลงกรณ์มหาวิทยาลัย  
ปีการศึกษา 2554  
ลิขสิทธิ์ของจุฬาลงกรณ์มหาวิทยาลัย

บทคัดย่อและแฟ้มข้อมูลฉบับเต็มของวิทยานิพนธ์ตั้งแต่ปีการศึกษา 2554 ที่ให้บริการในคลังปัญญาจุฬาฯ (CUIR)  
เป็นแฟ้มข้อมูลของนิสิตเจ้าของวิทยานิพนธ์ที่ส่งผ่านทางบัณฑิตวิทยาลัย

The abstract and full text of theses from the academic year 2011 in Chulalongkorn University Intellectual Repository (CUIR)  
are the thesis authors' files submitted through the Graduate School.

FABRICATION OF CARBON NANOTUBES – POLYANILINE COMPOSITE  
THIN FILMS USING LAYER-BY-LAYER TECHNIQUE  
FOR GAS SENSING APPLICATION

Mr.Ekarat Detsri

A Dissertation Submitted in Partial Fulfillment of the Requirements  
for the Degree of Doctor of Philosophy Program in Nanoscience and Technology  
(Interdisciplinary Program)  
Graduate School  
Chulalongkorn University  
Academic Year 2011  
Copyright of Chulalongkorn University



เอกรัฐ เดชศรี : การประดิษฐ์ฟิล์มบางจากวัสดุประกอบคาร์บอนนาโนทิวบ์ – พอลิอะนิลีน ด้วยเทคนิคเลเยอร์-บาย-เลเยอร์ สำหรับประยุกต์ตัวรับรู้แก๊ส (FABRICATION OF CARBON NANOTUBES – POLYANILINE COMPOSITE THIN FILMS USING LAYER-BY-LAYER TECHNIQUE FOR GAS SENSING APPLICATION) อ. ที่ปรึกษา วิทยานิพนธ์หลัก: ดร. สเตฟาน เทียร์ ดูบาส, 141 หน้า

งานวิจัยนี้ได้มีการใช้สารพอลิเอเล็กโตรไลต์ที่มีประจุบวกและประจุลบของท่อคาร์บอนในระดับนาโนเมมbranหลายชั้นที่ถูกเตรียมด้วยการดัดแปลงพื้นผิวแบบนอนโควาลนต์โดยใช้สารละลายพอลิอะนิลีนที่ละลายน้ำและพอลิไคโธลิกแอซิดโพลิเมอไรเซชัน คอลลอยด์ บนพื้นผิวของท่อคาร์บอน สำหรับการใช้ในการเตรียมฟิล์มบางแบบชั้นต่อชั้นของท่อคาร์บอนในระดับนาโนกับสารพอลิเอเล็กโตรไลต์ที่มีประจุบวกเช่นพอลิไคโธลิกแอซิดโพลิเมอไรเซชัน คอลลอยด์ และสารพอลิเอเล็กโตรไลต์ที่มีประจุลบเช่นพอลิสไตรีนซัลโฟเนต หรือพอลิอะนิลีนที่ละลายน้ำตามลำดับ ฟิล์มบางของวัสดุแต่งประกอบหลายชั้นได้ถูกเตรียมด้วยการดูดซับแบบสลับกันของสารพอลิเอเล็กโตรไลต์ที่มีประจุบวกและประจุลบ ซึ่งเทคนิคนี้เป็นเทคนิคทั่วไปที่มีศักยภาพในการสร้างฟิล์มบางสำหรับวัสดุแต่งประกอบของท่อคาร์บอน และยังสามารถเป็นวิธีง่าย ๆ ในการเตรียมฟิล์มบางวัสดุแต่งประกอบอื่นๆทั่วไป ในทางตรงกันข้าม งานวิจัยนี้ยังได้ทำการออกแบบและสังเคราะห์สารพอลิอะนิลีนที่ละลายน้ำ สำหรับใช้เป็นสารพอลิเอเล็กโตรไลต์อีกด้วย ซึ่งพอลิอะนิลีนที่ละลายน้ำจะถูกสังเคราะห์โดยการใช้เทคนิคการสังเคราะห์ที่พื้นผิวระหว่างอะนิลีนมอนอเมอร์และพอลิสไตรีน ซัลโฟเนต ซึ่งฟิล์มบางหลายชั้นจะถูกสังเคราะห์คุณสมบัติทั้งเชิงแสง และคุณสมบัติเชิงการนำไฟฟ้า โดยคุณสมบัติทางการนำไฟฟ้าของฟิล์มบางจะถูกประเมินค่าโดยการใช้เครื่องโพรมิเตอร์ และคุณสมบัติเชิงแสงจะถูกประเมินค่าโดยการใช้ยูวี วิสซิเบิลสเปกโตรสโกปี ความหนาและพื้นผิวของฟิล์มจะถูกประเมินค่าโดยการใช้ อะตอมมิค ฟอรัส ไมโครสโกปี ซึ่งการเกิดประจุที่พื้นผิวของฟิล์มบางจะแสดงธรรมชาติของการดูดซับด้วยแรงยึดเหนี่ยวทางไฟฟ้าสำหรับการสร้างฟิล์มบางแบบชั้นต่อชั้น โดยท่อคาร์บอนในระดับนาโนที่อยู่ในรูปของวัสดุแต่งประกอบฟิล์มบางสามารถที่จะพัฒนาการนำไฟฟ้าและสามารถจะนำไปสร้างเป็นอิเล็กทรอนิกส์สำหรับใช้เป็นตัวรับรู้ที่วัดได้ทั้งค่าเชิงแสงและการนำไฟฟ้า ซึ่งวัสดุแต่งประกอบของสารพอลิเอเล็กโตรไลต์ของท่อคาร์บอนในระดับนาโนและพอลิอะนิลีนมีความเป็นไปได้ที่จะถูกนำไปใช้สำหรับการประดิษฐ์ตัวรับรู้ต่อไป

สาขาวิชา..วิทยาศาสตร์นาโนและเทคโนโลยี.. ลายมือชื่อนิสิต.....  
ปีการศึกษา ....2554..... ลายมือชื่อ อ.ที่ปรึกษาวิทยานิพนธ์หลัก.....

## 4989738220 : MAJOR NANOSCIENCE AND TECHNOLOGY

KEYWORDS : CARBON NANOTUBES / POLYANILINE/ AMMONIA SENSOR/  
POLYELECTROLYTE MULTILAYER

EKARAT DETSRI : FABRICATION OF CARBON NANOTUBES -  
POLYANILINE COMPOSITE THIN FILMS USING LAYER-BY-LAYER  
TECHNIQUE FOR GAS SENSING APPLICATION

THESIS ADVISOR : STEPHAN THIERRY DUBAS, PH.D., 141 pp.

In this study, we have used anionic and cationic multi-wall carbon nanotube polyelectrolytes, prepared by the noncovalent surface modification of water soluble polyabiline and polydiallyldimethylamonium chloride on nanotube sidewall, for the layer-by-layer self assembly to prepare multilayers from carbon nanotube with polycation such as polydiallyldimethylamonium chloride, and polyanion such as poly(sryrenesulfonate) or water soluble polyabiline, respectively. The multilayer composite thin films are constructed by alternating of anionic and cationic polyelectrolyte. This is a general and powerful technique for the fabrication of thin carbon nanotubes films of arbitrary composition and architecture and allows also an easy preparation of all composite films. On the other hand, water soluble polyaniline was designed and synthesized for use as polyelectrolytes. The water soluble polyaniline was prepared by interfacial polymerization of aniline monomer in presence of poly (styrene sulfonate). The composite multilayer thin films were characterized for their optical and electrical properties. The electrical properties of the films were measured using a 4 point probe setup and the optical properties were measured by UV-Vis spectroscopy. The thickness and surface of the film was measured by atomic force microscopy. The charge compensation in multilayers is mainly intrinsic, which shows the electrostatic nature of the self assembly process. The CNT present in the composite film improve its conductivity and allow the fabrication of sensor which can be used both as an optical and electrical. This composite of polyelectrolyte, CNT and polyaniline is a promising composite film for gas sensing.

Field of study:..Nanoscience and Technology... Student's Signature .....

Academic Year : ...2011..... Advisor's Signature .....

## ACKNOWLEDGEMENTS

I would like to express my gratitude and sincere appreciations to my advisor Dr. Stephan Thierry Dubas for his helpful guidance, encouragement, time and for giving me an opportunity to study under his supervision. I would acknowledge my committee members, Associate Professor Dr. Vudhichai Parasuk for many insightful suggestions. Also I acknowledge sincerely Assistant Professor Dr. Sukkaneste Tungasamita, Dr. Ratthapol Rangkupan and Dr. Somboon Sahasitthiwat for being my committee member, providing valuable information and suggestions on this project.

I would also like to acknowledge the office staff and PEM students at the Nanoscience and Technology program. I also specially thank the Center for Innovative Nanoscience and Nanotechnology, (CIN grant 45-1.2/2552), Nanoscience and Technology program, and The 90<sup>th</sup> Anniversary of Chulalongkorn University Fund (Ratchadaphiseksomphot Endowment Fund) for financial support during my Ph.D. program.

Finally I would like to express my deepest gratitude to my dad Mr. Wilaisak, my mom Mrs. Prayoon and younger sister Miss Chatsuda for their love, understanding, encouragement, support and always stand by my side. I thank to you all.

# CONTENTS

	Page
ABSTRACT (THAI).....	iv
ABSTRACT (ENGLISH).....	v
ACKNOWLEDGEMENTS.....	vi
CONTENTS.....	vii
LIST OF TABLES.....	xv
LIST OF FIGURES.....	xvi
LIST OF ABBREVIATIONS.....	xxv
CHAPTER	1
I INTRODUCTION.....	1
II THEORY AND LITERATURE REVIEW.....	4
2.1 An Overview of Conducting Polymer.....	4
2.1.1. Concept of conduction mechanism.....	5
2.1.2 Concept of dopping.....	8
2.1.3 General synthesis of conducting polymer.....	10
2.1.4 Polyaniline.....	11
2.1.4.1 Synthesis of polyaniline.....	13
- Interfacial Polymerization or Template-guided synthesis	14
- Parameters controlling the interfacial polymerization.....	16
2.1.4.2 Doping and Conduction Mechanism of Polyaniline.....	18
2.2 An Overview of Carbon Nanotubes.....	19
2.2.1 Basic properties of CNTs.....	21
2.2.2 Surface modification of carbon nanotubes.....	23

2.3 An Overview of layer by layer self assembly technique.....	26
2.3.1 Parameter controlling layer-by-layer self assembly.....	28
2.4 Composite materials.....	32
<b>III EXPERIMENTAL.....</b>	<b>36</b>
3.1.Synthesis and characterization of water soluble polyaniline using interfacial polymerization method.....	36
3.1.1 Chemicals and Materials.....	36
3.1.2 Synthesis of water soluble Polyaniline.....	37
3.1.2.1 Effect of time onto the polymerization of water - soluble polyaniline.....	37
3.1.2.2 Effect of poly(sodium 4-styrenesulfonate, PSS) blending concentration.....	37
3.1.2.3 Effect of temperature onto the polymerization of water - soluble polyaniline.....	38
3.1.2.4 Effect of pH onto the polymerization of water – soluble polyaniline.....	39
3.1.2.5 Effect of oxidizing agent, Ammonium persulfate concentration onto the polymerization of water - soluble polyaniline.....	39
3.1.3 Characterization of water – soluble polyaniline.....	39
3.2 Layer-by-layer self assembly of water - soluble polyaniline.....	40
3.2.1 Chemical and materials.....	40
3.2.2 Preparation of polyelectrolyte multilayer thin films.....	41
3.2.2.1 Effect of dipping time onto the film fabrication.....	41
3.2.2.2 Effect of pH onto the film fabrication.....	41



3.2.2.3 Effect of NaCl concentration onto the film fabrication	42
3.2.2.4 Effect of polyaniline : poly(sodium 4-styrene sulfonate) with various concentration feed ratio of polymerization onto the film fabrication.....	44
3.2.2.5 Effect of number of layer onto the film fabrication.....	45
3.2.3 pH sensing of water - soluble polyaniline multilayer films and water - soluble polyaniline solution.....	45
3.2.4 Characterization of polyelectrolyte multilayer thin films.....	46
3.3 Dispersion of Multiwall Carbon Nanotubes with poly(diallyldimethyl ammonium chloride).....	46
3.3.1 Chemical and materials.....	46
3.3.2 Dispersion of Multiwall Carbon Nanotubes.....	47
3.3.2.1 Effect of PDADMAC concentration on the dispersion of MWCNTs.....	47
3.3.2.2 Effect of sonication times on MWCNTs dispersed with PDADMAC.....	47
3.3.3 Stability of MWCNTs dispersed with PDADMAC .....	48
3.3.3.1 Effect of salt type and salt concentration on the stability of MWCNTs.....	48
3.3.3.2 Effect of functionalization times on the stability of MWCNTs.....	48
3.3.3.3 Effect of pH on the stability of MWCNTs.....	48
3.3.4 Characterization of MWCNTs dispersed with PDADMAC.....	49
3.4 Dispersion of multiwall carbon nanotubes with water – soluble polyaniline blend poly(sodium 4-styrenesulfonate, PSS).....	49

3.4.1 Chemical and materials.....	49
3.4.2 Dispersion of Multiwall Carbon Nanotubes.....	50
3.4.2.1 Effect of Water - soluble polyaniline blend poly(sodium 4-styrenesulfonate, PSS) concentration on the dispersion of MWCNTs.....	50
3.4.2.2 Effect of pH on MWCNTs dispersed with water - soluble polyaniline blend poly(sodium 4-styrenesulfonate, PSS).....	51
3.4.3 Stability of MWCNTs dispersed with water - soluble polyaniline blend poly(sodium 4-styrenesulfonate, PSS).....	51
3.4.3.1 Effect of functionalization times on the stability of MWCNTs.....	51
3.4.4 Characterization of MWCNTs dispersed with water - soluble polyaniline blend poly(sodium 4-styrenesulfonate, PSS).....	52
3.5 Layer-by-layer self assembly of MWCNTs.....	52
3.5.1 Chemical and materials.....	52
3.5.1 Primer preparation.....	53
3.6 Polyelectrolyte multilayer films for volatile amine gas sensors.....	54
3.6.1 Chemical and materials.....	54
3.6.2 Gas sensor analysis.....	56
3.6.2.1 Effect of ammonia concentration on the sensing properties of polyelectrolyte multilayer films.....	56
3.7 Characterization technique.....	56
3.7.1 UV-Vis spectroscopy.....	56

3.7.2	Transmission electron microscopy, TEM.....	57
3.7.3	Scanning electron microscopy, SEM.....	57
3.7.4	Fourier transform Infrared spectroscopy, FTIR.....	58
3.7.5	Atomic force microscopy, AFM.....	58
<b>IV</b>	<b>RESULTS AND DISCUSSION.....</b>	<b>59</b>
4.1	Synthesis and characterization of water-soluble polyaniline using interfacial polymerization method.....	59
4.1.1	Synthesis of water - soluble polyaniline blend poly(sodium 4-styrenesulfonate).....	59
4.1.2	Effect of synthetic conditions on the interfacial polymerization of polyaniline.....	62
4.1.2.1	Effect of reaction time.....	63
4.1.2.2	Effect of poly(sodium 4-styrenesulfonate, PSS) blending solution.....	65
4.1.2.3	Effect of temperature onto the polymerization of water – soluble polyaniline.....	69
4.1.2.4	Effect of pH onto the polymerization of water – soluble polyaniline blend poly(sodium 4-styrenesulfonate)..	72
4.1.2.5	Effect of ammonium persulfate, oxidizing aconcentration onto the polymerization of water – soluble polyaniline blend poly(sodium 4-styrenesulfonate).....	73
4.2	Layer-by-layer self assembly of water – soluble polyaniline blend poly(sodium 4-styrenesulfonate).....	76
4.2.1	Fabrication and characterization of polymer multilayer thin	

films.....	76
4.2.1.1 Effect of dipping time onto the film fabrication.....	77
4.2.1.2 Effect of pH onto the film fabrication.....	78
4.2.1.3 Effect of NaCl concentration onto the film fabrication	80
A. Effect of NaCl concentration in water - soluble polyaniline blend poly(sodium 4-styrene sulfonate) solution onto the film fabrication.....	80
B. Effect of NaCl concentration in PDADMAC solution onto the film fabrication.....	81
4.2.1.4 Effect of Aniline:PSS concentration feed ratio for fabricated of polymer multilayer thin films.....	85
4.2.1.5 Effect of number of layer onto the film fabrication.....	89
4.3 pH sensing of water - soluble polyaniline multilayer films and water - soluble polyaniline solution.....	94
4.4 Dispersion of Multiwall Carbon Nanotubes with Poly(diallyldimethyl ammonium chloride).....	99
4.4.1 Effect of PDADMAC concentration on the dispersion of MWCNTs .....	99
4.4.2 Monolayer of MWCNTs dispersed with different concentration of PDADMAC.....	101
4.4.3 Effect of sonication times on MWCNTs dispersed with PDADMAC.....	102
4.4.3 Stability of MWCNTs dispersed with PDADMAC .....	103

4.4.3.1 Effect of functionalization times on the stability of MWCNTs.....	104
4.4.3.2 Effect of ionic interaction on the stability of MWCNTs.	1051
4.4.3.3 Effect of pH on MWCNTs dispersed with PDADMAC..	106
4.5 Dispersion of Multiwall Carbon Nanotubes with polyaniline blend poly(sodium 4-styrenesulfonate, PSS).....	109
4.5.1 Effect of water - soluble polyaniline blend poly(sodium 4-styrenesulfonate, PSS) concentration on the dispersion of MWCNTs.....	109
4.5.2 Effect of pH on the dispersion of MWCNTs.....	111
4.5.3 Stability of MWCNTs dispersed with water - soluble polyaniline blend poly(sodium 4-styrenesulfonate): functionalization times.....	112
4.6 Layer-by-layer self assembly of MWCNTs.....	114
4.6.1 Layer-by-layer self assembly of MWCNTs dispersed with poly(diallyldimethyl ammonium chloride / poly(sodium 4-styrene sulfonate); MWCNTs.PDADMAC/PSS.....	114
4.6.2 Layer-by-layer self assembly of MWCNTs dispersed with poly(diallyldimethyl ammonium chloride / water - soluble polyaniline blend poly(sodium 4-styrenesulfonate); MWCNTs.PDADMAC/PANi.PSS.....	119
4.6.3 Layer-by-layer self assembly of MWCNTs dispersed with water - soluble polyaniline blend poly(sodium 4-styrenesulfonate) / poly(diallyldimethyl ammonium chloride) multilayer thin films; MWCNTs.PANi.PSS/PDADMAC.....	124

4.6.4 Layer-by-layer self assembly of MWCNTs dispersed with Poly(diallydimethyl ammonium chloride) / MWCNTs dispersed water - soluble polyaniline blend poly(sodium 4-styrenesulfonate) multilayer thin films; MWCNTs.PANi.PSS/MWCNTs.PDADMAC..	131
4.7 Gas sensors.....	138
4.7.1 Dependence of the sensor response on NH <sub>3</sub> concentration....	138
<b>V CONCLUSIONS</b>	144
<b>REFERENCES.....</b>	146
<b>APPENDIX.....</b>	159
<b>BIOGRAPHY.....</b>	160

## LIST OF TABLES

TABLE		Page
1.1	Chemical structures of some interesting conjugated polymers.....	5
3.1	Characterisation techniques and their utilization of PANi.PSS.....	40
3.2	Characterisation techniques and their utilization of pH sensing of water - soluble polyaniline multilayer films and water - soluble polyaniline solution.....	46
3.3	Characterisation techniques and their utilization of MWCNTs dispersed with PDADMAC.....	49
3.4	Characterisation techniques and their utilization of MWCNTs dispersed with water - soluble polyaniline blend poly(sodium 4-styrenesulfonate, PSS).....	52
3.5	Characterisation techniques and their utilization of MWCNTs multilayer films.....	54
4.1	The summarization parameters to fabricate the polyaniline multilayered thin film.....	89

## LIST OF FIGURES

FIGURE		Page
2.1	Band structure of an electronically conducting polymer .....	6
2.2	Positively charge defect on polyaniline (a) polaron, (b) bipolaron.....	6
2.3	(a) The general structure of PANi that shows the average oxidation state (1-y). (b) The chemical structures of the three normally found oxidation state of PANi.....	13
2.4	Interfacial polymerization of polyaniline.....	15
2.5	Chemical polymerization of polyaniline.....	16
2.6	Molecular model of SWCNTs exhibiting different achiral and chiral conformations.....	20
2.7	Functionalization possibilities of SWCNTs: A) defect group functionalization, B) covalent sidewall functionalization, C) noncovalent functionalization with surfactant, D) noncovalent exohedral functionalization with polymers and E) endohedral functionalization.....	24
2.8	(A) Schematic diagram showing the film deposition process, (B) simplified molecular picture of the adsorption step of polyelectrolyte.....	27
2.9	Chemical structure of positive and negative polyelectrolytes: (1) poly(diallyldimethylammonium)chloride (PDADMAC), (2) poly(so-dium 4-styrenesulfonate) (PSS), (3) polyacrylic acid (PAA), (4) polyallylamine hydrochloride (PAH).....	28
2.10	Models of surface microstructure for polyionic molecular layers. (a)	



	PSS at the shortest deposition time (<5 min). (b) PSS at the longest deposition time (<10 min). (c) PSS/PAA complex bi layers. (d) Comparison with polymer brushes in the initial stage of tethering by on sticky end. (e) Polymer brushes in a dense state.....	30
3.1	Morphology image of water - soluble polyaniline characterized by scanning electron microscope (Phillips XL30CP).....	38
3.2	Schematic diagram representing the layer-by-layer deposition.....	41
3.3	Transmission electron microscopic image of MWCNTs (baytubes C 150 P, outer diameter distribution 5-20 nm and length 1 - >10 um) from Bayer Co. Ltd., Thailand.....	47
3.4	Transmission electron microscopic image of MWCNTs dispersed with water - soluble polyaniline blend poly(sodium 4-styrenesulfonate, PSS).....	50
3.5	Schematic diagram of experimental apparatus for evaluating sensitivity of developed sensor.....	55
4.1	Schematic representation the formation of water - soluble polyaniline blend poly(sodium 4-styrenesulfonate).....	60
4.2	Mechanism representation the formation of water - soluble polyaniline blend poly(sodium 4-styrenesulfonate).....	61
4.3	UV-Vis spectra of water - soluble polyaniline blend poly(sodium 4-styrenesulfonate), (a) Emeraldine salt and (b) Emeraldine base.....	61
4.4	Reaction progress of the polymerization of water - soluble polyaniline blend poly(sodium 4-styrenesulfonate).....	63
4.5	Kinetic polymerization of water - soluble polyaniline blend poly(sodium 4-styrenesulfonate) by interfacial polymerization.....	64

4.6	Plot of the Time Vs $\lambda_{max}$ of the kinetic polymerization of water - soluble polyaniline blend poly(sodium 4-styrenesulfonate) by interfacial polymerization.....	64
4.7	UV-Vis spectra of water - soluble polyaniline blend poly(sodium 4-styrenesulfonate) with the different PSS concentration ratio of 3-200 mM.....	65
4.8	FT-IR spectra of (a) poly(sodium 4-styrenesulfonate) and (b) polyaniline.....	67
4.9	FT-IR of water - soluble polyaniline blend poly(sodium 4-styrenesulfonate) with the different PSS concentration 3-200 mM...	68
4.10	UV-Vis spectra of water - soluble polyaniline blend poly(sodium 4-styrenesulfonate) with the different temperature at 4, 30 and 40 °C.	70
4.11	Plot of the changes in absorbance and % weight of water - soluble polyaniline blend poly(sodium 4-styrenesulfonate) with the different synthesis temperature at 4, 30 and 40 °C.....	70
4.12	Morphology image of water - soluble polyaniline blend poly(sodium 4-styrenesulfonate) at 4 and 30 °C .....	72
4.13	UV-Vis spectra of water - soluble polyaniline blend poly(sodium 4-styrenesulfonate) with the different pH of 0.6, 1, 2 and 3.....	73
4.14	UV-Vis spectra of water - soluble polyaniline blend poly(sodium 4-styrenesulfonate) with the different APS.....	74
4.15	The optimum conditions to synthesis water-soluble polyaniline blend poly(sodium 4-styrenesulfonate).....	75
4.16	Schematic mechanism of layer-by-layer self assembly of water - soluble polyaniline blend poly(sodium 4-styrene sulfonate) /	

	poly(diallyldimethyl ammonium chloride) multilayer thin films.....	75
4.17	Diagram depicting the steps used in the layer-by-layer deposition of water - soluble polyaniline blend poly(sodium 4-styrene sulfonate) / poly(diallyldimethyl ammonium chloride) multilayer thin films.....	77
4.18	The plot of the dipping time of (PANi-PSS/PDADMAC) multilayer thin film.....	78
4.19	Normalized plot of the pH onto the assemblies of (PANi.PSS/PDADMAC) multilayer films.....	79
4.20	Effect of NaCl concentration in water - soluble polyaniline blend poly(sodium 4-styrene sulfonate) solution onto the assemblies of (PANi-PSS/PDADMAC) multilayer films, insert graph show the picture of water - soluble polyaniline blend poly(sodium 4-styrene sulfonate) films at various NaCl concentration of 0.1, 0.5, 1.0, 1.5 and 2.0 M when fix the number of layer at 9.....	80
4.21	Plots of the changes in absorbance of the (PANi-PSS/PDADMAC) <sub>9</sub> multilayer films of various NaCl concentration in 5, 10 and 50 mM PADADMAC solution.....	82
4.22	Effect of NaCl concentration in 5 mM PDADMAC solution.....	83
4.23	Effect of NaCl concentration in 10 mM PDADMAC solution.....	83
4.24	Effect of NaCl concentration in 50 mM PDADMAC solution.....	84
4.25	The changes in absorbance of (PANi-PSS/PDADMAC) <sub>5lys</sub> multilayer films at various concentration feed ratio of PANi-PSS10:3, 10:5, 10:10, 10:20, 10:50, 10:100, 10:150 and 10:200 mM.	85
4.26	Competition study of Layer-by-Layer polymer multilayer thin films.....	87

4.27	The changes in resistivity of (PANi-PSS/PDADMAC) <sub>21lys</sub> multilayer films at various concentration feed ratio of PANi-PSS....	88
4.28	The absorbance value as the function of number of (PANi-PSS/PDADMAC) <sub>lys</sub> multilayer films.....	90
4.29	Representative digital picture images of assembled (PANi.PSS/PDADMAC) <sub>lys</sub> multilayer films.....	90
4.30	AFM pictures for the (PANi-PSS/PDADMAC) <sub>lys</sub> multilayer films deposited on glass substrate: (A) 1 $\mu$ m x 100 nm dimension and (B) 1 $\mu$ m x 500 nm nm dimension in 19 layers.....	91
4.31	Thickness of (PANi-PSS/PDADMAC) <sub>lys</sub> multilayer films.....	92
4.32	Specific conductivity of the (PANi-PSS/PDADMAC) <sub>lys</sub> multilayer films.....	92
4.33	Electronic absorption spectra of polyaniline solution in different pH.	94
4.34	The relationship between $\lambda_{max}$ and solution pH.....	95
4.35	The absorbance change of polyaniline solution vs pH at 762 and 545 nm.....	96
4.36	Electronic absorption spectra of (PANi-PSS/PDADMAC) <sub>lys</sub> multilayer in different pH .....	96
4.37	The relationship between $\lambda_{max}$ and solution pH of (PANi-PSS/PDADMAC) <sub>lys</sub> multilayer.....	97
4.38	The absorbance change of (PANi-PSS/PDADMAC) <sub>lys</sub> multilayer vs pH at 763 and 517 nm.....	98
4.39	Effect of PDADMAC concentration of 0, 0.01, 0.05, 0.1, 0.2, 0.3, 1.0 and 3.0 mM on the dispersion of MWCNTs.....	100
4.40	Model of noncovalent surface modification of MWCNTs with	

	PDADMAC.....	101
4.41	Monolayer of MWCNTs dispersed with the different concentration of PDADMAC of 0, 0.01, 0.05, 0.1, 0.2, 0.3 and 1.0 mM.....	102
4.42	Effect of sonication time onto the dispersion of MWCNTs with PDADMAC.....	103
4.43	Stability of noncovalent surface modification of MWCNTs dispersed with PDADMAC, as the function of time.....	104
4.44	Stability of noncovalent surface modification of MWCNTs dispersed with PDADMAC, as the function of salt type and salt concentration: where a = NaCl, b = Na <sub>2</sub> SO <sub>4</sub> and c = Na <sub>3</sub> HPO <sub>4</sub> ).....	105
4.45	Stability of noncovalent surface modification of MWCNTs dispersed with PDADMAC, as the function of pH.....	107
4.46	TEM micrograph of MWCMTs dispersed in PDADMAC (a) scale bar 50 nm, (b) scale bar 20 nm and (c) scale bar 7 nm.....	108
4.47	Effect of water - soluble polyaniline blend poly(sodium 4-styrenesulfonate, PSS) concentration (0, 0.01, 0.02, 0.05, 0.1, 0.13 and 0.15 % weight) onto the dispersion of MWCNTs.....	110
4.48	Monolayer of MWCNTs dispersed with the different concentration of water - soluble polyaniline blend poly(sodium 4-styrenesulfonate, PSS) of 0, 0.01, 0.02, 0.05, 0.1, 0.13 and 0.15 % weight on glass substrate.....	110
4.49	Effect of pH of water - soluble polyaniline blend poly(sodium 4-styrenesulfonate) onto the dispersion of MWCNTs.....	111

4.50	Stability of noncovalent surface modification of MWCNTs dispersed with water - soluble polyaniline blend poly(sodium 4-styrenesulfonate, PSS), as the function of time.....	112
4.51	TEM micrograph of MWCMTs dispersed in water - soluble polyaniline blend poly(sodium 4-styrenesulfonate) (a) scale bar 100 nm and (b) scale bar 50 nm.....	113
4.52	Schematic mechanism of layer-by-layer self assembly of MWCNTs.PDADMAC / PSS multilayer thin films.....	115
4.53	Plot of the changes in absorbance of Layer-by-layer self assembly of MWCNTs.PDADMAC / PSS.....	115
4.54	Thickness of MWCNTs.PDADMAC / PSS multilayer thin films.....	116
4.55	AFM pictures for the MWCNTs.PDADMAC / PSS 15 layers.....	116
4.56	Specific conductivity of MWCNTs dispersed with poly(diallyldimethyl ammonium chloride) / poly(sodium 4-styrene sulfonate) multilayer thin films.....	117
4.57	The UV-Vis spectra of 15 layers (MWCNTs.PDADMAC)/PSS multilayer thin films at pH 1 to 12.....	118
4.58	Specific conductivity of 15 layers (MWCNTs.PDADMAC)/PSS multilayer thin films by varying pH.....	118
4.59	Schematic mechanism of layer-by-layer self assembly of MWCNTs. PDADMAC / PANi.PSS multilayer thin films.....	119
4.60	Plot of the changes in absorbance of Layer-by-layer self assembly of MWCNTs. PDADMAC / PANi.PSS multilayer thin films.....	120
4.61	Thickness of MWCNTs. PDADMAC / PANi.PSS multilayer thin films.....	121

4.62	AFM pictures for the MWCNTs. PDADMAC / PANi.PSS multilayer thin films, at 15 layers.....	121
4.63	Specific conductivity of MWCNTs. PDADMAC / PANi.PSS multilayer thin films.....	107
4.64	The UV-Vis spectra of 15 layers (MWCNTs. PDADMAC) / PANi.PSS multilayer thin films at pH 1 to 12.....	123
4.65	Specific conductivity of 15 layers (MWCNTs. PDADMAC) / PANi.PSS multilayer thin films by varying pH from 1-12.....	123
4.66	Schematic mechanism of layer-by-layer self assembly of MWCNTs.PANi.PSS/PDADMAC multilayer thin films.....	125
4.67	Plot of the changes in absorbance of Layer-by-layer self assembly of (MWCNTs.PANi.PSS <sub>0.01% weight</sub> ) / PDADMAC multilayer thin films.....	126
4.68	Plot of the changes in absorbance of Layer-by-layer self assembly of (MWCNTs.PANi.PSS <sub>0.02 % weight</sub> ) / PDADMAC multilayer thin films.....	126
4.69	Plot of the changes in absorbance of Layer-by-layer self assembly of (MWCNTs.PANi.PSS <sub>0.03 % weight</sub> ) / PDADMAC multilayer thin films.....	127
4.70	Thickness of MWCNTs.PANi.PSS/PDADMAC multilayer thin films.....	128
4.71	AFM pictures for the MWCNTs.PANi.PSS/PDADMAC multilayer thin films at (a) 1, (b) 3, (c) 9 and (d) 15 layers.....	128
4.72	Specific conductivity of MWCNTs.PANi.PSS/PDADMAC.....	129

4.73	The UV-Vis spectra of 15 layers (MWCNTs.PANi.PSS <sub>0.01% weight</sub> ) /PDADMAC multilayer thin films at pH 1 to 12.....	130
4.74	Specific conductivity of 15 layers (MWCNTs.PANi.PSS <sub>0.01% weight</sub> ) /PDADMAC multilayer thin films by varying pH from 1-12.....	130
4.75	Schematic mechanism of layer-by-layer self assembly of MWCNTs.PDADMAC / MWCNTs.PANi.PSS multilayer thin films	132
4.76	Plot of the changes in absorbance of Layer-by-layer self assembly of MWCNTs.PDADMAC / MWCNTs.PANi.PSS multilayer thin films.....	132
4.77	Thickness of MWCNTs.PDADMAC / MWCNTs.PANi.PSS multilayer thin films.....	133
4.78	Representative digital picture images of assembled MWCNTs.PDADMAC / MWCNTs.PANi.PSS multilayer thin films.....	133
4.79	AFM pictures for the MWCNTs.PDADMAC / MWCNTs.PANi.PSS multilayer thin films at (a) 2, (b) 4, (c) 6, (d) 8, (e) 10 and (f) 16 layers.....	134
4.80	Specific conductivity of MWCNTs.PDADMAC / MWCNTs.PANi.PSS multilayer thin films.....	135
4.81	The UV-Vis spectra of 16 layers (MWCNTs.PDADMAC) / (MWCNTs.PANi.PSS) multilayer thin films at pH 1 to 12.....	136
4.82	Specific conductivity of 16 layers (MWCNTs.PDADMAC) / (MWCNTs.PANi.PSS) multilayer thin films by varying pH from 1-12.....	137
4.83	Relative resistance variation of (MWCNTs.PDADMAC) /	



	(MWCNTs.PANi.PSS) multilayer thin films based sensor versus time exposed to different concentrations of NH <sub>3</sub> at room temperature.....	140
4.84	Relative resistance variation of (MWCNTs.PANi.PSS) / PDADMAC multilayer thin films based sensor versus time exposed to different concentrations of NH <sub>3</sub> at room temperature.....	141
4.85	Relative resistance variation of (MWCNTs.PDADMAC) / PANi.PSS multilayer thin films based sensor versus time exposed to different concentrations of NH <sub>3</sub> at room temperature.....	141
4.86	Relative resistance variation of (MWCNTs.PDADMAC) / PSS multilayer thin films based sensor versus time exposed to different concentrations of NH <sub>3</sub> at room temperature.....	142

## LIST OF ABBREVIATIONS

PANi	:	Polyaniline
CNTs	:	Carbon nanotubes
MWCNTs	:	Multiwall carbon nanotubes
SWCNTs	:	Singlewall carbon nanotubes
PEM	:	Polyelectrolyte multilayer thin films
LbL	:	Layer-by-Layer technique
PDADMAC	:	Poly(diallyldimethylammonium chloride)
PSS	:	Poly(sodium 4-styrenesulfonate)
APS	:	Ammonium persulfate
mM	:	milli Molar
M	:	Molar
nm	:	nanometer
$\lambda$	:	Lampda
min	:	minute

# CHAPTER I

## INTRODUCTION

Composites of polymer and carbon nanotubes have received considerable research interest because of dramatic improvement of conducting, mechanical thermal and optical properties. Polymer-carbon nanotubes composites can be made with different polymeric matrix and the combined synergistic and conducting properties using MWCNTs make them attractive for technological use. Apart from the increase of conductivity, thermal stability and new electronic properties can be found in polymer-carbon nanotubes composites that use a conducting polymer.

Among attractive conducting polymer, polyaniline have been studied in a wide variety of scientific research and application. Because polyaniline possess unique properties, high conductivity, high chemical durability and reversible control of conductivity both by protonation and by charge-transfer doping. For these reasons, polyaniline have been widely used to prepare the composite with MWCNTs. The polyaniline and MWCNTs composites show enhanced electronic and conductivity properties. There are many methods for preparing the PANi and MWCNTs composites such as polymerization of the corresponding monomer in the presence of CNTs by either chemical or electrochemical properties. One simple and versatile method to prepare the composite of PANi and MWCNTs is using the layer-by-layer, LbL, self assembly method or electrostatic self assembly, ESA. This technique can produce conformal ultrathin composite films and highly tunable surfaces. The polyelectrolyte multilayer composite films exhibit a linear growth regime where the

thickness increase linear with the number of deposited layers, leading to nano or micrometer thin films.

In this work, conducting polymer, water soluble polyaniline blend poly(sodium 4-styrenesulfonate), PANi. PSS was synthesized by interfacial polymerization technique. The electrostatic interaction between  $-\text{SO}_3^-$  groups of poly(sodium 4-styrenesulfonate), PSS and  $(-\text{NH}_3^+)$  groups of polyaniline, could be generated the water soluble properties of polyaniline. The polyaniline multilayers were fabricated by LBL self assembly method for used as the optical pH sensor. As for the MWCNTs were modified by noncovalent surface modification in order to improve the dispersion and stability. Negatively charged MWCNTs have been functionalized on their exterior wall with water soluble polyaniline blend poly(sodium 4-styrenesulfonate), PANi.PSS yielding MWCNTs.PANi.PSS which is having  $\pi$ - $\pi$  stacking interaction between side wall MWCNTs and aromatic groups of PANi. On the other hand, the positively charged MWCNTs have been functionalized by polymer wrapping using poly(diallyldimethylammonium chloride), PDADMAC yielding MWCNTs. PDADMAC which the hydrophobic interaction. LbL MWCNTs films, which consist of well-dispersed MWCNTs, have been produced by LbL using stable dispersion of negatively and positively charged. Unlike other multilayer assemblies that contain MWCNTs as one or two or more components, these systems incorporate MWCNTs with out the incorporation of adding organic materials: this different can enable the development of 100 % MWCNTs thin films with properties that can be manipulated using assembly conditions. MWCNTs multilayer thin films show conductivity-dependent thickness and surface topology, which are characteristic of LbL thin films.

## **CHAPTER II**

### **THEORY AND LITERATURE REVIEW**

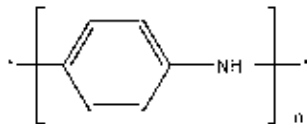
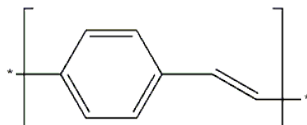
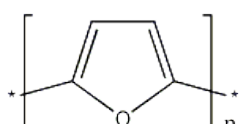
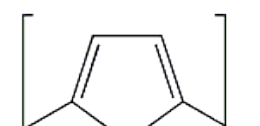
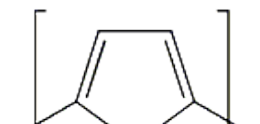
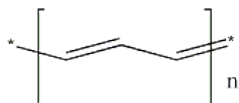
#### **2.1 An Overview of Conducting Polymer**

Conducting polymers are polymers that inherently conduct electricity [1]. Electronically conducting polymers are extensively conjugated molecules with substantial  $\pi$  electron delocalization along the polymer chain giving rise to interesting electrical and optical properties [2]. These properties make these materials suitable for many application in the field of electrochromic display devices [3], sensor or biosensor technology [4], energy storage [5], electromagnetic shielding [6] and molecular electronic [7]. The certain advantage of these materials over their inorganic counterpart [8] such as easy processing by chemical or electrical oxidative polymerization of the monomer and compatibility with plastic [9] have made them become a new materials that would lead to the next generation of powerful materials.

In 1976, the first synthesis electrically conducting polymer, doped polyacetylene, was reported by Hideki Shirakawa [10]. The subsequent discovery by Alan J. Heeger and Alan G. MacDiarmid that the polyacetylene polymer would undergo an increase in conductivity of 6 orders of magnitude by oxidative doping with iodine [10] from  $10^{-4} - 10^2$  S/cm. Since 1976, a number of conducting polymers, namely polypyrrole, polyaniline polyfuran, polythiophene and etc, have become the focus of much study. The structure of these molecules are shown in Table 1. The important of conducting polymers is exemplified by the award of the 2000 Nobel

Prize in Chemistry for “The discovery and development of conducting polymer” [11] to Hideki Shirakawa, Alan J. Heeger and Alan G. MacDiarmid.

Table 1.1 Chemical structures of some interesting conjugated polymers [12].

Name	Structure
Polyaniline	
Poly(p-phenylenevinylene)	
Polyfuran	
Polypyrrole	
Polythiophene	
Polyacetylene	

All conjugated polymers presented in Table 1.1 have chemical structures for semiconductors. The highest occupied molecular orbital of monomer orbital (HOMO) was formed the occupied  $\pi$ -band (valance band) and the lowestest unoccupied molecular orbital of monomer orbital (LUMO) was formed the

unoccupied  $\pi^*$ -band (conduction band) [13]. Figure 2.1. The conductivity of the conjugated polymer (undoped) is transformed from an insulating form to the metallic formed by the processes called doping. The doping processes could be introduced the new dopant energy level into the band gap[14].

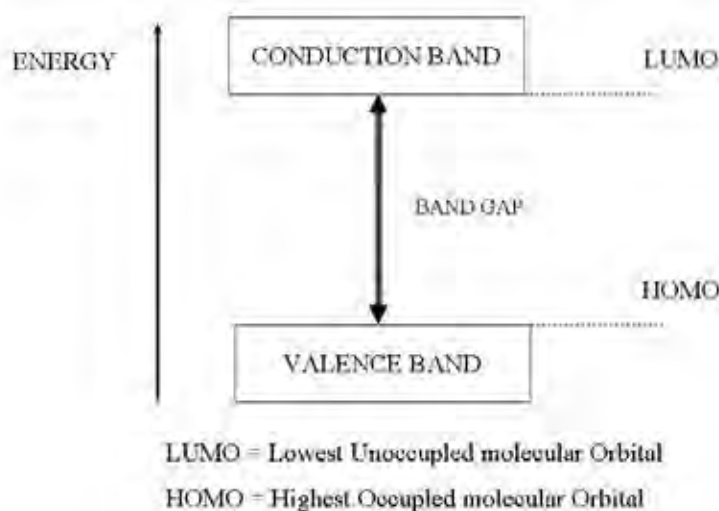


Figure 2.1 Band structure of an electronically conducting polymer [13].

Normally, the electrical conductivity of conducting polymers depends on many parameters: the density of mobile charges or the number of carriers per unit volume ( $n$ ), the electron charge ( $e$ ) and the carrier mobility ( $\mu$ ). The relationship between an electrical conductivity ( $\sigma$ ) and those parameters are expressed via the general equation [15].

$$\sigma = ne\mu \quad (1)$$

Because the band gap of conjugated polymers (undoped) is usually fairly large,  $n$  is very small under ambient conditions. Consequently, conjugated polymers are insulator in their neutral state and no intrinsically conducting organic polymer is

known at this time. Although conducting polymers possess a relatively large number of delocalized  $\pi$  electron, a fairly large energy band gap exist between the valence band and the conduction band, thus the polymer are considered to be semi-conducting, at best. These polymer must be doped (usually meaning altering the number of  $\pi$  electron) in order to render the polymer truly conducting. Doping of polymers creates new states (doner or acceptor state) which exist within the band gap, and are energetically accessible to the  $\pi$  electrons, resulting in significant increases in conductivity [15].

Doping in conducting polymers refers to the redox process that transform polymers from an insulating form to their conducting form. The process can be reversed to produce the original polymer with little or no degradation of the polymer backbone. Both doping and undoping processes involving dopant counter ions which act to stabilize the doped state, maybe carried out chemically or electrochemically. The conductivity of the polymers can be controlled by controlling the doping level during the doping process. This permits the optimization for the best properties in each type of polymers. This permits the optimization of properties in each type of polymer. Doping introduces a new dopant energy level into the band gap; conduction is facilitated and the electrical conductivity is strong dependent on the doping level as doner or acceptor species are incorporated. The dopants used to induced an insulator-metal transition in electron polymers can be both n-type (electron donating) or p-type (electron acceptor). The doping process can be divided into 3 types [16]: redox doping involving dopant ions, redox doping involving no dopant ions and non redox doping.



**1. Redox doping involving dopant ions:** The redox process involves a change in the number of electrons associated with the polymer backbone. This doping type undergoes either p- or n- redox doping by chemical.

- Chemical p-doping: P-doping involves the partial oxidation of the  $\pi$  electron in the polymer backbone resulting in a decrease of the number of electron. P-doping was first discovery by treating trans-polyacetylene with an oxidizing agent such as iodine. The electrical conductivity of polymers doped with this process can increase from  $10^{-5} - 10^3$  S/cm [17].

- Chemical n-doping: N-doping is the partial reduction of the  $\pi$  electron system on the polymer backbone. This type of doping was discovered by treating a trans- polyacetylene with the reducing agent such as lithium amalgam or sodium naphtalide [18].

Both chemical p- and n-doping processes can doped not only polyacetylene but also other conductive polymer as well. Counter dopant ion will stabilize the charges on the polymer backbone. In each case, spectroscopic signature of polaron and bipolaron are obtained.

**2. Redox doping involving no dopant ions:**

- Photodoping: This type of doping can be done by exposing the polymer such trans- polyacetylene to the mediation of energy greater than its band gap, so the electron are promoted across the gap and the polymer undergoes photodoping. The charges that present in polymer chain can delocalization along the polymer chain and photoconductivity is observed.

- Charge injection doping: This doping types uses a metal/insulator/semiconductor (MIS) configuration; metal and conductive polymer

are separated by a thin layer of a high electric dielectric strength insulator. A potential is applied across the structure to create a surface charge layer or the accumulation layer which has been extensively investigated for conductive polymer. The resulting charges are present in the polymer without associated dopant ions [19].

**3. Non redox doping:** In contrast to redox doping, in this doping type the number of electrons associated with the polymer backbone does not change. The first example of the doping of an organic polymer is the emeraldine base form of polyaniline. This can be accomplished by treating emeraldine base with aqueous protonic acid which results in an increase in conductivity by about 9-10 order of magnitude and produces the protonated emeraldine salt [20].

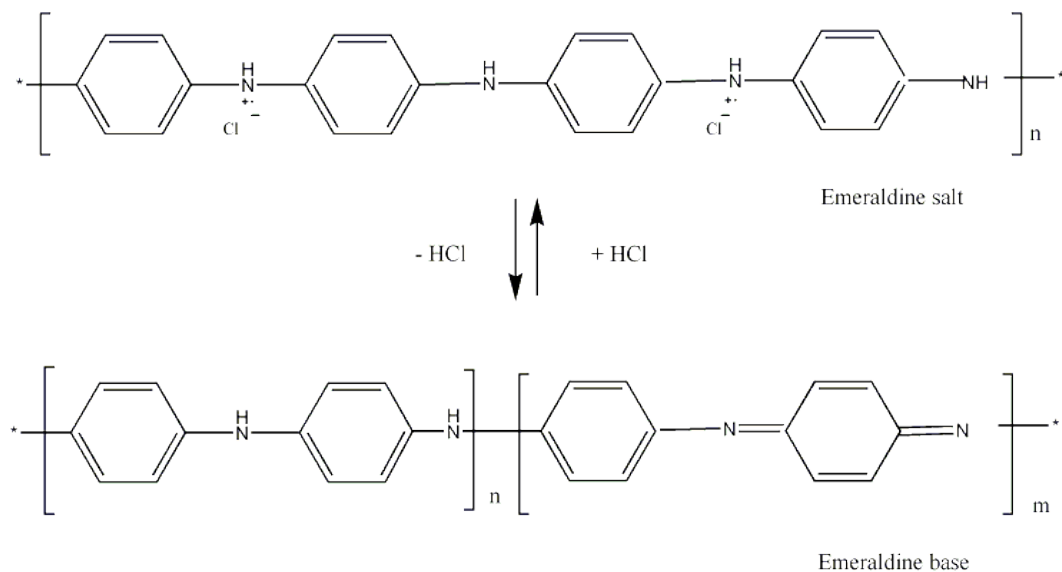


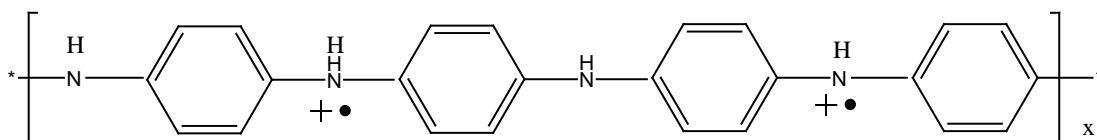
Figure 2.2 Doping process of Polyaniline [20].

After doping, the doped conducting polymer shows good electrical conductivity for two reasons: 1. Doping lead to injection of carrier into  $\pi$  electron

system. 2. The  $\pi$ -bonding lead to  $\pi$  electron delocalization along the polymer chain and, thereby, to the possibility of charge carrier mobility.

It is generally agreed that the mechanism of conductivity in conjugated polymers are based on the motion of charged defects with the conjugated framework. Oxidation of polymer initially generates a radical cation with both spin and charge. Borrowing from solid state physics terminology, these species are referred to as a polaron and comprises both the hold site and the structure distortion which accompanies it. This condition is depicted as shown in Figure 2.3 (a) [21]. The cation and radical form a bound species, since any increase in the distance between them would necessitate the creation of additional higher energy quinoid unit. Theoretical treatments have demonstrated that two nearby polarons combine to form the lower energy bipolarons as shown in Figure 2.3 (b) [21]. One bipolaron is more stable than two polarons despite the coulombic repulsion of the two ions. Since the defect is simply a boundary between two moieties of equal energy, the infinit conjugation chain on either side, it can migrate in either direction without affecting the energy of the backbone, provided that there is no significant energy barrier to the process. It is this charge carrier mobility that leads to the high conductivity of these polymers.

(a)



(b)

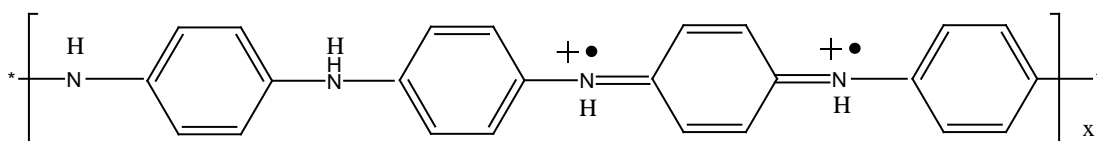


Figure 2.3 Positively charge defect on polyaniline (a) polaron, (b) bipolaron [21].

### 2.1.1 General synthesis of conducting polymer

Conducting polymers can be produced using either chemical or electrochemical oxidation of the monomer [22]. Polymerization involves formation of low molecular weight oligomers that are further oxidized at lower potentials than the initial monomer to form a polymer that eventually precipitates or is electrodeposited onto the electrode surface.

- Chemical oxidation polymerization: This is the common method to synthesis conducting polymer. It has been desirable for mass production. . Chemical oxidation polymerization is performed by react monomer with oxidizing agent such as ammonium persulfate. In case of polyaniline, the chemical oxidation polymerization of aniline has been carried out by react aniline monomer with oxidizing agent in acidic solution [23]. The acidic condition provides the solubilization of the monomers as well as the formation of emeraldine salt as a conducting polyaniline. The aniline monomer forms the anilinium ion in acidic medium and chemical polymerization results in the formation of protonated, partially oxidized form of polyaniline.

- Electrochemical polymerization: Compared with chemical oxidation polymerization, electrochemical polymerization is performed at an electrode (conductive substrate) [24]. Whereas the powder forms are obtained by chemical polymerization, the electrochemical polymerization method leads to films deposited on the anode. In case of polyaniline electrochemical polymerization, the radical cation of aniline monomer is formed on the electrode surface by oxidation of the monomer [25]. This process is considered to be the rate determining step. Radical coupling and elimination of two protons make mainly para-formed dimer. Chain propagation

proceeds with oxidation of dimer and aniline monomer on the electrode surface. In this step, the radical cation of the oligomer couples with a radical cation of aniline monomer. In the final step, polyaniline is doped by the acid present in solution. The growth of polyaniline has been considered to be self catalyzed. This means that the polymer are formed at the higher rate as the more monomer are deposited onto the polymer surface. It involves the adsorption of the anilinium ion onto the oxidized form of polyaniline, followed by electron transfer to form the radical cation and subsequent reoxidation of the polymer to its most oxidized state.

## 2.2 Polyaniline

As one of the most important conducting polymers, PANi was discovered in 1934 as probably the oldest known synthetic organic polymer. PANi is one of the most studied conducting polymers due to its many attractive properties such as ease of synthesis [26], being cheap [26], and of relatively stable electric conductivity [27], with interesting electrochemical and optical properties [28] as the resulting potential application as electrochromic [29], battery electrode [30], biosensors [31], etc.

Polyaniline has a general formula containing mixed oxidation state polymer composed of reduced benzenoid units and oxidized quinoid units Figure 2.4 (A). The general formula of polyaniline is shown in Figure 2.4 (B). PANi can exist in three oxidation state [32] ranging from the fully reduced Leucoemeraldine base (LEB) where  $y = 1$ . Pernigraniline (PNB) is the fully oxidized state where  $y = 0$ . The emeraldine form of polyaniline is referred to as emeraldine base (EB) where  $y = 0.5$ . The half-oxidised emeraldine state is composed of an alternating sequence of two benzenoid units and one quinoid unit. Emeraldine base is regarded as the most useful form of polyaniline due to its high stability at room temperature [33]. In comparison,

the LEB is easily oxidized while the PNB is easily degraded [34]. Each of the above mentioned three form of PANi are an insulator [35], although they possess other interesting physical and chemical properties. However, the insulating EB form can be non-redox doped with protonic acid to yield the Emeraldine salt (ES) form, which shows the conductivity [36]. ES can also be obtained through a redox-doping process in acidic conditions from its corresponding reduced LEB form or oxidized PNB form by either a chemical or an electrochemical step [37]. Nevertheless, the non-redox doping processes is different from the redox doping in that it does not involve the addition or removal of electrons from the polymer backbone. Instead, the imine nitrogen atoms of the polymer are protonated to give a polaronic form where both spin and charge are delocalised along the entire polymer backbone. Both the redox doping process and the non-redox doping process are reversible, the conductive ES form can be converted back to its corresponding insulating base form if the condition change [38].

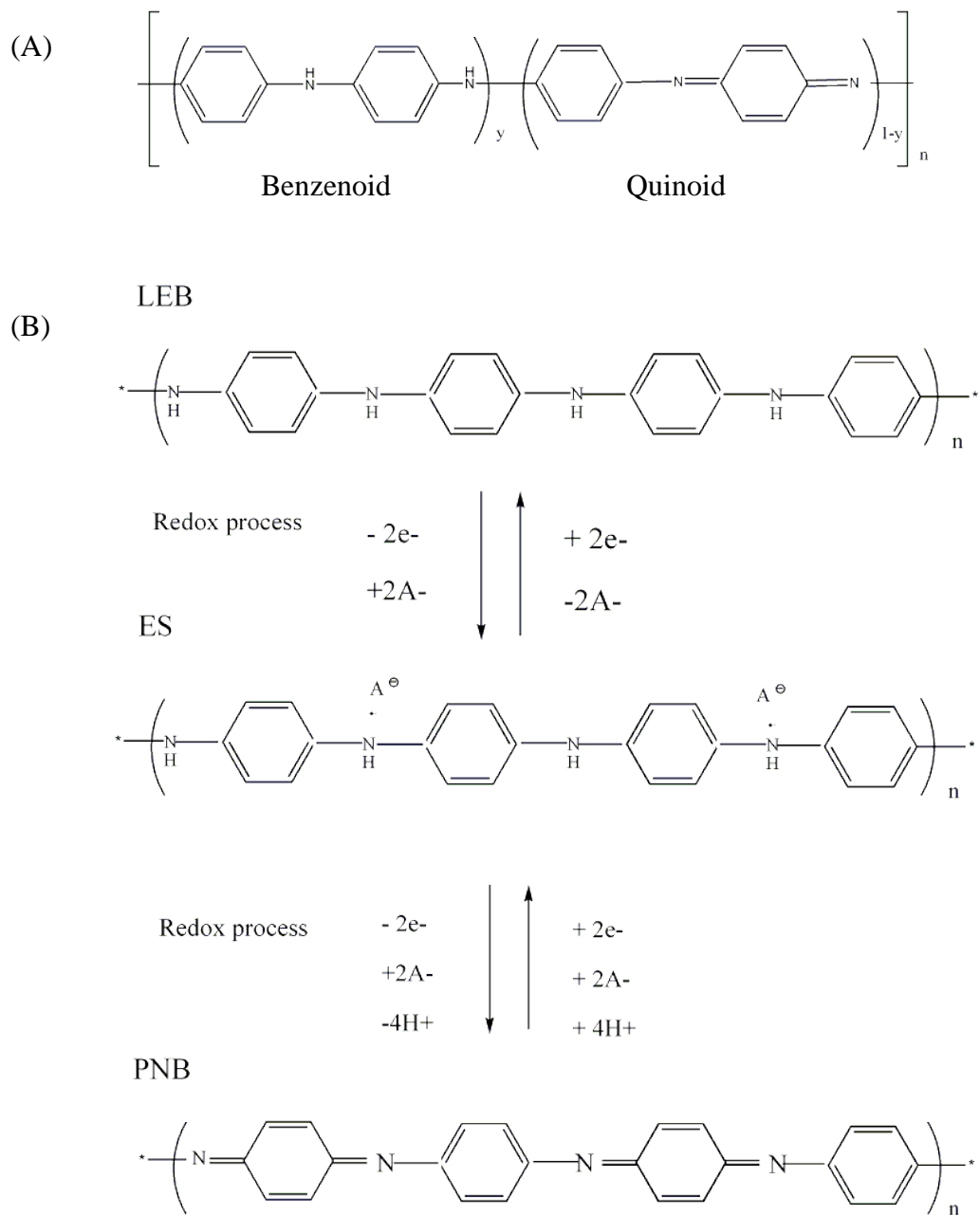


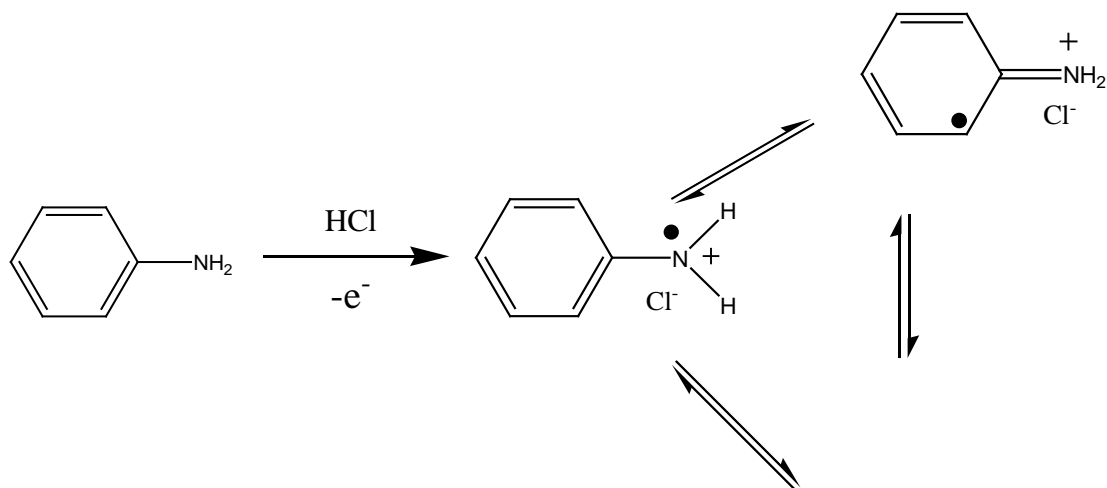
Figure 2.4 (a) The general structure of PANi that shows the average oxidation state (1-y). (b) The chemical structures of the three normally found oxidation state of PANi [38].

### 2.2.1 Synthesis of polyaniline

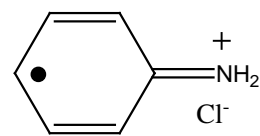
The most common synthesis of PANi involves oxidative polymerization, in which the polymerization and doping occur concurrently, and may be accomplished either electrochemical or chemical polymerization. Electrochemical polymerization method trend to have lower yields than the chemical polymerization method. Furthermore, the chemical polymerization methods are far more amenable to large-scale production. A large number of chemical polymerization methods have been utilized to polymerize aniline, the majority of which take place in solution and may be categorized as monophasic or biphasic. So in this research will focus on the biphasic chemical polymerization method.

The chemical polymerization mechanism of PANi is presented in Figure 2.5. The first step in the polymerization mechanism is supposed to be the oxidation of aniline, resulting in a resonance-stabilized anilinium cation in acid solution. This is followed by coupling of anilinium cations, resulting in dicationic dimer species. The dicationic dimer species then undergoes re-aromatization to its neutral stage to form p-aminodiphenylamine. Then the dicationic dimer species couples with an anilinium cation, resulting in propagation of the chain. The last stage, the oxidative of the growing polymer to a radical cation and doping by acid (HCl) present in solution.

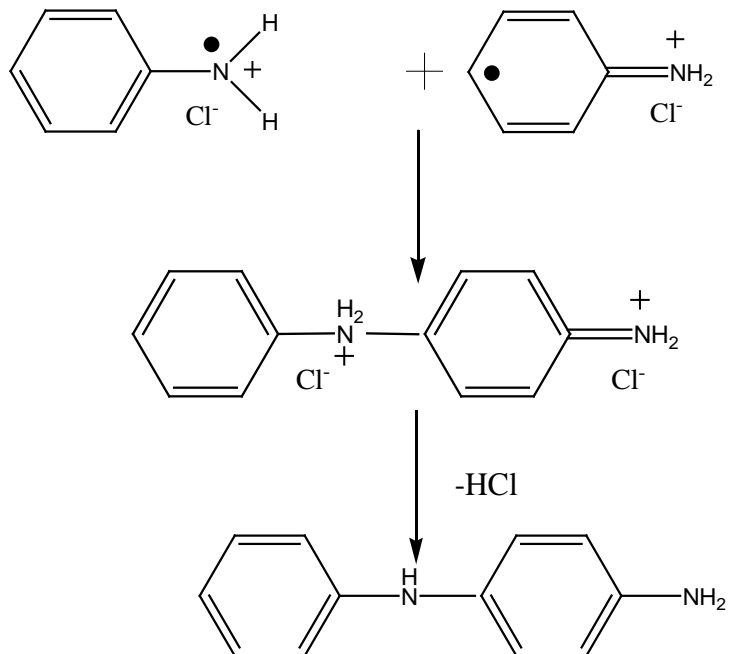
#### Step 1. Oxidation of monomer



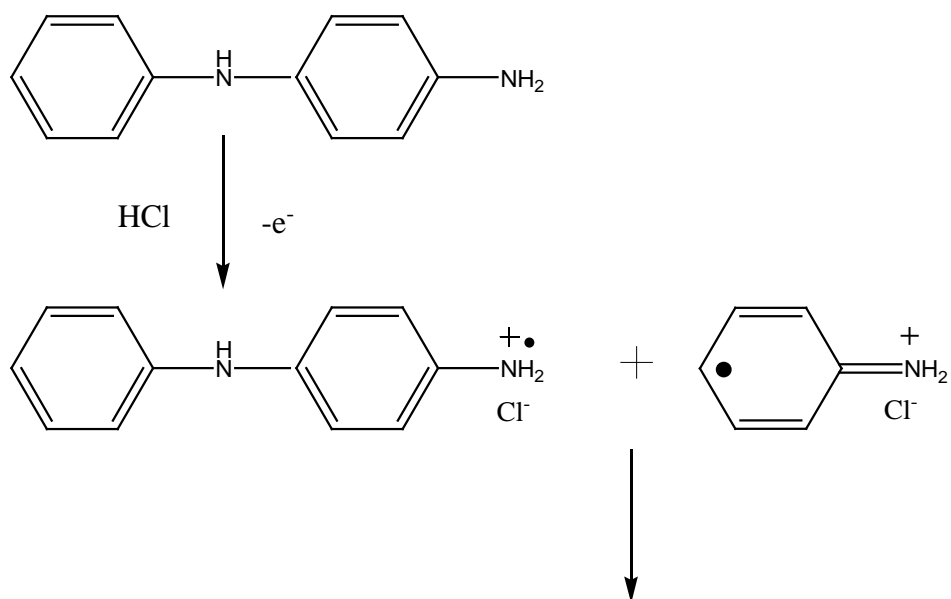


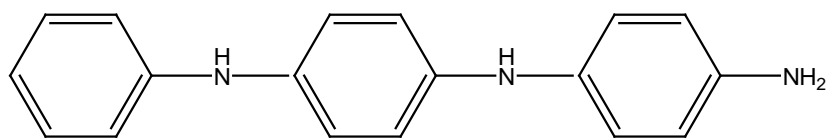


Step 2. Radical coupling and rearomatization



Step 3. Chain propagation





Step 4. Oxidation and doping of the polymer

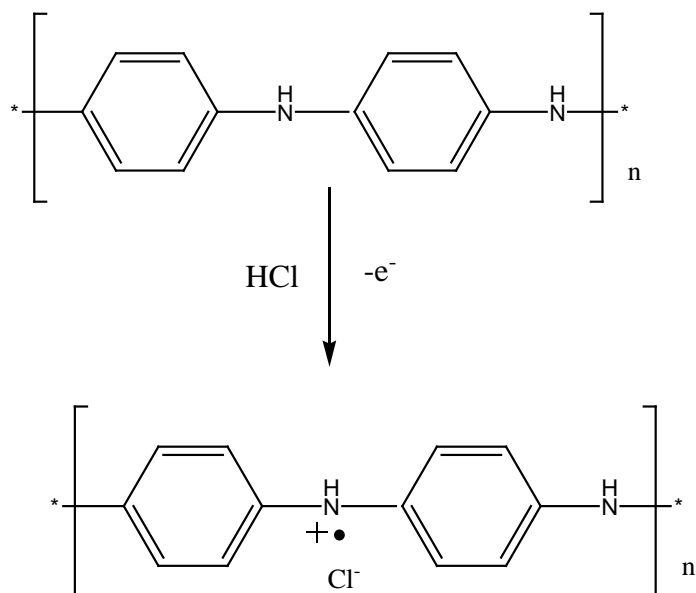


Figure 2.5 Polymerization mechanism of polyaniline [39].

However, because of its low solubility in most common solvents and water, the industrial application of polyaniline is limited. Efforts have been directed toward overcoming such limitations. One approach is to introduce acid group (such as -COOH, -SO<sub>3</sub>H, etc) into the polyaniline chain [40]. Another way is to polymerize the protonic-acid moiety containing aniline derivatives such as aminobenzylphosphoric acid, to give poly(*o*-aminobenzylphosphoric acid) [41] or to copolymerize aniline with similar monomers, such as *N*-(4-sulfophenyl)aniline [42] and *o*-anthranilic acid [43] to yield of poly(aniline-*co*-*N*-(4-sulfophenyl) aniline) and poly(aniline-*co*-*o*-anthranilic acid), respectively. But in this research work, water-soluble self-doped

polyaniline has been proposed by blending polyaniline onto a water-soluble polymer, poly(sodium 4-styrenesulfonate), having pendant aniline monomer and acid doped to obtain water - soluble polyaniline blend poly(sodium 4-styrenesulfonate) [44]. This technique was call Interfacial polymerization.

### **2.2.1.1 Interfacial Polymerization**

Interfacial polymerization technique is the technique employing the polyelectrolyte to bind to and preferentially align the aniline monomers prior to polymerization. During polymerization, the anionic polyelectrolyte such as poly(sodium 4-styrenesulfonate) [45] and poly(acrylate) [46] also provide the required counterions for charge compensation in the doped PANi products. This can lead to water soluble or water dispersed emeraldine salt products. The interfacial polymerization synthesis has the advantage of being a simple process capable of producing water soluble PANi.

The interfacial polymerization of polyaniline is performed in an aqueous–organic biphasis system (Figure 2.6) with aniline monomer dissolved in  $\text{CHCl}_3$  solution and the oxidizing agent- ammonium persulfate, dissolved in an aqueous acid HCl solution with poly(sodium 4-styrenesulfonate), PSS as the blending solution. This process is well-known chemical oxidative polymerization of aniline in a strongly acid environment. The idea of using PSS as the blending for polyaniline, due to PSS is a strong polyelectrolyte which completely dissociated in water so it can act as an anionic dopant and as the template for the formation of PANi with high dispersibility.



Figure 2.6 Interfacial polymerization of polyaniline.

PANi.PSS was then grown from aqueous solution by the anilinium cations created in the interface and adsorbed through the electrostatic interaction onto a large amount of  $-\text{SO}_3^-$  groups of PSS (Figure 2.7) to form an aniline-PSS complex. Subsequently, the polymerization of the adsorbed anilinium cations were changed into PANi.PSS network by ammonium persulfate, oxidizing agent. The inter polymer matrices joined each other during polymerization in the presence of PSS resulting macro PANi.PSS network. The enhance polymerization observed is hypothesized to arise from strong electrostatic interaction between amine nitrogen of PANi backbone and  $-\text{SO}_3^-$  groups of PSS.

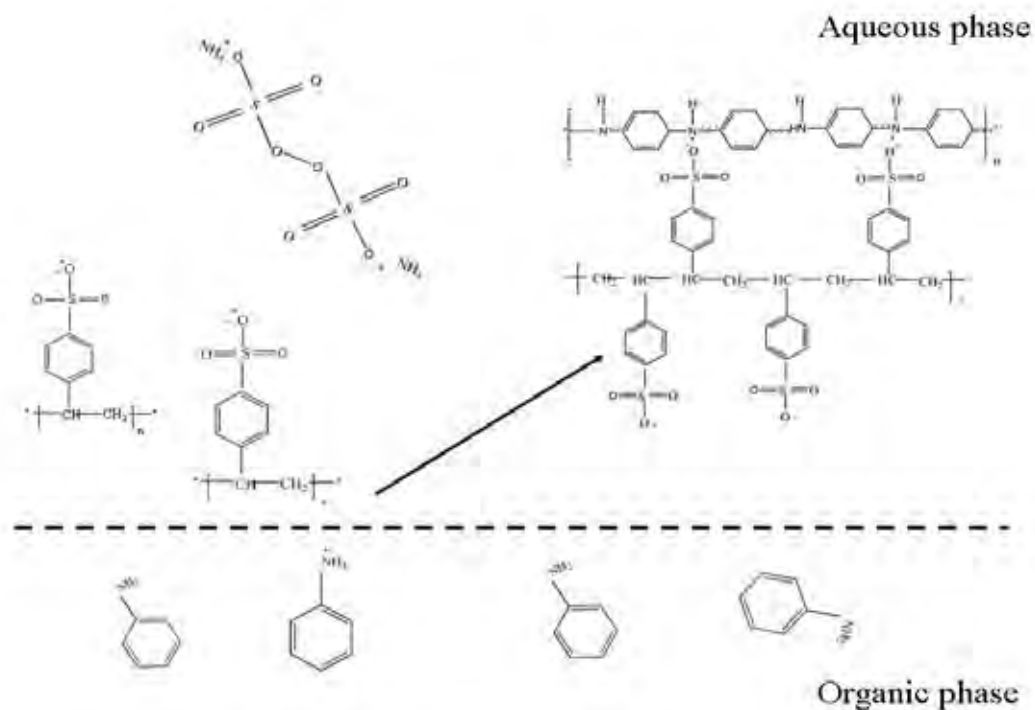


Figure 2.7 Mechanism representation the formation of water - soluble polyaniline blend poly(sodium 4-styrenesulfonate) [47].

The polymerization are found in the top aqueous layer after a short induction period ranging from 10 sec. to several minutes depending on the acid used, the green polyaniline or emeraldine salt or protonated polyaniline appears at the interface. As the reaction proceeds, the color of the aqueous phase becomes dark-green, and finally stop changing, indicating the completion of the reaction. An overnight reaction time is generally sufficient. The resulting PANi.PSS are not precipitated because the strong electrostatic interaction between amine nitrogen of PANi backbone and  $\text{-SO}_3^-$  groups of PSS. The PANi.PSS are well dispersed in aqueous solution for long period storage periods. The efficiency of PSS blended on PANi is often evaluated in term of stability against dispersion or aggregation. The aggregation occurs when the amount  $\text{-SO}_3^-$  site

of PSS is not balance with the amount of amine nitrogen of PANi, leading to their precipitation.

### **2.2.1.2 Ultraviolet-Visible spectroscopy of polyaniline**

Conjugated molecules are often highly colored as their  $\pi$ - $\pi^*$  energy band-gap falls within the visible region; those wavelengths which are not absorbed are transmitted, resulting in the observed color. During polymerization, the polyaniline blend poly(sodium 4-styrenesulfonate) are found at the interface. The color of the polymer solution product are turn from blue to green and to the dark green at the end. The change in polymer color is due to the change in polyaniline structure. The first blue color are observed at the protonated-pernigraniline [48]. As the reaction proceeds, the color of the aqueous phase becomes green as indicate as the protonated-emeraldine [48]. At the end of the polymerization the color of product solution turn to dark green due to the highly conjugated protonated-emeraldine [48].

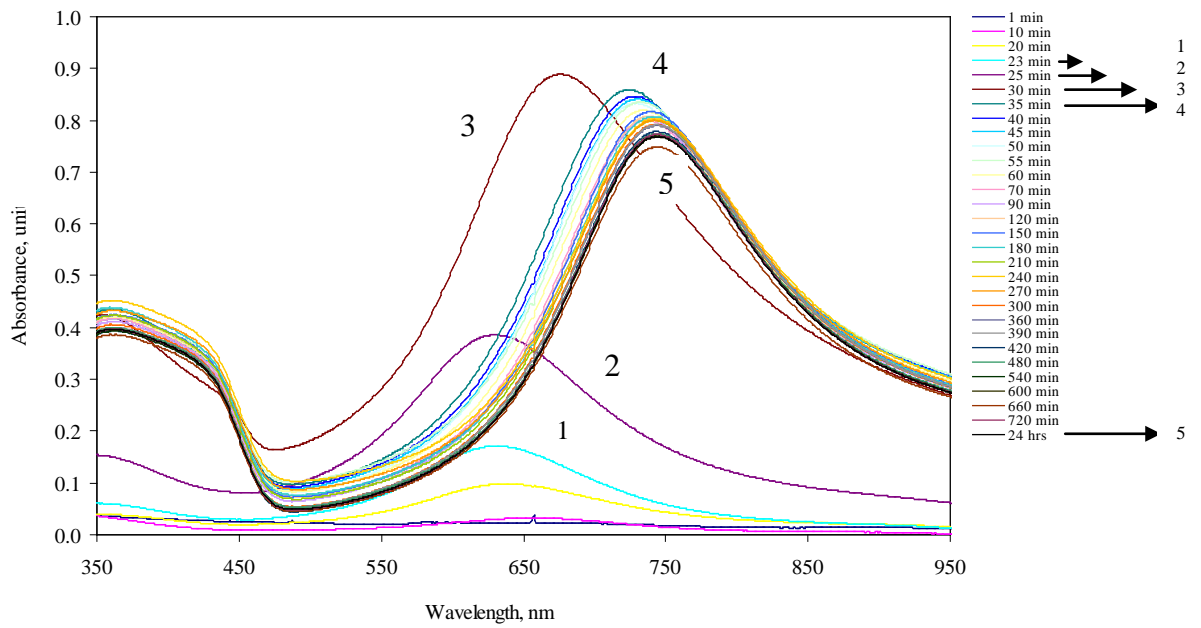


Figure 2.8 Kinetic polymerization of water - soluble polyaniline blend poly(sodium 4-styrenesulfonate) by interfacial polymerization.

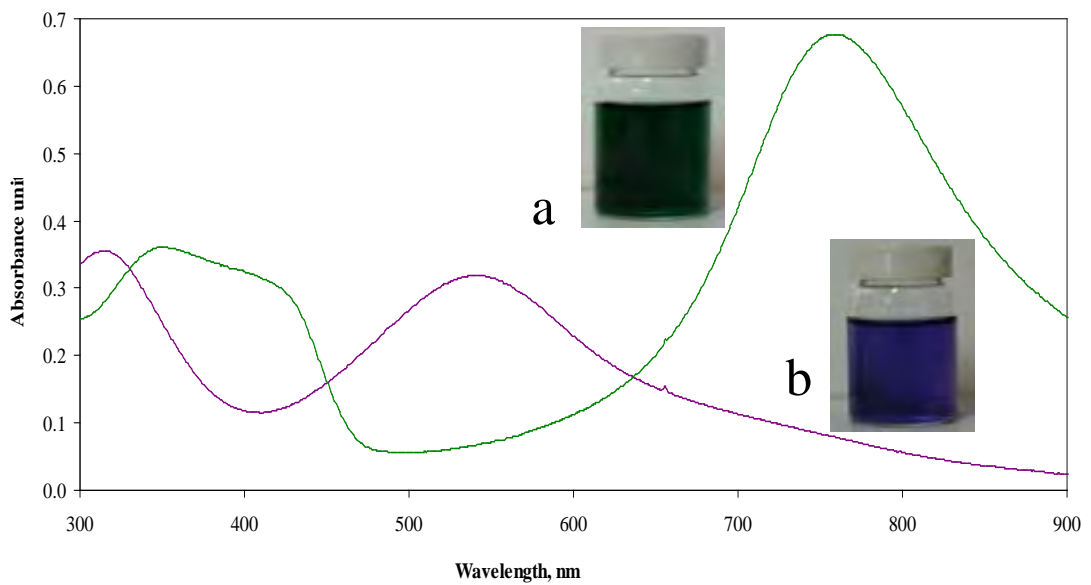


Figure 2.9 UV-Vis spectra of water - soluble polyaniline blend poly(sodium 4-styrenesulfonate), (a) Emeraldine salt and (b) Emeraldine base.

The different electronic spectra of PANi.PSS from interfacial polymerization are shown in Figure 2.9. The characteristic absorbance of PANi.PSS as the doped forms of emeraldine salt or protonated polyaniline (a) are shown three characteristic

absorption bands at 350, 420 and 770 nm corresponding to  $\pi$ - $\pi^*$  band-gap electron transition within benzenoid segments, low wavelength polaron- $\pi^*$  band and high wavelength  $\pi$ -polaron band, respectively [49]. For emeraldine base (b), the protonated polyaniline was treated with NaOH. In alkaline solution, PANi.PSS undergoes dedoping which is characteristic by a shift in the  $\pi$ - $\pi^*$  band-gap at 310 nm. And there is a strong band at 550 nm that had been attributed to a local charge transfer between a quinoid ring and the adjacent imine-phenyl-amine units giving rise to an intramolecular charge transfer exciton [50].

**2.2.1.3 Parameters controlling the interfacial polymerization:** The parameters controlling the synthesis of polyaniline were studied because there are important for the polymerization.

**1. *Polymerization temperature:*** The polymerizations of aniline with ammonium persulfate were performed at room temperature. However, later studies showed that PANi obtained was of relatively low molecular weight [51] and contained significant defect sites [52] such as undesirable branching due to ortho-coupling [53]. Subsequently, the most widely employed temperature for polymerization of aniline monomers has been control at 1-5 °C, as described by MacDiarmid et al. [54] providing PANi, whose EB forms have molecular weights ( $M_w$ ) of 30,000 – 60,000 g/mol.

**2. *Nature of the acid and pH:*** The nature and concentration of the protonic acid employed in aniline polymerization with ammonium persulfate, oxidizing agent, have been reported to have a significant effect on the physicochemical properties and molecular weight of the PANi.-ES products. The polymerization time using HClO<sub>4</sub> as the dopant acid was also observed to be twice as long as with HCl, HNO<sub>3</sub> or H<sub>2</sub>SO<sub>4</sub>,



[55] which may be associated with more compact morphology for PANi product [56]. As for the pH of the oxidative polymerization of aniline by ammonium persulfate, oxidizing agent, greatly affects the nature of products. The formation of various PANi products have been reported by MacDiarmid et al [57] when the oxidative polymerization was carried out at acidic conditions,  $\text{pH} > 3$ . The solution pH was dropped as the reaction proceeds due to production of protons in the course of aniline polymerization. It is generally accepted that acidic conditions are required for the polymerization of aniline and substituted aniline to form a conjugated PANi with higher yield and conductivity [58]. When the conventional polymerization was diluted (at pH 3-4) at the early stages to isolate the first product formed, or when the pH of polymerization was held constant by the buffer solution, a brown product formed. This brown product had different morphology and different optical and magnetic properties from those of PANi [59].

**3. Nature of oxidant:** A wide range of other chemical oxidant has also been successfully employed for the polymerization of aniline monomers. Pron et al. [60] studied the polymerization of aniline monomer using four different types of oxidant such as ammonium persulfate, hydrogen peroxide, potassium dichromate and potassium iodate. Except hydrogen peroxide, the other three oxidant resulted in PANi products of similar conductivity. The conductivity of PANi synthesized with hydrogen peroxide was much lower. Armes and Miller [61] reported that the conductivity of PANi was depended on the ammonium persulfate:aniline ratio, for the oxidant:aniline molar ratios below 1; however the yield of PANi increased linearly up to a ratio of 1. Both yield and conductivity were decreased via over-oxidant of the polymer at higher oxidant:monomer initial molar ratio. Cao et al [62] found that the oxidant:aniline used had a minor effect on the conductivity of PANi produced but the

major effect on the yield produced. The authors concluded that the high concentration of oxidant promoted the formation of soluble oligomers which resulted in a lower final yield.

### **2.3 An Overview of Carbon Nanotubes**

Carbon nanotubes (CNTs) have been extensively studied since their discovery in 1991 by Sumio Iijima [63]. CNTs are unique nanostructure for their size, shape and exhibit remarkable electronic, physical and mechanical properties [64]. Owing to their outstanding electronic, thermal, structure properties, chemical stability, low density, high mechanical strength, large surface area, high modulus and high conductivity, CNTs are suitable for broad range of application in many fields as gas storage devices [65], toxic gas sensor [66], conducting paintings [67], and flat panel display [68]. CNTs can be single-walled and multi-walled carbon nanotubes. Single-walled carbon nanotubes, SWCNTs can be considered to be formed by the rolling up a single layer of graphite sheet to make a seamless cylinder with a diameter of 0.4- 2.0 nm [69]. The symmetric cylinder results in the wrapping of the grapheme sheet can only roll in a discrete set of direction to form a closed cylinder. Once 2 atoms in the grapheme sheet are chosen, grapheme sheet is rolled until the 2 atoms coincide. According to the structure of SWCNTs, their physical and chemical properties are controlled by two separate regions. One is the sidewall of tubes, and the other is the end cap of the tube. Multi-walled carbon nanotubes, MWCNTs can be thought of the nanotubes contain multiple concentric graphite tubes with the increasing diameter 2-100 nm. Therefore, the length and diameter of MWCNTs differ from SWCNTs which can also result different properties. In contrast, MWCNTs require no catalyst for the growth, metal catalyst such as iron, cobalt or nickel is only necessary for the growth

of SWCNTs. Both MWCNTs and SWCNTs possess high tensile strengths and exhibit either electrically conductive or semiconductive which depend on their helicity. CNTs usually exist in 3 common chiralities: armchair, zigzag and chiral nanotubes (Figure 2.10) depending on how the two-dimensional grapheme sheet is rolled up.

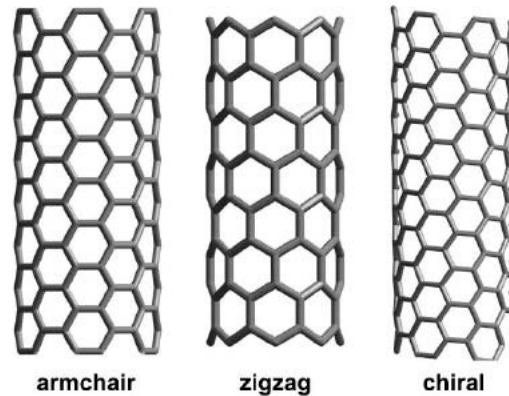


Figure 2.10 Molecular model of SWCNTs exhibiting different achiral and chiral conformations [70]

### 2.3.1 Basic properties of CNTs

The important properties of CNTs are categorized as follows. [71]

**1. Chemistry reactivity:** The reactivity of CNTs is directly depends on the pi-orbital mismatch caused by an increased curvature. That means a distinction could be considered between the sidewall and the end caps of a nanotube. Based on the above explanation, the reactivity increases with the decreasing of the diameter of nanotube. Any covalent chemical modification of either sidewalls or end caps would be possible. Therefore, the solubility of CNTs in various solvents can be controlled this way. [72]

**2. Electrical conductivity** CNTs with a small diameter either semi-conducting or metallic is related to their chiral vector. Thus far, the variations in conducting

properties are caused by the molecular structure resulting in a different band structure and thus a different bandgap. For example, a (m,n) nanotube is metallic as accounts that:  $n=m$  or  $(n-m) = 3i$ , where  $i$  is an integer and  $n$  and  $m$  are defining the nanotube. For the same reason, the resistance to conduction is determined by quantum mechanical aspects and is proved to be independent of the nanotube length. [73]

**3. Optical activity:** The optical activity is revealed with the chiral nanotubes that caused when the nanotube enlarge and thus the chiral nanotubes will disappear. For the same reason, the other physical properties are affected by these parameters. With the optical activity properties of CNTs, the employing of CNTs plays an important role for optical devices. [74]

**4. Mechanical strength:** The Young modulus especially in the axial direction is one of the most critical factor that determine whether how mechanical strength of CNTs would be. Due to the CNTs have a large Young modulus, the nanotube exhibits flexibility that results in the expansion in length. Overall, the CNTs are potentially allowed to employ for the composite material application that require anisotropic properties. [75]

### **2.3.2 Carbon nanotubes synthesis**

To date, CNTs are produced by 3 main techniques, namely electric arc discharge, laser ablation and chemical vapour deposition.

**1. Arc discharge :** In arc discharge, carbon atoms are evaporated by plasma of helium gas generated using electric arc between 2 graphite electrodes. The metal catalyst powder such as iron, nickel and cobalt generally filled in one of the electrode

in a helium atmosphere. By product of ordered nanotubes were made from an ionized carbon plasma and joule heating from the discharge generated the plasma [76].

**2. Laser ablation:** Laser ablation method has been used to produce an ensemble of carbonaceous material which contains nanotubes (30-70%), amorphous carbon and carbon particles. This technique utilized a laser to evaporate a graphite target which is usually filled with a flowed of gas was passed through the growth chamber to move the grown nanotubes forwards and collected on a cold end (finger) [77].

**3. Chemical vapour deposition (CVD):** The growth process involves 3 main factors consisting of transition-metal nanoparticle catalyst, hydrocarbons and growth temperature. The nanotubes are formed by the dissociation of hydrocarbon molecules catalyzed using the transition-metal catalyst, and the dissolution and saturation of carbon atoms in the metal nanoparticles under high temperature. Diameter and length of carbon nanotube can be controlled by considering the catalyst size and reaction time. For the growth of MWNTs, the carbon feedstock typical catalyst is iron, nickel or cobalt nanoparticle. The formation of metal-carbon solution due to the soluble of carbon in the metal catalyst occurs at high temperatures and leads to the growth step [78].

### **2.3.3 Surface modification of carbon nanotubes**

The effective utilization of CNTs in composite applications depends strongly on the ability to disperse them individually and uniformly throughout the matrix, without destroying their structure or reducing their aspect ratio. The major problem of CNTs is focused onto the dispersion in aqueous or organic solution due to the van der waals forces between nanotubes surface and CNTs trend to aggregate to each other as

a bundle. To solve this problem, CNTs were modified the surface in order to reduce the van der Waals forces of intertube for improving their dispersion. The surface modification of CNTs can be grouped into two broad categories; 1) covalent surface modification through reaction onto  $\pi$ -conjugated skeleton of CNTs and 2) noncovalent surface modification or wrapping of various molecules on the sidewall of CNTs. To provide a wide variety of functional groups on carbon nanotubes surface, covalent surface modification were the impact method for dispersion and stability improvement. However the disadvantage of covalent surface modification are that the abundant of conjugated bond which were the important for electronic properties of carbon nanotubes, were loose during the favor chemical reaction on the nanotubes surface. While the noncovalent surface modification still provided the carbon nanotubes integrity using polymer, surfactant biomolecules base on the interaction as electrostatic, hydrogen bonding, hydrophobic and even van der Waals [79].

### **2.3.3.1 Covalent surface modification**

The covalent surface modification of multiwall carbon nanotubes has been widely investigated and produced an array of modified nanotubes structures bearing small molecules, polymers, and inorganic species. However, sidewall functionalized of CNTs is strongly. Furthermore, change to CNTs properties caused by covalently attached functional groups can be dramatic and permanent. Adding any covalent functionality to the CNTs inevitably changes the CNTs electronic structure and might not be suitable for application that rely on high electrical and thermal conductivity of CNTs. As a results, the desired multifunctionality of CNTs might be sacrificed. For example in a mixture of concentrated nitric and sulfuric acids, the oxygen-containing groups are introduced to the ends and sidewall of the tubes. These groups, which are

chemically attached to the tubes, are mostly represented by  $-\text{COOH}$  groups, less by  $-\text{C}=\text{O}$ , and  $-\text{OH}$  groups. These groups can serve as starting points for further functionalization of the nanotubes.

### **2.3.3.2 Noncovalent surface modification**

The noncovalent surface modification of multiwall carbon nanotubes or wrapping of various molecules on the sidewall of CNTs still provided the carbon integrity using using polymer or surfactant. The noncovalent surface modification interaction are based on electrostatic, hydrogen bonding, hydrophobic,  $\pi$ - $\pi$  stacking interaction and even van der Waals. The advantage of this method is the preservation of electronic structure of carbon nanotubes surface.

Wang Y. [80] presented their work that focuses on the dispersion of SWCNTs in PDADMAC solution. The hydrophobic interaction between SWCNTs and PDADMAC was considered responsible for the solubility. The mixture of 1 % PDADMAC solution and 4 mg SWCNTs was shown the high dispersion efficiency for at least 7 months stability. The SWCNTs.PDADMAC system represent the composite platform for the development of glucose biosensors based on the LbL assembled multilayer films.

Noncovalent surface modification of MWCNTs with polystyrene-g-(glycidyl methacrylate-co-styrene) was studied by Lui T.Y. [81] The strong interaction have been proved to exist between aromatic rings and the surface of MWCNTs by  $\pi$ - $\pi$  stacking interaction. The mixture solutions can be stable for months without microscopic precipitation. TEM images showed that the MWCNTs bundles were efficiently exfoliated into individual MWCNTs. Moreover, individual MWCNTs can

be stabilized in good solvent such as ethanol through intertube steric repulsion introduced by the stretched polymer main chain.

Moore V.C. [82] demonstrated a noncovalent surface modification of SWCNTs by the surfactant of sodium dodecylbenzene sulfonate (SDBS). The high molecular weight of SDBS was shown the high dispersion efficiency. The mixture of SWCNTs and SDBS can be dissolved in water with the solubility as high as 5.0 mg/ml.

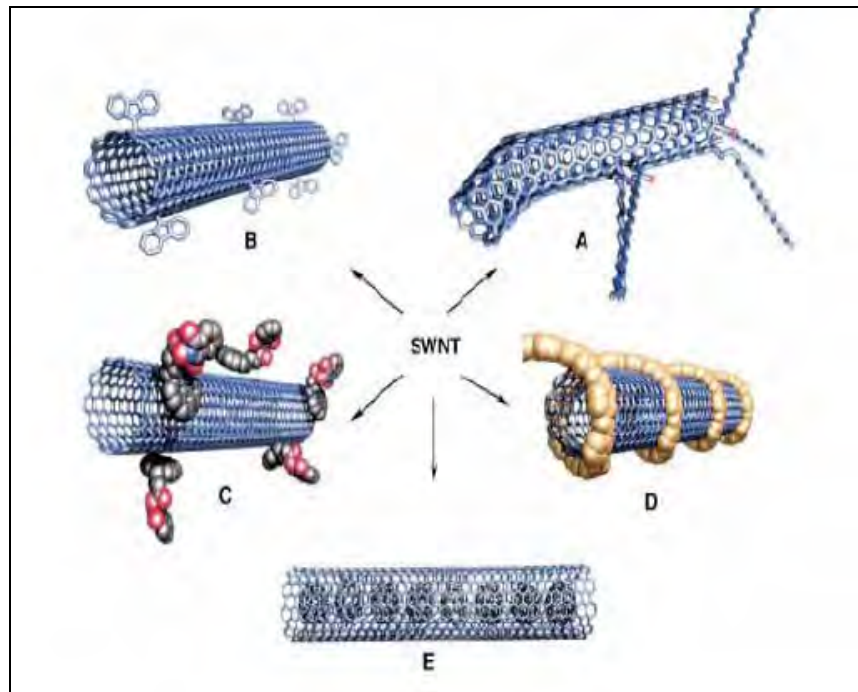


Figure 2.11 Functionalization possibilities of SWCNTs: A) defect group functionalization, B) covalent sidewall functionalization, C) noncovalent functionalization with surfactant, D) noncovalent exohedral functionalization with polymers and E) endohedral functionalization [83].

This thesis deal with noncovalent exohedral functionalization of MWCNTs using polyelectrolyte such as poly(diallyldimethylammonium chloride), PDADMAC



and water-soluble polyaniline. Noncovalent exohedral functionalization still electronic property of CNTs because there are not abundant of conjugation bond which were important for electronic properties. The interaction of noncovalent surface modification of CNTs are based on van der waals, hydrophobic and  $\pi$ - $\pi$  stacking interactions, respectively.

#### **2.4 An Overview of layer by layer self assembly technique**

Multilayer thin films of organic compounds or nanoparticles on solid surfaces or substrates have been studied and investigated for more than 70 years because they allowed the fabrication of multicomposite molecular assemblies of tailored architecture [84]. The structure, composition and uniformity of the surface of such films play the important roles in many applications such as electronic and optoelectronic devices, sensors, and protective coatings [85]. Many techniques including spin coating, solution casting, thermal evaporation, Langmuir-Blodgett (LB), and Layer-by-layer (LbL) self assemble deposition have been developed and studied to assemble and fabricate the organic semiconductors or nanoparticles as thin films. The solution deposition technique, which is the low-cost technology, offers the greatest advantages in term of economic feasibility for device fabrication at the industrial scale. Recently, there were many great interests in the preparation of well-ordered, ultrathin organic films by Layer-by-layer self assembly, LbL for use as thin film coatings, electro-optic devices and various display devices. This electrostatic LbL self assembly technique was first developed in early 1990s by Decher and coworker. This technique was developed for the construction of multicomposite films of rod-like molecules equipped with ionic groups at both ends, polyelectrolytes or other charged materials through the adsorption from aqueous solution. This method

involves strong electrostatic interaction between a charged surface and the oppositely charged molecules (polycation and polyanion) which is the energetic driving force for multilayer formation. The schematic diagram showing the fabrication of multilayers which composed of polyions or other charged molecules or colloidal object is shown in Figure 2.12. In principle, there are no restriction with respect to substrate size and topology due to the process involves only adsorption from solution. As shown in Figure 2.12 (A), the thin deposition on glass substrate from ordinary beakers can be performed either manually or by an automated device. A well-cleaned substrate is first deposited with polyelectrolyte (positive charged in this sample) prior to deposition of interested materials. This charged substrate is then sequentially immersed into the solution of polyanion and polycation, respectively. A representation for the buildup of multilayer film at molecular level is shown in Figure 2.12 (B). The counterions have been omitted and the stoichiometry of charged groups between polyanions and between the substrate and polyanion is arbitrary in this example. The typical and commercial polyelectrolytes are also shown in Figure 2.13.

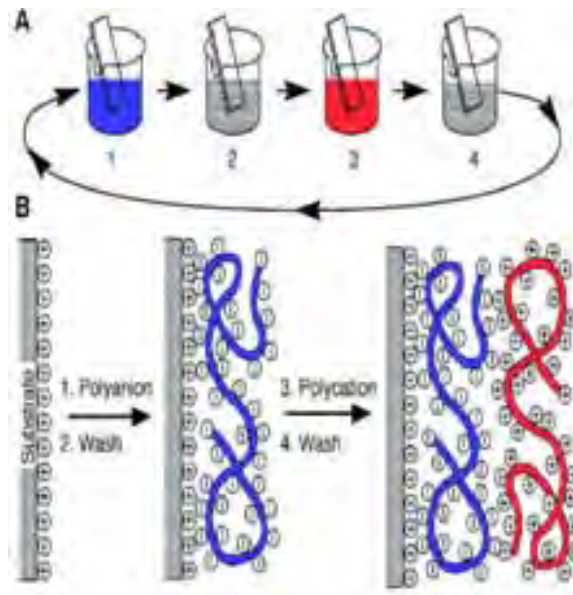


Figure 2.12 (A) Schematic diagram showing the film deposition process, (B) simplified molecular picture of the adsorption step of polyelectrolyte [86].

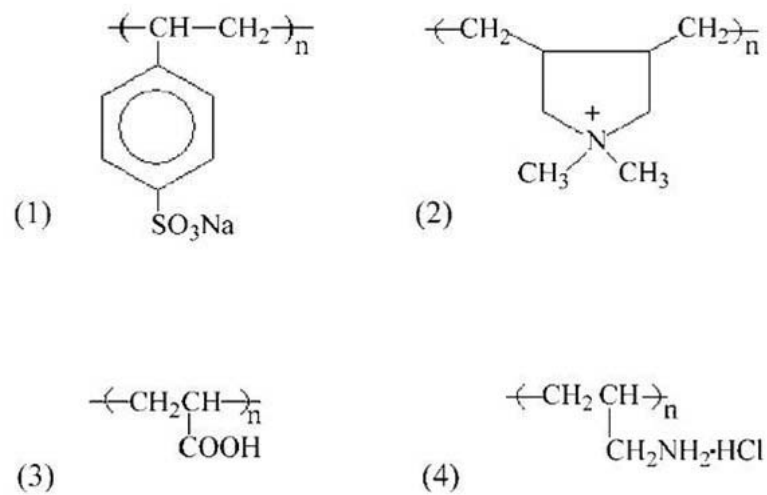


Figure 2.13 Chemical structure of positive and negative polyelectrolytes: (1) poly(diallyldimethylammonium)chloride (PDADMAC), (2) poly(so-dium 4-styrenesulfonate) (PSS), (3) polyacrylic acid (PAA), (4) polyallylamine hydrochloride (PAH) [87].

Typically, films are deposited from the concentration of solutions in several milligram per milliliter. These concentrations are much greater than that required for reaching the plateau of the adsorption isotherm to ensure that the solutions do not become depleted during the film fabrication which composed of several layers. In addition, one or more washing steps are usually performed after each layer adsorption to avoid contamination for the next adsorption solution by liquid adhering to the substrate from the previous adsorption step. The washing step can also help to stabilize weakly adsorbed polymer layers. The appropriate adsorption times of each layer depend on the type of materials, molar masses, concentrations and agitation of solution which ranging from minutes in the case of polyelectrolyte to hours.

A model of the film formation by adsorption of charged polyelectrolyte on an oppositely charged surface could help for better understanding of whole adsorption process. Tsukruk et al [88] has investigated the LbL process by the model concept with both poly(styrenesulfonate, PSS and poly(allylamine), PAA molecular layers versus deposition time, Figure 2.14. It is speculated that assembly of polyions on charged surface is indeed a two stage process. At the very initial stage of film formation, with in the first 1-2 min of self assembly, charged PSS polymer chains are adsorbed homogeneously, mainly on selected sites of oppositely charged substrates with high concentration of local charges. Apparently at this stage of deposition, chain are tethered to the surface by only a few segments and thus virtually preserve their coiled conformation. And then polymer chains are relaxed to a dense packing during the long second stage of self assembly. Presumably, a stable homogeneous polymer monolayer which covers the original surface is formed only after complete relaxation of adsorbed macromolecules. Concerning the deposition time,  $t$ , a longer deposition time allows macromolecules to equilibrate and form a complete monolayer. Polymer

islands are gradually spread out over the surface: their height decreases to 1-1.5 nm for adsorption times after 10-30 min. This process results in homogeneous coverage of the surface with flattened macromolecular chains.

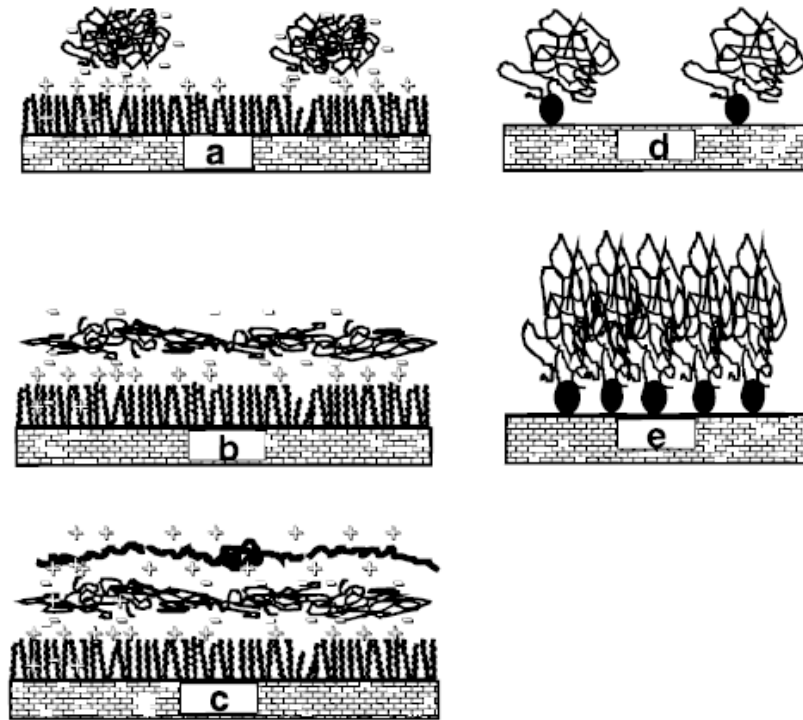


Figure 2.14 Models of surface microstructure for polyionic molecular layers. (a) PSS at the shortest deposition time (<5 min). (b) PSS at the longest deposition time (<10 min). (c) PSS/PAA complex bi layers. (d) Comparison with polymer brushes in the initial stage of tethering by on sticky end. (e) Polymer brushes in a dense state [88].

The major advantages of layer-by-layer deposition methods are as followed: 1) Many different materials can be incorporated in individual multilayer films 2) The films architectures are completely determined by the deposition sequence. Furthermore, no special film balance is required for this technique which indeed the technique has been referred to as a molecular beaker epitaxy. Several applications of this technique

have been reported due to its simplicity in processability, versatile and use of water-based solutions.

#### **2.4.1 Parameter controlling layer-by-layer self assembly**

- **pH:** Control of surface and interface properties are critically important for layer-by-layer self assembly technique. The pH-controlled layer-by-layer assembly provides enormous flexibility in controlling both the molecular organization and properties of polyelectrolyte multilayer thin films. With suitable adjustments of pH of the dipping solutions, it is possible to manipulate dramatically the molecular organization, competition, surface properties and chemistry of the multilayer assembled created by this process. In principle, the macromolecules chemical structure can be transform into a polyelectrolyte structure by covalently attaching a reasonable number of ionic groups in an aqueous medium of appropriate pH. The pH of the polyelectrolyte solution has affect to the charge density of the polymer. This charge carrier density is defined as the average number of ionic sites per monomer unit in the case of polymer. Example of poly(acrylic acid), is the weak polyelectrolyte which have carboxylic groups on the polymer backbone. The poly(acrylic acid) would retain the ionic character in the polymer chain when adjust the pH solution more than 4.4.

- **Ionic strength:** The ionic strength had effect to the formation of the polyelectrolyte multilayer films due to the screening of the charges along the polyelectrolyte chains, the polymer molecules are more entangled with increasing salt concentration. The results are in larger thickness and a stronger internal and external roughness of the adsorbed layers. The increase in thickness is proportional to ionic strength. The effect of NaCl has triple as it act on the conformation of the

polyelectrolytes in solution. First, effect of the conformation of the polyelectrolytes in solution has already been discussed and it is known that high concentration induce a coiling of polymer chains by screening of electrostatic charges on the polyelectrolyte. Second, effect is also due to the screening of the electrostatic repulsion during adsorption onto the substrate, which induce a higher loading and diffusion rate of the polyelectrolytes onto the substrate. Finally, the effect of ionic strength is to swelling the film by competitive interaction with polyelectrolyte-polyelectrolyte bound through the extrinsic compensation. The swelling of the PEM matrix lead to a looser network and allow the diffusion of polyelectrolytes chains inside the film.

- **Dipping time:** Another parameter which can be used to control the growth of multilayers is the dipping time. Because the adsorption of polyelectrolyte at the thin film water interface is controlled by a diffusion process time play a major role in the formation of the multilayer. When negatively charged surface is dipped in a positively charge polyelectrolyte, the electrostatic interaction are sufficient to allow a complex to be formed between the polyelectrolyte on the surface and the oppositely charged polyelectrolyte in solution. While the deposition occur, the surface charge become less negative and more positive as more polycation polyelectrolyte adsorb onto the surface. When the surface is completely adsorped with the polycationic polyelectrolyte the adsorption of new polyelectrolyte is stop due to electrostatic repulsion.

## 2.5 Composite materials

A composite material is made of two or more constituents with significantly different physical or chemical properties. They are distinguished by the nature of their constituents and by the geometry and arrangement of the disperse phase in the metric.

The properties of the new materials are dependent upon the properties of the constituent materials, as well as the properties of the interface.

It is well known that nano-composite materials have much attention from the scientific community because of the unique and unexpected properties which make them attractive candidates for diverse applications such as nanoelectronic, biosensors, and so on. Recently, fabrication of carbon nanotubes/ conducting polymers composite has gained great interest, and it has been demonstrated that the obtained carbon nanotubes/ conducting polymers composite possess the properties of each of the constituents with a synergistic effect. The reason that the conductive polymers are the best candidate to fabricate the composite material is the conjugated groups of polymer, which would interact strongly with the planar of carbon nanotubes. Polyaniline is the one of the most extensively studied conductive polymers [89]. Potential applications include use in rechargeable batteries, sensors, switchable membrane and electrochromic devices, due to its environmental stability and controllable conductivity over a wide range by protonation and charge transfer doping. The composite of carbon nanotubes and polyaniline were also prepared and investigated by many researchers. Almost all reported carbon nanotubes and polyaniline composite show enhanced electronic properties, with some of them finding practical applications as printed electrodes in transistors with high performance contacts and logic gates. However, the reported methods for preparing the carbon nanotubes and polyaniline composite are almost the same such as by;

1. Polymerization of the corresponding monomer in the presence of carbon nanotubes, either by chemical method or by the electrochemical techniques.



2. Many techniques including spin coating, solution casting, thermal evaporation, and Langmuir-Blodgett (LB) have been developed and studied to assemble and fabricate the carbon nanotubes and polyaniline composite thin films

Using these different techniques a great number of carbon nanotubes and polyaniline composite can be processed. In addition, until now no reports were available about the properties of carbon nanotubes and polyaniline composite in neutral conditions, which is an important aspect to learn for their potential biological applications. Here we report another simple way of incorporating carbon nanotubes into polyaniline by layer-by-layer method. Recently, the LbL method has been demonstrated very successfully in the preparation of carbon nanotubes/ non-conducting polymer such as PDADMAC composite. The obtained multilayer films were highly homogeneous and showed drastically improved mechanical properties as compared to those prepared by other methods [90]. Here we first demonstrated, by the LbL method, the preparation of conducting polymer, polyaniline with carbon nanotubes due to we had expected that CNTs could enhance the conductivity of conducting polymer, polyaniline.

### ***Processing methods of PANi – CNT composites***

The main challenge in the polymer-CNTs composite preparation is the implementation of CNTs' amazing properties on the nanoscale composite, combining the choice of materials with the appropriate processing methods [91]. The process to composite two different materials of PANi – CNT via LbL self-assembly method is shown below.

***Preprocessing:*** In this case of CNTs used as the polyelectrolyte for the LbL, a preprocessing step has to be added to prepare the materials. Deagglomeration of nanotubes ropes for dispersing individual nanotubes. The efficiency of CNTs in composite materials applications depends strongly on the ability to disperse them individually and uniformly throughout the matrix, without destroying their structure, or reducing their aspect ratios. The CNTs could be incorporated into the polymer matrix by noncovalent interactions based on the hydrophobic or  $\pi$ - $\pi$  stacking interaction or van der Waals interactions depend on the type of dispersing agent.

***Layer-by-layer processing:*** Layer-by-layer processing uses a solution in which CNTs and polymer are first dispersed and then made the multilayer with the other polymers. In this technique the main challenge is to obtain a stable composite multilayer thin films.

CNTs have been incorporated into conducting polymer, polyaniline matrix to enhance different polymer properties, like to improve conductivity of polymer, improve thermal resistance, improve mechanical strength. Another goal is to overcome the drawbacks of CNTs for large-scale applications such as improve their solubility, their dispersibility, their reactivity and enhance their interfacial interactions in composites.

## **2.6 Conductivity measurement**

Conductivity is defined as the ability of the substance to conduct electrical current. It is commonly represented by  $\sigma$  and has the SI units of siemens per centimetre (S/cm). The conductivity is the reciprocal of electric resistivity ( $\rho$ , the SI unit is the ohm centimetre,  $\Omega$ .cm). One of the most common methods to measuring

the surface resistivity is by using two or four point probe. This method uses probes aligned linearly or square pattern that contact the surface of the material. Measuring surface resistivity with four probes date back to 1996 where Wenner discussed using the technique to measure the earth's resistivity. Both two and four probe methods are the most popular methods for measuring resistivity.

Four-point probe technique was used to measure the electrical conductivity of polymer thin films. The schematic of four-probe used in this work is shown in Figure 2.11. Probe tips made from copper were press against the surface of thin films. The conductivity was obtained by introducing current (I) to the two outer tips and determined the voltage drop (V) across two inner tips. The conductivity was calculated from equation 2.

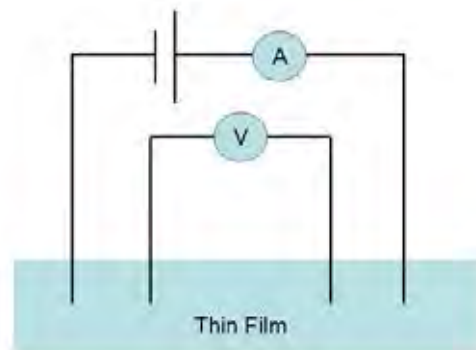


Figure 2.15 Schematic of four-point probe.

$$\sigma = 1/\rho = I / (K \times V \times t) \quad (2)$$

Where

$\sigma$  is the conductivity (S/cm)

$\rho$  is the resistivity ( $\Omega \cdot \text{cm}$ )

V is the applied voltage (V) to the tip

I is the measured current (A) across two tip

T is the thickness of the films (cm)

K is the geometric correction factor

Most surface resistivity measurements are made on semiconductor wafers or thin films on a small surface area substrate. Since the measurements are made on finite sized areas, correction factors have to be used based on the sample geometry. This correction factor depends on the sample thickness, edge effect and the location of the probe on the sample. Many studies have been performed on correction factors, with tables outlining the necessary adjustments. Other considerations that need to be considered for accurate four-point probe measurements are the spacing of the probes, and temperature effects. Small spacing differences in probe spacing can cause the resistivity values widely across a sample surface.

**Electrical measurements of polyaniline films, carbon nanotube films and carbon nanotubes polyaniline composite films:**

Polyaniline has an electronic conduction mechanism that seems to be unique among conducting polymer, because it is doped by protonation. There are many methods to fabricate conducting polyaniline thin films such as spin coating, solution casting, thermal evaporation, Langmuir-Blodgett and layer-by-layer self assembly technique. Each film fabrication method shows the different architectures that affect the conductivity.

Siti Amira Othman *et al.* were successful in preparing polyaniline thin films by Langmuir-Blodgett technique. The conductivity of polyaniline thin films were measured by four point probe. By applying the resistivity,  $\rho$ , from the equation of  $1/\rho = I / (K \times V \times t)$ . The resistivity of polyaniline thin films was found around  $4.640 \times 10^7 \Omega \cdot \text{cm}$ . Conductivity of the polymer thin films is an inverse of resistivity.

Recently, the conductivity of carbon nanotubes polyaniline composite film was proposed by P.C. Ramamurthy. The composite of carbon nanotubes and polyaniline were fabricated by spin coating. The conductivity measurements were carried out on the freestanding composite films using a four point probe method. The conductivity of composite films values range from 11 S/cm to 23 S/cm when increasing SWCNTs concentration from 1 – 10 % SWCNTs loading. On the other hand the conductivity of carbon nanotubes was found at 8 S/cm when fixed the SWCNTs concentration at 10 % SWCNTs loading.

Jianbo Lu *et al.* and coworker have been reported the conductivity of pure polyaniline and carbon nanotubes polyaniline composite. The polymer thin films and polymer-composite thin films were fabricated by Langmuir-Blodgett technique. The conductivity measurements of thin films were carried out using a four point probe method. The conductivity of the polyaniline and carbon nanotubes polyaniline composite were found  $7.235 \times 10^{-7}$  and  $5.212 \times 10^{-4}$  S/cm, respectively.

Ji-Er Huang *et al.* were successful to fabricate composite thin films of carbon nanotubes and polyaniline. The conductivity of polyaniline thin films were measured by four point probe technique at room temperature. The conductivity of carbon nanotubes polyaniline composite were found in the range of  $1.2 \times 10^{-3}$  -  $1.5 \times 10^{-2}$  S/m. as carbon nanotubes content ranging from 0-8 % wt.

## **CHAPTER III**

### **EXPERIMENTAL**

There are five parts in this thesis mainly focused on the synthesis and characterization of water-soluble polyaniline, dispersion of multiwall carbon nanotubes with the different types of polymer and also studied their application. In the first part, the water-soluble polyaniline was synthesized using interfacial polymerization method. The characterization methodologies were investigated. In the second part, the water-soluble polyaniline films were prepared by layer-by-layer self assembly method and employed as the pH sensor. The third and fourth part involved in a new fabrication method to disperse multiwall carbon nanotubes by poly(diallyldimethylammonium chloride), PDADMAC and water-soluble polyaniline and, respectively. The last part studied the layer-by-layer self assembly of multiwall carbon nanotubes - water-soluble polyaniline composite films.

### **3.1 Synthesis and characterization of water-soluble polyaniline using interfacial polymerization method**

#### **3.1.1 Chemical and materials**

Aniline monomer ( $C_6H_5NH_2$ ), ammonium persulfate (APS,  $(NH_4)_2S_2O_8$ ), chloroform ( $CHCl_3$ ) and hydrochloric acid (HCl) were purchased from Aldrich Chemicals. All other chemicals were analytical grade and used without further purification. All aqueous solutions were prepared with doubly-distilled water.

### **3.1.2 Synthesis of water - soluble polyaniline**

Water - soluble polyaniline in the presence of poly(sodium 4-styrenesulfonate, PSS) was prepared by interfacial polymerization technique. The experimental was performed into two phases of aqueous and organic solution. In aqueous phase, the PSS was reacted with oxidizing agent, Ammonium persulfate (APS) and HCl dopant concentration. The aqueous solution was carefully poured into aniline monomer dissolved in chloroform solution. The reaction was kept at 4 °C without agitation for 24 hours. The green water-soluble polyaniline was formed at the interface within a few minutes. Afterward the aqueous solution was separate from the organic solution. The resultant aqueous product which remain the green solution was obtained in its salt form (ES): Emeraldine hydrochloride (PANi-HCl) The above obtained (PANi-HCl) salt form was converted into the Emeraldine base (EB) from by treating it with a 0.1 M NaOH solution.

#### **3.1.2.1 Effect of time onto the polymerization of water - soluble polyaniline**

UV-Vis spectroscopy was used to monitor the polymerization time of water - soluble polyaniline. 10 mM aniline monomer was dissolved in CHCl<sub>3</sub> solution and reacted with 10 mM poly(sodium 4-styrenesulfonate, PSS) blending solution, and 5 mM ammonium persulfate in acid media. The absorbance of the solution was measured since the polymer formed at the interface until 24 hours was reached. In each step, the polymerization was kept at 4 °C.

#### **3.1.2.2 Effect of poly(sodium 4-styrenesulfonate, PSS) blending concentration**

1 M HCl acid dopant concentration, 5 mM Ammonium persulfate (APS) oxidizing agent and the different PSS concentration 1, 3, 5, 10, 20, 50, 100, 150 and

200 mM were feed into 10 mM Aniline monomer in chloroform solution. The mixture solution were stored at 4 °C for 24 hours. The resultant aqueous product was measured by UV-Vis spectroscopy at wavelength of 350 – 1,000 nm.

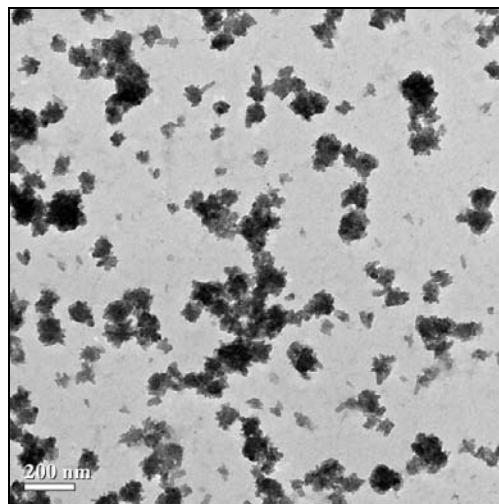


Figure 3.1 Morphology image of water - soluble polyaniline characterized by scanning electron microscope (Phillips XL30CP)

### **3.1.2.3 Effect of temperature onto the polymerization of water - soluble polyaniline**

For study the preparation of water - soluble polyaniline in the different temperature, in clean 250 mL Erlenmeyer flask, 80 mL of water was mixed with 10 mM 10 mL PSS solution and reacted with 5 mM 10 mL of oxidizing agent ammonium persulfate in HCl acid concentration. The reaction was kept for 24 hours at 4, 10, 25 and 40 °C, respectively. The aqueous product was measured by UV-Vis spectroscopy.



#### **3.1.2.4 Effect of pH onto the polymerization of water - soluble polyaniline**

This experiment was conducted in order to ensure that pH is an important constituent for preparation of water - soluble polyaniline. The 130 mL of synthetic solution contained 10 mM 30 mL aniline monomer dissolved in chloroform solution was reacted with 100 mL of blending PSS solution and ammonium persulfate. The reacting solution was adjusted to different pH ranging from 1, 2, 3, 4 and 5. The resultant aqueous product was measured by UV-Vis spectroscopy at wavelength of 350 – 1,000 nm.

#### **3.1.2.5 Effect of oxidizing agent, Ammonium persulfate concentration onto the polymerization of water - soluble polyaniline**

The oxidation potential for polymerization of water - soluble polyaniline is depended on the concentration of oxidizing agent. The effect of oxidizing concentration was studied by using the different concentration of ammonium persulfate from 1, 3, 5, 7 and 10 mM in 1 M acid media under polymerization processes. The performance of oxidizing concentration was evaluated by UV-Vis spectrometer.

#### **3.1.3 Characterization of water - soluble polyaniline**

Water - soluble polyaniline usually exists in four common structure: leucoemeraldine, pernigraniline, emeraldine base and emeraldine hydrochloride. Of these four forms, only emeraldine hydrochloride on interfacial polymerization synthetic is focused. The main characterization techniques involved physical properties are arranged in Table 3.1

Table 3.1 Characterisation techniques and their utilization of PANi.PSS

Techniques	Information
UV-Vis spectrometer	Absorption spectra
Fourier transform infrared spectrophotometer	Functional group
Scanning electron microscope	Surface morphology

### 3.2 Layer-by-layer self assembly of water - soluble polyaniline

LbL self assembly of polyaniline thin films was made by the procedure reported by Decher. This experimental was studied the possibility of the fabrication of polyaniline thin films via the usage of polyaniline solution from the interfacial polymerization.

#### 3.2.1 Chemical and materials

In order to deposit alternating charged multilayers sequentially, two solutions of opposite electrical charge polyelectrolyte were prepared. The anionic polyelectrolyte, water - soluble polyaniline was prepared by interfacial polymerization technique as explained in part 3.1. The cationic polyelectrolyte, poly(diallyldimethyl ammonium chloride, PDADMAC, molecular weight = 200,000-350,000) was purchased from Aldrich Chemicals. Sodium chloride was purchased from Carlo Erba, Thailand. All chemicals were used as received without any further purification. All aqueous solutions were prepared with doubly-distilled water.

### 3.2.2 Preparation of polyelectrolyte multilayer thin films

#### 3.2.2.1 Effect of dipping time onto the film fabrication

The 5 layers of positively-charged hydrophilic glass slide substrate was immersed into the solution of pH 6 water-soluble polyaniline blend poly(sodium 4-styrene sulfonate). The deposition time was varied for 15 sec to 10 mins until the polymer was saturated onto the substrate. Each period with different time, the film was determined by UV-Vis spectroscopy at wavelength of 350 – 900 nm. The schematic diagram representing the layer-by-layer deposition procedure is shown in Figure 3.2.

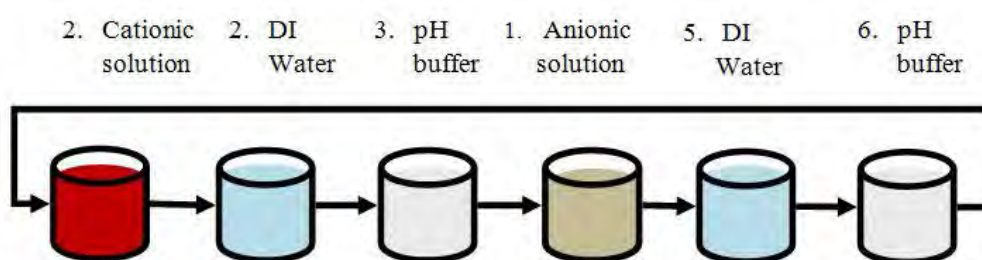


Figure 3.2 Schematic diagram representing the layer-by-layer deposition. [91]

#### 3.2.2.2 Effect of pH onto the film fabrication

##### Chemical preparation:

1. Water-soluble polyaniline blend poly(sodium 4-styrene sulfonate)

0.25 % weight water-soluble polyaniline blend poly(sodium 4-styrene sulfonate) was adjusted to the different pH of 2, 3, 4, 5, 6, 7, 8, 9, 10 and 11. Each 80 mL of water-soluble polyaniline blend poly(sodium 4-styrene sulfonate) with different pH solution were transferred into 100 mL beaker. Then 2 M of NaCl was added to the solution.

## 2. Poly(diallyldimethyl ammonium chloride)

10 mM of poly(diallyldimethyl ammonium chloride) was adjusted to the different pH of 2, 3, 4, 5, 6, 7, 8, 9, 10 and 11. Each 80 mL of PDADMAC with have different pH solution were transferred into 100 mL beaker. Then 1 M of NaCl was added to the solution.

### Film fabrication:

The polymer multilayer thin films were fabricated by immerse 5 layers of positively-charges hydrophilic glass slide substrate onto the water - soluble polyaniline blend poly(sodium 4-styrene sulfonate) solution for 5 mins and then rinsed with water for 2 mins. Then the film was immersed in the solution of poly(diallyldimethyl ammonium chloride) and rinsed with water again. The polyaniline multilayer thin films was fabricated for 11 layers. Before measure the performance of the films by UV-Vis spectrometer, the polyaniline multilayer thin films were dipped in 1 M HCl acid for 24 hrs.

### **3.2.2.3 Effect of NaCl concentration onto the film fabrication**

A. Effect of NaCl concentration in water - soluble polyaniline blend poly(sodium 4-styrene sulfonate)

#### Chemical preparation:

1. Water - soluble polyaniline blend poly(sodium 4-styrene sulfonate)

80 mL of pH 6 of water - soluble polyaniline blend poly(sodium 4-styrene sulfonate) were mixed with the different concentration of NaCl. In this experiment, NaCl which have the concentration of 0.5, 1.0, 1.5 and 2.0 mM was added to the polyaniline solution.

## 2. Poly(diallyldimethyl ammonium chloride)

10 mM of poly(diallyldimethyl ammonium chloride) was adjusted to pH 6. The PDADMAC solution volume 80 mL was transferred to 100 mL beaker. Then 1 M of NaCl was added to the solution.

### Film fabrication:

The film fabrication was studied with the same process of 3.2.2.3 A.

## B. Effect of NaCl concentration in poly(diallyldimethyl ammonium chloride)

### Chemical preparation:

#### 1. Poly(diallyldimethyl ammonium chloride)

80 mL of pH 6 of poly(diallyldimethyl ammonium chloride) were mixed with the different concentration of NaCl. In this experiment, NaCl which have the concentration of 0.02, 0.1, 0.5, 1.0 and 2.0 M was added to the Poly(diallyldimethyl ammonium chloride) solution.

#### 2. Water - soluble polyaniline blend poly(sodium 4-styrene sulfonate)

Water - soluble polyaniline blend poly(sodium 4-styrene sulfonate) was adjusted to pH 6. The polymer solution volume 80 mL was transferred to 100 mL beaker. Then 2 M of NaCl was added to the solution.

### Film fabrication:

The film fabrication was studied with the same process of 3.2.2.3 A.

#### **3.2.2.4 Effect of polyaniline : poly(sodium 4-styrene sulfonate) with various concentration feed ratio of polymerization onto the film fabrication**

Polyelectrolyte multilayer technique was used to prepare polyaniline multilayer thin films. Water - soluble polyaniline blend poly(sodium 4-styrene sulfonate) from the interfacial polymerization process which have the different aniline : PSS ratio (10:3, 10:5, 10:10, 10:20, 10:50, 10:100, 10:150 and 10:200 mM) were used as the negative polyelectrolyte. The layer-by-layer deposition process was performed manually mainly as the following steps:

1. The glass slide substrates were functionalized with strong polyelectrolyte of 10 mM of poly(diallyldimethyl ammonium chloride) and poly(sodium 4-styrene sulfonate) for 5 layers in order to generate the positively-charges hydrophilic properties of the substrate.

2. The substrates were then immersed into the solution of water - soluble polyaniline blend poly(sodium 4-styrene sulfonate) pH 6 and then rinsed with water for 5 min and 2 min, respectively.

3. Then the film was immersed in the solution of poly(diallyldimethyl ammonium chloride) pH 6 for 5 min and rinsing with water to remove the excess of material.

The alternate layer-by-layer films of water - soluble polyaniline blend poly(sodium 4-styrene sulfonate) with poly(diallyldimethyl ammonium chloride) were achieved by repeating this process until the desired number of layer was reached. For the UV-Vis spectroscopy measurement, the multilayer films were dipped in 1 M HCl acid for 24 hrs in order to generate the protonated form of polyaniline.

### **3.2.2.5 Effect of number of layer onto the film fabrication**

#### Chemical preparation:

##### 1. Poly(diallyldimethyl ammonium chloride)

10 mM poly(diallyldimethyl ammonium chloride) was adjusted to pH 6. The polymer solution volume 80 mL was transferred to 100 mL beaker. Then 0.02 M of NaCl was added to the solution.

##### 2. Water - soluble polyaniline blend poly(sodium 4-styrene sulfonate)

Water - soluble polyaniline blend poly(sodium 4-styrene sulfonate) was adjusted to pH 6. The polymer solution volume 80 mL was transferred to 100 mL beaker. Then 2 M of NaCl was added to the solution.

#### Film fabrication:

The film fabrication was studied with the same process of 3.2.1.3 A. But the number of layer were achieved by repeating this process until the desired number of layer was reached.

### **3.2.3 pH sensing of water - soluble polyaniline multilayer films and water - soluble polyaniline solution**

The pH sensing properties of the water - soluble polyaniline multilayer films and water - soluble polyaniline solutions were investigated by recording their optical response at different pH buffer solution. The polyaniline multilayer films were placed in the 250 mL of the different pH acetate and phosphate buffer and recorded the optical response by UV-Vis spectrometer.

### 3.2.4 Characterization of polyelectrolyte multilayer thin films

In order to know the characteristic of water - soluble polyaniline multilayer films, the main characterization techniques involved physical properties are arranged to studied in Table 3.2

Table 3.2 Characterisation techniques and their utilization of pH sensing of water - soluble polyaniline multilayer films and water - soluble polyaniline solution

Techniques	Information
UV-Vis spectrometer	Absorption spectra
Atomic force microscopy	Surface morphology, thickness
Conductivity	Conductance

### 3.3 Dispersion of Multiwall Carbon Nanotubes with Poly(diallydimethyl ammonium chloride)

#### 3.3.1 Chemical and materials

Multiwall carbon nanotubes: MWCNTs (baytubes C 150 P, outer diameter distribution 5-20 nm and length 1 - >10 um, were kindly donated from Bayer Co. Ltd., Thailand. Poly(diallydimethyl ammonium chloride, PDADMAC, molecular weight = 200,000-350,000) was purchased from Aldrich Chemicals. All other chemicals were analytical grade and used without further purification. All aqueous solutions were prepared with doubly-distilled water.



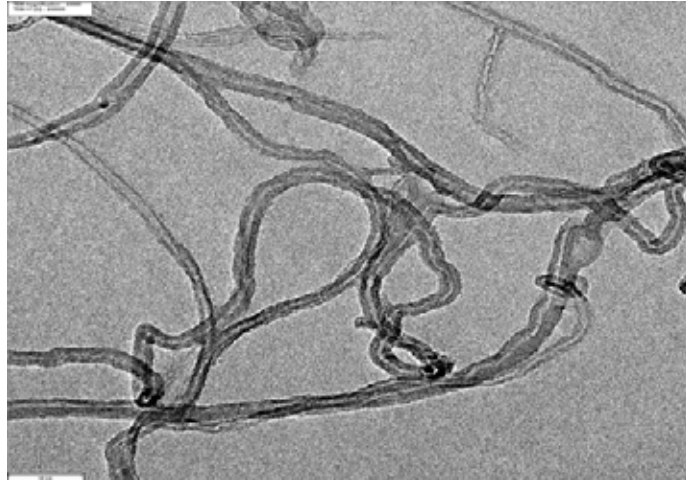


Figure 3.3 Transmission electron microscopic image of MWCNTs (baytubes C 150 P, outer diameter distribution 5-20 nm and length 1 - >10  $\mu\text{m}$ ) from Bayer Co. Ltd., Thailand.

### **3.3.2 Dispersion of Multiwall Carbon Nanotubes**

#### **3.3.2.1 Effect of PDADMAC concentration on the dispersion of MWCNTs**

For the dispersion of MWCNTs, 5 mg MWCNTs were mixed in 100 mL of the different concentration of PDADMAC (0, 0.01, 0.05, 0.1, 0.2, 0.3, 1.0, 3.0 and 5.0 mM) to obtain homogeneous solution. The mixture was sonicated using probe sonicator at ice bath for 1 hr. In each period with different PDADMAC concentration, the solution of MWCNTs were determined by UV-Vis spectroscopy. The wavelength of 550 nm was chosen as it represents the midway of the visible range.

#### **3.3.2.2 Effect of sonication times on MWCNTs dispersed with PDADMAC**

5 mg MWCNTs were mixed with 100 mL of 0.1 mM PDADMAC solution. The mixtures were sonicated at different time intervals ranging from 0.15, 0.30, 1.0,

1.5, 2.0 and 3.0 hours. The mixture solution was stored at room temperature for 24 hours and measured the turbidity by UV-Vis spectroscopy.

### **3.3.3 Stability of MWCNTs dispersed with PDADMAC**

#### **3.3.3.1 Effect of salt type and salt concentration on the stability of MWCNTs**

100 mL of 5 mg MWCNTs and 0.1 mM PDADMAC were mixed with the different types of salt (NaCl, Na<sub>2</sub>SO<sub>4</sub> and Na<sub>3</sub>PO<sub>4</sub>) and different salt concentration (0.01, 0.02, 0.05, 0.08, 0.10, 0.15, 0.25, 0.50 and 1.00 M) into 250 mL erlenmeyer flask. The mixture solution was stored at room temperature for 24 hours and measured the turbidity by UV-Vis spectroscopy at wavelength 550 nm.

#### **3.3.3.2 Effect of functionalization times on the stability of MWCNTs**

The dispersion of MWCNTs with PDADMAC were prepared by dispersing 5 mg MWCNTs in 0.1 mM PDADMAC solution. The mixture solutions were stored at room temperature for 24 hours and measured the turbidity by UV-Vis spectroscopy at wavelength 550 nm.

#### **3.3.3.3 Effect of pH on the stability of MWCNTs**

The 50 mL of dispersion of 5 mg MWCNTs with 0.1 mM PDADMAC solution were mixed with 20 mL of the different pH buffer (pH 1-12). The mixture solutions were stored at room temperature for 24 hours and measured the turbidity by UV-Vis spectroscopy at wavelength 550 nm.

### 3.3.4 Characterization of MWCNTs dispersed with PDADMAC

For the MWCNTs dispersed with PDADMAC, there are many parameters such as surface morphology, nanostructure, UV-Vis absorption may involve the performance of MWCNTs. Generally, it is difficult to control the physical properties of the material precisely due to some parameters are related to each other. To understand the properties of MWCNTs dispersed with PDADMAC, the Table 3.3 outlines the characterization methods commonly used.

Table 3.3 Characterisation techniques and their utilization of MWCNTs dispersed with PDADMAC

Techniques	Information
UV-Vis spectrometer	Absorption spectra
Transmission electron microscope	Surface morphology, nanostructure

### 3.4 Dispersion of multiwall carbon nanotubes with water - soluble polyaniline blend poly(sodium 4-styrenesulfonate, PSS)

#### 3.4.1 Chemical and materials

Multiwall carbon nanotubes: MWCNTs (baytubes C 150 P, outer diameter distribution 5-20 nm and length 1 - >10 um, were kindly donated from Bayer Co. Ltd., Thailand. Poly(diallyldimethyl ammonium chloride, PDADMAC, molecular weight = 200,000-350,000), aniline monomer ( $C_6H_5NH_2$ ), ammonium persulfate (APS,  $(NH_4)_2S_2O_8$ , chloroform ( $CHCl_3$ ) and hydrochloric acid (HCl) were purchased from Aldrich Chemicals. All other chemicals were analytical grade and used without further purification. All aqueous solutions were prepared with doubly-distilled water.

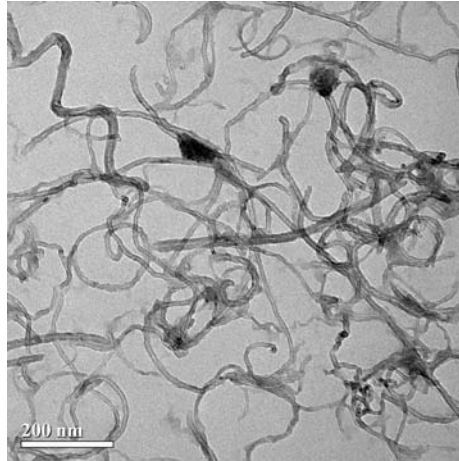


Figure 3.4 Transmission electron microscopic image of MWCNTs dispersed with water - soluble polyaniline blend poly(sodium 4-styrenesulfonate, PSS).

### **3.4.2 Dispersion of Multiwall Carbon Nanotubes**

#### **3.4.2.1 Effect of Water - soluble polyaniline blend poly(sodium 4-styrenesulfonate, PSS) concentration on the dispersion of MWCNTs**

The dispersion of MWCNTs by water - soluble polyaniline blend poly(sodium 4-styrenesulfonate, PSS) was carried out by mixing 5 mg of MWCNTs with the different concentration of water - soluble polyaniline blend poly(sodium 4-styrenesulfonate) solution, (0.01, 0.02, 0.05, 0.08, 0.10, 0.15 and 0.20 % weight). The mixture was sonicated using probe sonicator at ice bath for 1 hr. The mixture solutions were stored at room temperature for 24 hours. In each period with different water - soluble polyaniline blend poly(sodium 4-styrenesulfonate) concentration, the solution of MWCNTs were determined by UV-Vis spectroscopy at wavelength of 550 nm.

### **3.4.2.2 Effect of pH on MWCNTs dispersed with water - soluble polyaniline blend poly(sodium 4-styrenesulfonate, PSS)**

A 100 mL of 0.1 mM PDADMAC solutions at different pH ranging from 1-12 were added into 5 mg MWCNTs into a 100 mL beaker. The mixture solutions were sonicated at 100 percent power for 1 hour. In each period with different pH, the solution of MWCNTs were determined by UV-Vis spectroscopy.

### **3.4.3 Stability of MWCNTs dispersed with water - soluble polyaniline blend poly(sodium 4-styrenesulfonate, PSS)**

#### **3.4.3.1 Effect of functionalization times on the stability of MWCNTs**

The dispersion of MWCNTs with water - soluble polyaniline blend poly(sodium 4-styrenesulfonate, PSS) were prepared by dispersing 5 mg MWCNTs in 0.01 % of water - soluble polyaniline blend poly(sodium 4-styrenesulfonate, PSS) , solution. The mixture solutions were stored at room temperature for 24 hours and measured the turbidity by UV-Vis spectroscopy at wavelength 550 nm.

### **3.4.4 Characterization of MWCNTs dispersed with water - soluble polyaniline blend poly(sodium 4-styrenesulfonate, PSS)**

MWCNTs dispersed with water - soluble polyaniline blend poly(sodium 4-styrenesulfonate, PSS) have attracted interest because of their superior properties and unique features arising from MWCNTs dispersed with PDADMAC. The incorporation MWCNTs into the water - soluble polyaniline blend poly(sodium 4-styrenesulfonate, PSS) will significantly improve a lot more chemical and physical properties. In this study carried out so far, the preparation and the considerable

investigation were being studied. Several characterization techniques employed in this study is shown in Table 3.4.

Table 3.4 Characterisation techniques and their utilization of MWCNTs dispersed with water - soluble polyaniline blend poly(sodium 4-styrenesulfonate, PSS)

<b>Techniques</b>	<b>Information</b>
UV-Vis spectrometer	Absorption spectra
Transmission electron microscope	Surface morphology, nanostructure

### 3.5 Layer-by-layer self assembly of MWCNTs

#### 3.5.1 Chemical and materials

This experimental was conducted to fabricate the multilayer thin films of the different types of polyelectrolyte. The chemicals which were used for fabricate the multilayer thin films were shown below:

<b>No</b>	<b>Polyelectrolyte</b>	
	<i>Positive charges (+)</i>	<i>Negative charges (-)</i>
1	MWCNTs dispersed with Poly(diallyldimethyl ammonium chloride, PDADMAC	Poly(sodium 4-styrene sulfonate),PSS
2	Poly(diallyldimethyl ammonium chloride, PDADMAC	MWCNTs dispersed water - soluble polyaniline blend poly(sodium 4-styrenesulfonate, PSS)
3	MWCNTs dispersed with Poly(diallyldimethyl ammonium	Water - soluble polyaniline blend poly(sodium 4-styrenesulfonate, PSS)

	chloride, PDADMAC	
4	MWCNTs dispersed with Poly(diallyldimethyl ammonium chloride, PDADMAC	MWCNTs dispersed water - soluble polyaniline blend poly(sodium 4-styrenesulfonate, PSS)

Remark: All solution were prepared freshly before fabrication polyelectrolyte multilayer thin films.

NaCl was purchased from Aldrich Chemicals. The chemical was analytical grade and used without further purification. Aqueous solutions were prepared with doubly-distilled water.

### 3.5.1 Primer preparation

First, the freshly prepared glass slide substrate was functionalized with a layer of poly(diallyldimethyl ammonium chloride) and poly(sodium 4-styrene sulfonate) for 4 layers in order to generate the hydrophilic properties of the substrate. The functionalized glass slide substrates were negatively charged. It was expected that the deposition of primer should provide high charge density for glass slide substrate.

### 3.5.2 Layer-by-layer self assembly of MWCNTs with the different types of polyelectrolyte solution

The multilayer thin films were fabricated by a home build automated dipping machine. Multilayer thin films of polyelectrolyte were prepared by repeating the following step on the glass slide substrate n times:

Example: Preparation of MWCNTs dispersed with Poly(diallyldimethyl ammonium chloride) / Poly(sodium 4-styrene sulfonate) multilayer thin films.

Four layers of glass slide primer substrate was immersed in the MWCNTs dispersed with Poly(diallyldimethyl ammonium chloride) for 10 min then rinsing with buffer solution pH 8 to remove excess material. Then immersed alternately in the solution of Poly(sodium 4-styrene sulfonate) for 5 min and rinsing with buffer solution pH 8. Repeating all steps in order to get a multilayer films which a desired thickness.

(Remark: Other polyelectrolyte multilayer films were fabricated with the same procedure of MWCNTs dispersed with Poly(diallyldimethyl ammonium chloride) / Poly(sodium 4-styrene sulfonate) multilayer thin films)

Table 3.5 Characterisation techniques and their utilization of MWCNTs multilayer films

Techniques	Information
UV-Vis spectrometer	Absorption spectra
Atomic force microscopy	Surface morphology, thickness
Conductivity	Conductance

### 3.8 Characterization technique

#### 3.8.1 UV-Vis spectroscopy

A UV-Vis spectroscopy is a group of spectroscopic techniques where the transmission of light pass through a solution form of substance is studied. If light is absorbed, the radian power of light beam decreases. A UV-Vis spectroscopy consisting of a light source, a dispersive system combined in a monochromator and a detector. UV-Vis spectroscopy has the UV in the range of 200 – 400 nm and 400 – 800 nm in the visible range. This technique has a board range of applications in



chemistry, provides the information of the UV spectrum, light intensity and can be used to quantitate a light transmitted of a compound in a solution. This technique can be used for measure the % polymerization of polyaniline, absorbance of polymer thin films, dispersion of MWCNTs in polymer and optical sensor performances.

### **3.8.2 Transmission electron microscopy, TEM**

TEM is a microscopic technique used in the field of nanotechnology and development in many fields such as heterogeneous, catalysis and semiconductor devices. Typically, TEM requires the electron source to emit electrons from the top of the microscope pass through the vacuum column. The electromagnetic lenses are for focusing the electron into a thin beam, they are then focused onto the sample. The unscattered electrons are remained in the beam can be detected which results in the shadow image of the sample on the fluorescence screen or photographic film. Details of images can be studied with its different parts displayed in varied dark shade on the screen depending on the density of the material presents. This technique will be used for observe the dispersion of MWCNTs with polymer.

### **3.8.3 Scanning electron microscopy, SEM**

The SEM is one of the electron microscope instruments capable of producing high resolution image of the sample surface and analysis of the microstructural characteristic of solid specimen. The basic components of SEM are the lenses, electron gun, electron collector, visual and recording cathode ray tubes as well as the electronics with cathode ray tubes. This technique will be used for observe the surface of polymer multilayer thin films and MWCNTs.

#### **3.8.4 Fourier transform Infrared spectroscopy, FTIR**

FTIR is a technique which is used to obtain an infrared spectrum of absorption, emission, photoconductivity or Raman scattering of a solid, liquid or gas. FTIR is most useful for identifying chemicals that are either organic or inorganic. It can be utilized to quantitate some components of an unknown mixture. The resulting spectrum represents the molecular absorption and transmission, creating a molecular fingerprint of the sample. This technique will be used to analyze the functional groups of polymer under the process of polymerization.

#### **3.8.5 Atomic force microscopy, AFM**

Atomic force microscopy (AFM) or scanning force microscopy (SFM) is a very high-resolution type of scanning probe microscopy, with demonstrated resolution on the order of fractions of a nanometer. AFM provides a 3D profile of the surface on a nanoscale, by measuring forces between a sharp probe (<10 nm) and surface at very short distance (0.2-10 nm probe-sample separation). The probe is supported on a flexible cantilever. The AFM tip “gently” touches the surface and records the small force between the probe and the surface. The AFM has the advantage of imaging almost any type of surface, including polymers, ceramics, composites, glass, and biological samples. This technique will be used to analyze the surface morphology and thickness of multilayer thin films.

# CHAPTER IV

## RESULTS AND DISCUSSION

### 4.1 Synthesis and characterization of water-soluble polyaniline using interfacial polymerization method

The first part of this work, the preparation of water-soluble polyaniline from interfacial polymerization technique was investigated, in order to use as the polyelectrolyte for polymer thin film fabrication by layer-by-layer self assembly technique. Shown in Figure 4.1 is the scheme of the interfacial polymerization of polyaniline in the presence of poly(sodium 4-styrenesulfonate). The interfacial polymerization of polyaniline were investigated by a combination of two phases of aqueous and organic phases with aniline monomer dissolved in  $\text{CHCl}_3$  solution and the oxidizing agent ammonium persulfate, dissolved in an aqueous acid  $\text{HCl}$  solution with poly(sodium 4-styrenesulfonate), PSS as the blending solution.



Figure 4.1 Schematic representation the interfacial polymerization of water - soluble polyaniline blend poly(sodium 4-styrenesulfonate).

From the interfacial polymerization, protonated – polyaniline blend poly(sodium 4-styrenesulfonate) can be synthesized by controlling the influence of experimental conditions on the polymerization. The properties of polyaniline are affected by polymerization conditions, such as temperature, pH, time, and oxidant/monomer ratio. All parameters have also been widely studied.

1. The influence of synthetic temperature: In this experiment the effect of temperature onto the polymerization was controlled at 4°C. Generally, a decrease in polymerization temperature results in the higher yield and molecular weight of polymer product. Adam *et al.* [] found that the molecular weight of polyaniline increased from 19,400 Da at 18 °C to 86,000 Da at 4°C. Moreover, Stejska *et al.* [] reported that the molecular weight and conductivity of polyaniline increased as the reaction temperature was lowered.
2. The influence of pH: It is generally accepted that acid conditions are required for the polymerization of aniline and result in conjugated conducting polyaniline with higher yield and conductivity []. The pH of the oxidative polymerization of aniline by ammonium persulfate greatly affects the nature of product. The formation of polyaniline products have been recently reported by MacDiarmid [] and Stejskal [] when the oxidative polymerization of aniline is carried out at strong acidic conditions (pH>3), the polyaniline product was shown the high conductivity due to increasing the degree of protonation of the imine group of polyaniline. When the convention polymerization was diluted (at a pH of 3-4), the brown product formed []. This brown product had different morphology (hollow microspheres) and different optical and

magnetic properties. So in this experiment, the interfacial polymerization of polyaniline blend poly(sodium 4-styrenesulfonate) was carried out in pH 0.6.

3. The influence of time: There have been more studies on the effect of time onto the polymerization. Cao *et al.* [] have reported the effect of time onto the polymerization. The polymerization time was found to relate with the polymer yield and conductivity. The presence of high polymer yield and conductivity, when the polymerization time was carried out more than 24 hours. So in this experiment, the interfacial polymerization of polyaniline blend poly(sodium 4-styrenesulfonate) was carried out for the polymerization time more than 24 hours.
4. The influence of oxidant/monomer ratio: The initial molar ratio of the reactants used has a significant influence on the properties of polyaniline. Armes and Miller [] reported that the conductivity of polyaniline was independent on the ammonium persulfate/aniline ratio for oxidant/aniline molar ratios below 1; however the yield of polyaniline increased linearly up to a ratio of 1. Both yield and conductivity were decreased via over-oxidant of the polymer at higher oxidant/monomer initial concentration ratios. This study concluded that the most efficient ratio for polyaniline was about 1.15 or less. So in this experiment, the interfacial polymerization of polyaniline blend poly(sodium 4-styrenesulfonate) was carried out by controlling the oxidant/monomer concentration ratio on 0.5.

From the literature, the standard synthetic conditions were used to synthesis polyaniline in the presence of poly(sodium 4-styrenesulfonate) by interfacial polymerization. The conditions are listed in Table 4.1.

Table 4.1 The synthetic conditions for interfacial polymerization of polyaniline in the presence of poly(sodium 4-styrenesulfonate).

<b>Parameter</b>	<b>Control</b>
The influence of synthetic temperature	4°C
The influence of pH	0.6
The influence of time	24 hours
The influence of oxidant/monomer ratio	0.5

This experiment was focused on the polymerization of water-soluble polyaniline for used as the polyelectrolyte for polymer thin films fabrication using layer-by-layer self assembly technique. Poly(sodium 4-styrenesulfonate) was used as the blending solution for polyaniline formation. The idea of using PSS as the blending for polyaniline, due to PSS is a strong polyelectrolyte which completely dissociated in water so it can act as an anionic dopant and as the template for the formation of PANi with high dispersibility. So the effect of poly(sodium 4-styrenesulfonate) concentration was also investigated.

#### **4.1.1 Effect of poly(sodium 4-styrenesulfonate, PSS) concentration**

In this experiment, PSS was used to generate the water – soluble properties of polyaniline. The dispersible PANi.PSS was studied via the polymerization route with various PSS concentration of 3-200 mM with a fixed of standard synthetic condition (Table 4.1). The UV-Vis spectra of the water - soluble polyaniline blend poly(sodium 4-styrenesulfonate) with the different PSS concentration was showed in Figure 4.2.

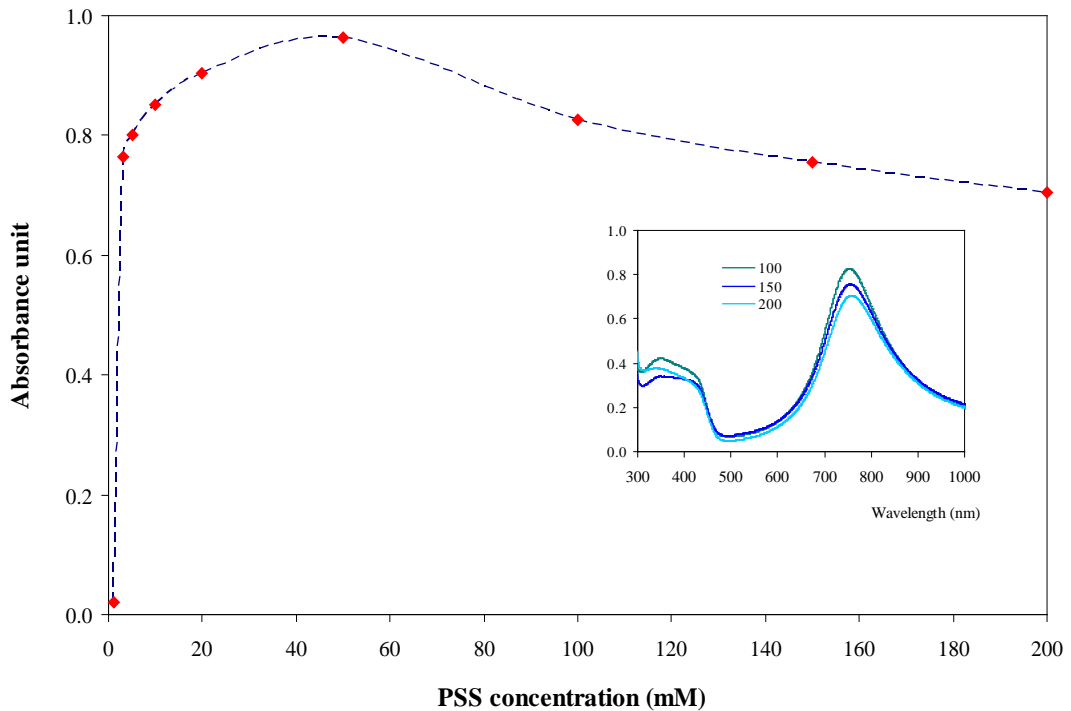


Figure 4.2 UV-Vis spectra of water - soluble polyaniline blend poly(sodium 4-styrenesulfonate) with the different PSS concentration 3-200 mM.

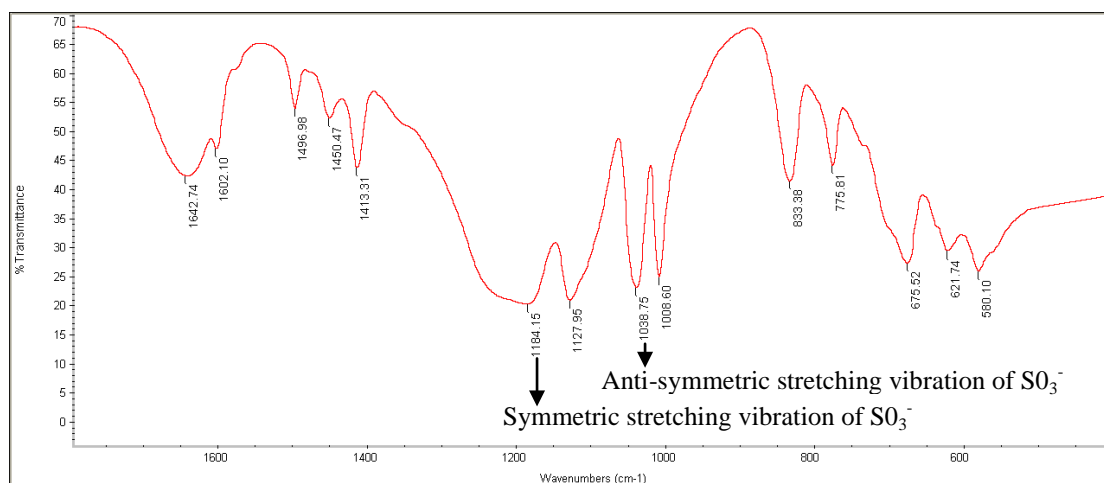
The resulting PANi.PSS was shown the good dispersion when the concentration of PSS more than 3 mM. Here, PSS acted as an anionic dopant and as the template for the formation of polyaniline with high dispersibility. The trend of the spectrums were found to increase with increasing the PSS concentration from 3 to 50 mM, then its decrease turns out to be slightly afterward when the PSS concentration increase from 100 to 200 mM. The formation mechanism of different concentration of PSS plays a vital role on polyaniline can be explained into two ways. The first, in the low PSS concentration (3 to 50 mM). The absorbance was found to increase due to the strong electrostatic interaction between  $-\text{SO}_3^-$  groups of PSS and  $(-\text{NH}_3^+)$  groups of polyaniline backbone. In the theoretical, PSS is a strong polyelectrolyte which completely dissociates into water and adopting a stretched. So, the anilinium cation

can be adsorbed completely through the electrostatic interaction onto a large amount of sulfonic groups of PSS. On the other hand, the increase in PSS concentration (100 to 200 mM) in aqueous phase was not shown the strong polymerization interaction but also shown the low polymerization interaction due to the influence of viscosity of PSS in aqueous phase [96]. The aniline monomer can be slightly to immersed and adsorbed at the sulfonate groups of PSS. So the polymerization yield was found to decreased.

In order to confirm the successful polymerization of water – soluble polyaniline in the presence of PSS by interfacial polymerization, FT-IR was used to analyze the functional groups of water - soluble polyaniline blend poly(sodium 4-styrenesulfonate). The FT-IR spectra of (a) pure poly(sodium 4-styrenesulfonate) and (b) pure polyaniline were shown in Figure 4.3 . The FT-IR spectrum of PSS (-a-) shows a characteristic peak at  $1,184\text{cm}^{-1}$  and  $1,037\text{ cm}^{-1}$  for the symmetric-stretching and antisymmetric-stretching vibration of  $-\text{SO}_3^-$  groups, respectively. The peak at  $1,127\text{ cm}^{-1}$  and  $1,008\text{ cm}^{-1}$  are attributed to in-plan skeleton vibration and in-plan bending vibration of the benzene ring, respectively. []



(a) Pure poly(sodium 4-styrenesulfonate)



(b) Pure polyaniline

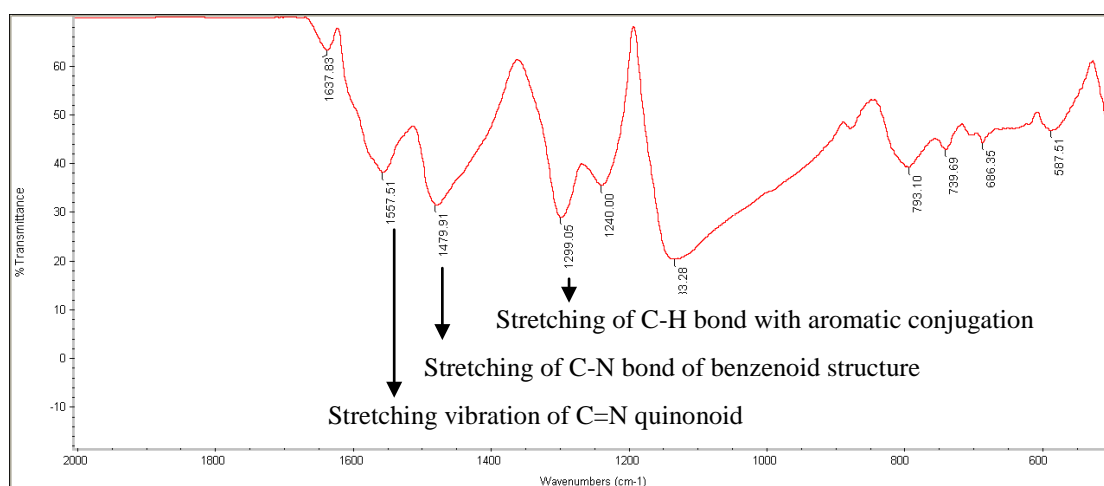


Figure 4.3 FT-IR spectra of (a) poly(sodium 4-styrenesulfonate) and (b) polyaniline.

As for the FT-IR spectra of pure polyaniline, the absorption peak observed at 1557, 1479 and 1299 cm<sup>-1</sup> corresponding to the stretching of C=N bond of quinoid structure, the stretching of the C-N bond of benzenoid structure and the stretching of the C-H bond with aromatic conjugation, respectively. []

(c) Water - soluble polyaniline blend poly(sodium 4-styrenesulfonate)

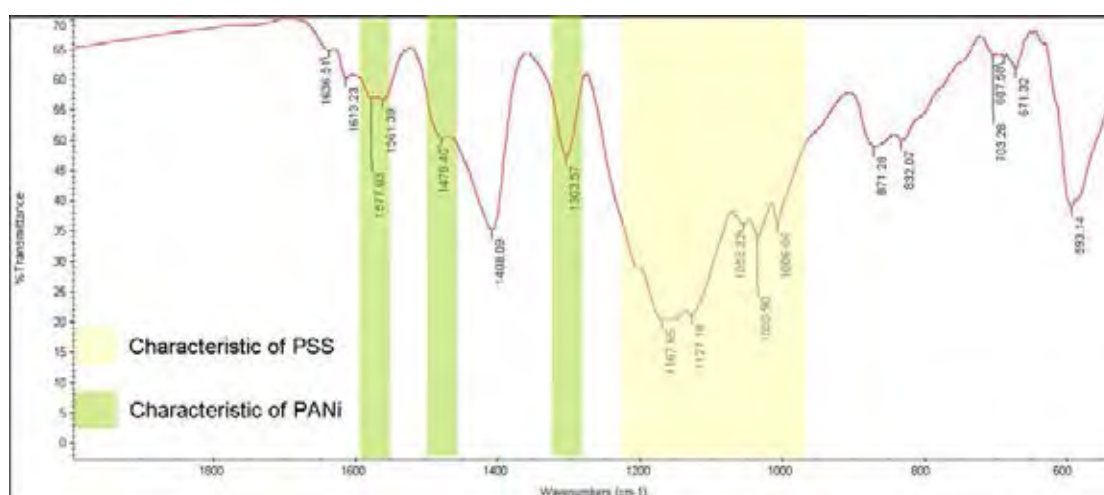


Figure 4.4 FT-IR of water - soluble polyaniline blend poly(sodium 4-styrenesulfonate) with the PSS concentration of 5 mM.

The FT-IR spectra of PANi:PSS with the different PSS concentration were shown in Figure 4.4. All characteristic absorbance peaks of pure poly(sodium 4-styrenesulfonate) and pure polyaniline could also be observed in the FT-IR spectra of water - soluble polyaniline blend poly(sodium 4-styrenesulfonate). The main characteristic absorption peaks of  $\text{SO}_3^-$  group are appeared around  $1,184, \text{cm}^{-1}$  and  $1,037 \text{ cm}^{-1}$  of all condition Aniline:PSS concentration ratio demonstrating the successful polymerization of polyaniline in the presence of PSS using interfacial polymerization. The characteristic symmetric-stretching and antisymmetric-stretching vibration peaks of  $\text{SO}_3^-$  group were observed at  $1,184 \text{ cm}^{-1}$  and  $1,037 \text{ cm}^{-1}$  in all curves of Figure 4.4 and are consistent with the increasing concentration feed ratio of Aniline:PSS concentration.

In conclusion: Water - soluble polyaniline blend poly(sodium 4-styrenesulfonate) was synthesized by interfacial polymerization. The influence of the range of experimental

conditions on the polymerization on the characterization of PANi.PSS conducting polymer was systematically investigated in order to achieve the optimal conditions. Optimization studied of the interfacial polymerization polymerization of PANi.PSS reveal that the experimental conditions such as temperature, pH, oxidant concentration, polyelectrolyte concentration and polymerization time have a dramatic effect on the properties of PANi.PSS. All of the polymerization parameters were shown in Figure 4.5.

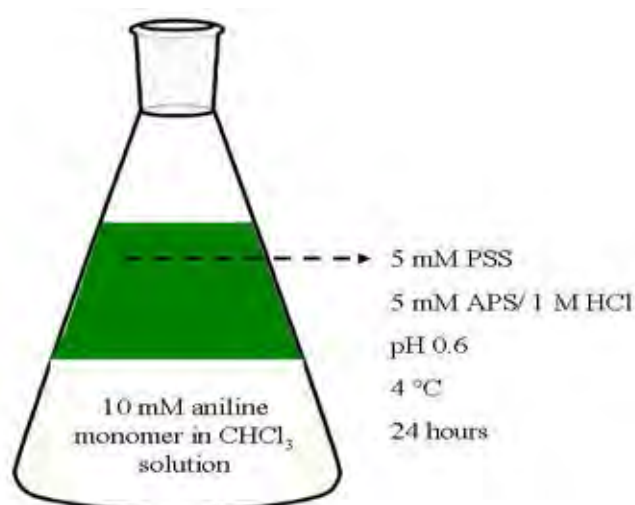


Figure 4.5 The optimum conditions to synthesis water-soluble polyaniline blend poly(sodium 4-styrenesulfonate)

#### **4.2 Layer-by-layer self assembly of water – soluble polyaniline blend poly(sodium 4-styrenesulfonate)**

The layer-by-layer polymer multilayer thin films were mostly performed in aqueous solution in order to fabricate the homogeneous thin film. In this study, layer-by-layer polymer multilayer thin films were prepared from two kinds of water - soluble polyelectrolyte, which have two different electroactive groups. The first polymer was anionic, PANi.PSS, which was synthesized by interfacial polymerization

method. Another polymer was cationic, poly(diallyldimethyl ammonium chloride, PDADMAC). The layer-by-layer polymer multilayer thin films were formed by the alternating deposition of the positively charged of polyelectrolyte between PANi.PSS and PDADMAC. The electrostatic attraction between the sulfonic group of PANi.PSS and quaternary ammonium group of PDADMAC could be fabricated the polymer multilayer thin films.

#### 4.2.1 Effect of dipping time onto the film fabrication

The one parameter which can used to control the growth of polymer multilayer thin films are the dipping time. Because the adsorption of polymer at the thin film water interface is controlled by a diffusion process time play a major role in the formation of the multilayer.

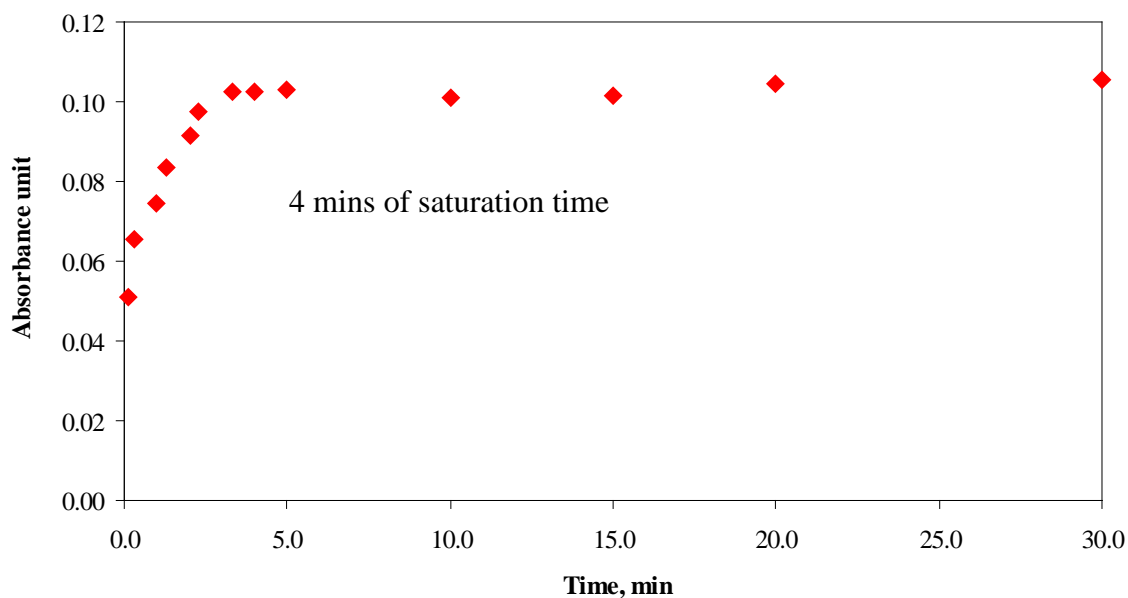


Figure 4.6 The plot of the dipping time of (PANi.PSS/PDADMAC) multilayer thin film

Effect of dipping time onto the assemblies of PANi-PSS/PDADMAC multilayer thin films were shown in Figure 4.6. When the 5 layers of positively-charged hydrophilic substrate was dipped in a PANi.PSS solution, the electrostatic interaction are sufficient to allow a complex to be formed within 10 sec. While the deposition occurs, the surface charge becomes less positive and more negative as more polycation PANi.PSS adsorb on the surface. The absorbance was found to increase from 10 sec to 4 min which suggests the quick adsorption of polyaniline onto the glass substrate. Afterward, the trend was found to be stable when the dipping time increases from 5 to 30 min. This means, when the surface is completely coated with the PANi.PSS the adsorption is stopped due to the electrostatic repulsion.

#### **4.2.2 Effect of pH onto the film fabrication**

The pH-controlled layer-by-layer assembly of polyelectrolytes provides enormous flexibility in controlling both the molecular organization and properties of polyelectrolyte multilayer thin films. With suitable adjustment of pH of the PANi.PSS solution, it is possible to manipulate dramatically the molecular organization, composition, surface properties and chemistry of the multilayer assemblies created by this process. This experiment was carried out by adjusting the pH of PANi.PSS solution in the pH range 6 to 10 by fixing the % weight concentration of each polymer solution. The UV-Vis spectra of PANi.PSS in different subphases were shown in Figure 4.7.

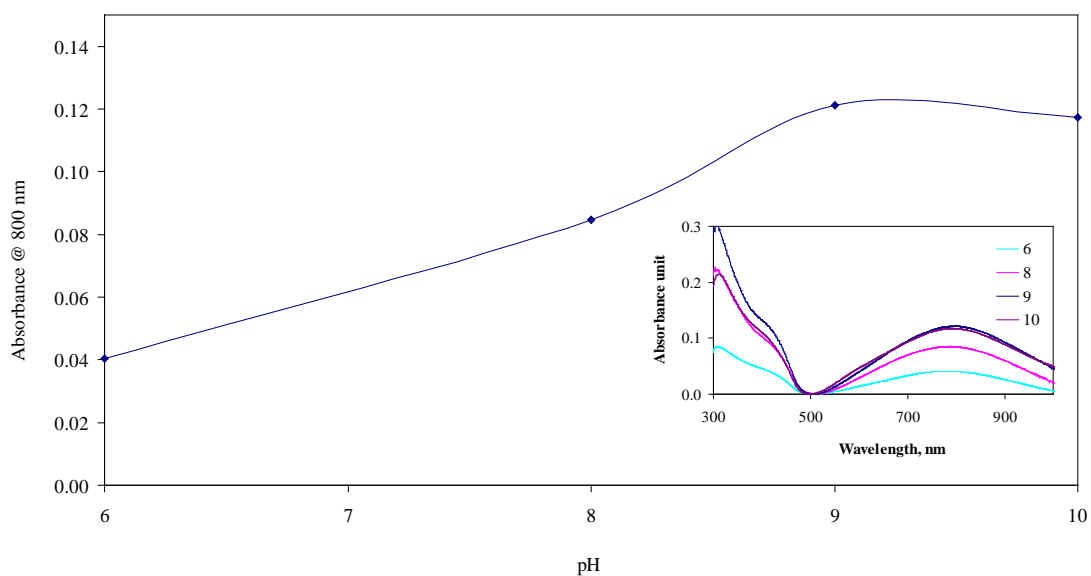


Figure 4.7 The plot of the effect of pH onto the (PANI.PSS/PDADMAC) multilayer thin film fabrication. Insert graph shown the normalized plot of the pH onto the assemblies of (PANI.PSS/PDADMAC) multilayer films.

The trend of progressive deposition in each pH onto the LbL self assembly of (PANI.PSS/PDADMAC) multilayer films is observed. It is interesting to observe that the absorption peak was found increased with increasing the pH of PANi solution from 6 to 9. The maximum absorption peak was found at pH 9. The appearance of the high deposition at pH 9 is due to high charge density of PANi.PSS solution. Then the pH trend was found to decrease a little bit to pH 10. PANi.PSS was completely ionized at pH 9, ( $pK_a = 9$  [ ]) and could be act as the anionic polyelectrolyte for film assembly. The charge carrier density or charge density is defined as the average number of ionic sites per monomer unit. The distribution of ionic site along the chain can also influence of polyelectrolyte properties significantly.

#### 4.2.3 Effect of NaCl concentration onto the film fabrication

##### A. Effect of NaCl concentration in PANI.PSS solution onto film fabrication

Polyelectrolyte multilayers are made by the alternating adsorption of oppositely charged polymer. NaCl, in the solution contacting the multilayer, is known to participate in many aspects of polyelectrolyte multilayer formation and function. Figure 4.8 showed the plot and picture of the films corresponding to various added amount of NaCl in the PANi.PSS solution.

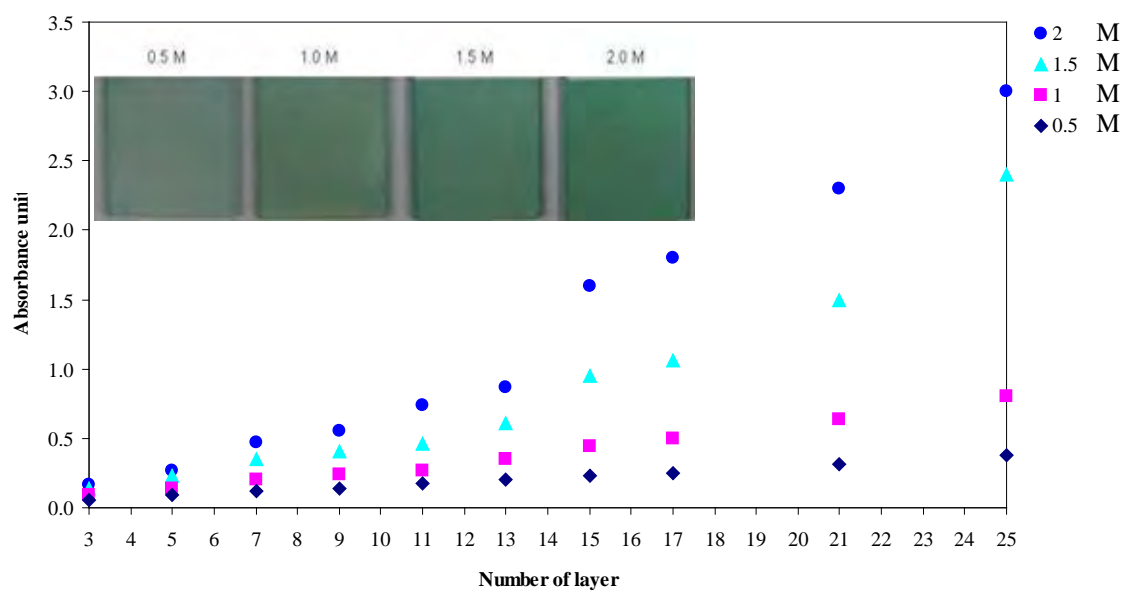


Figure 4.8 Effect of NaCl concentration in PANi.PSS solution onto the assemblies of (PANi.PSS/PDADMAC) multilayer films, insert graph show the picture of PANi.PSS films at various NaCl concentration of 0.5, 1.0, 1.5 and 2.0 M when fix the number of layer at 9.

It can be seen that when increasing the NaCl concentration from 0.5 to 2.0 M, the film appeared greener, with display the high absorbance at 2 M NaCl added. When adding NaCl in the solution, two majors effects including the kinetic of adsorption and the saturation level of polymer onto the film were observed. The initial increase in saturation can be explained by the decrease in electrostatic repulsion of the PANi.PSS solution adsorbed onto the surface. The salt ions play a screening role which cancel the repulsion of the PANi.PSS having the same charge and therefore, decrease the bjerum length. The decrease in repulsion between adsorbed polymer led to an increase in packing of polymer and therefore, more efficient adsorption of the polymer.

#### **B. Effect of NaCl concentration in PDADMAC solution onto the film fabrication**

Normally, the salt concentration is expected to increase the content of free site in the polyelectrolyte multilayer complex. Not only in the PANi.PSS, polyanionic sources but also in PDADMAC, polycationic source was investigated. In this studied, the influent of NaCl with have the concentration of 0.2, 0.5, 1.0 and 2.0 M were feed in various PADADMAC concentration of 5, 10 and 50 mM. Typical results are shown in Figure 4.9.



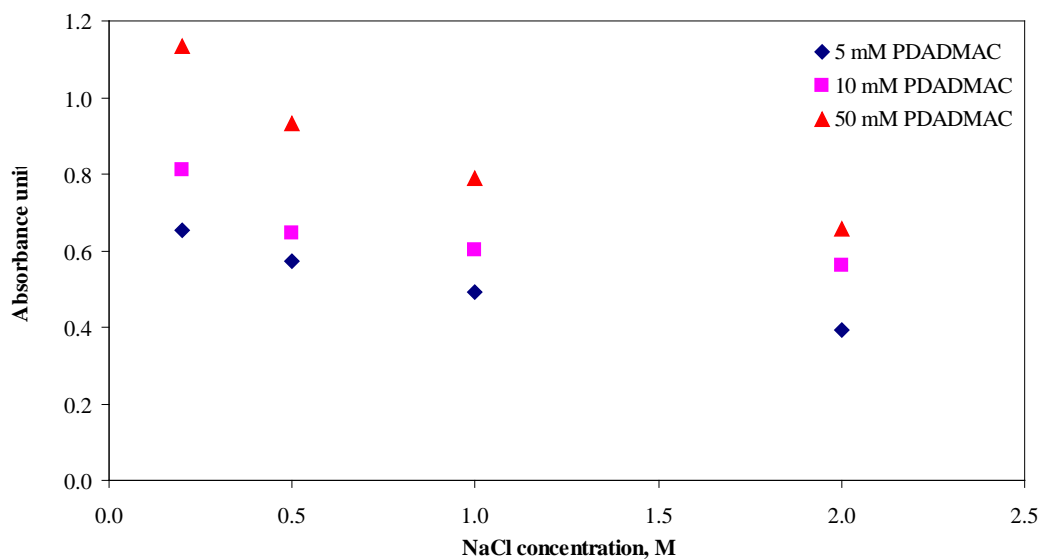


Figure 4.9 Plots of the changes in absorbance of the (PANI.PSS/PDADMAC)<sub>9lys</sub> multilayer films of various NaCl concentration in 5, 10 and 50 mM PADADMAC solution

The results are the changes in absorbance of (PANI.PSS/PDADMAC)<sub>9lys</sub> multilayer films with NaCl concentrations were increased from 0.2, 0.5, 1.0 and 2.0 M in various PADADMAC concentration of 5, 10 and 50 mM. It can be seen that the kinetic of adsorption display the maximum at the NaCl concentration of 0.2 M and then when further increasing NaCl concentration from 0.5, 1.0 and 2.0 M, the kinetic adsorption of (PANI.PSS/PDADMAC)<sub>9lys</sub> multilayer films appeared decreases. Figure 4.10 - 4.12 were used to investigated the reason, why the desorption of polymer are decrease when increase the NaCl concentration in PDADMAC solution.

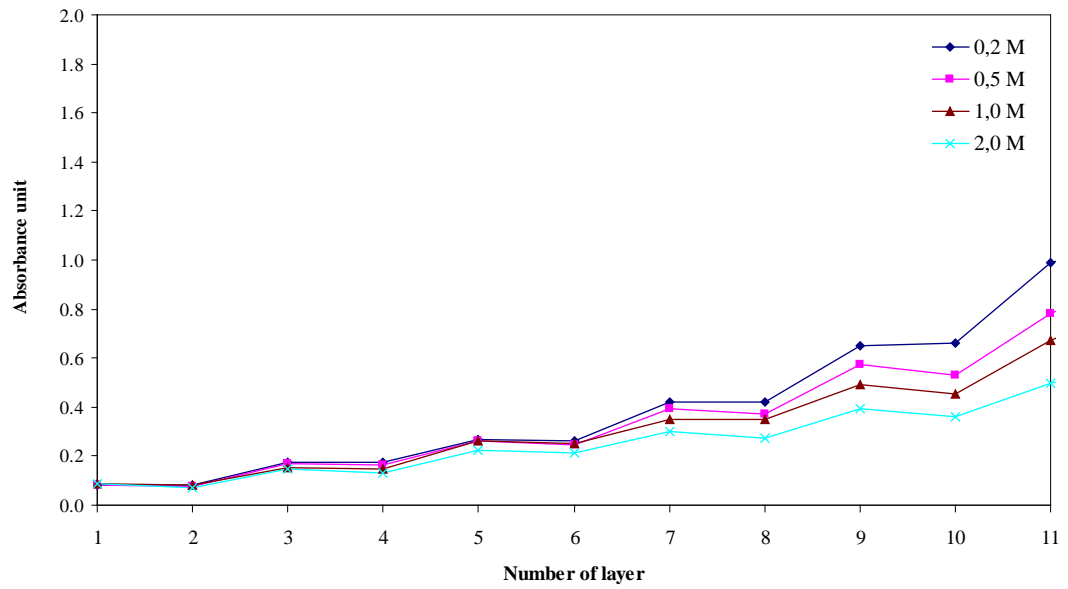


Figure 4.10 Effect of NaCl concentration in 5 mM PDADMAC solution.

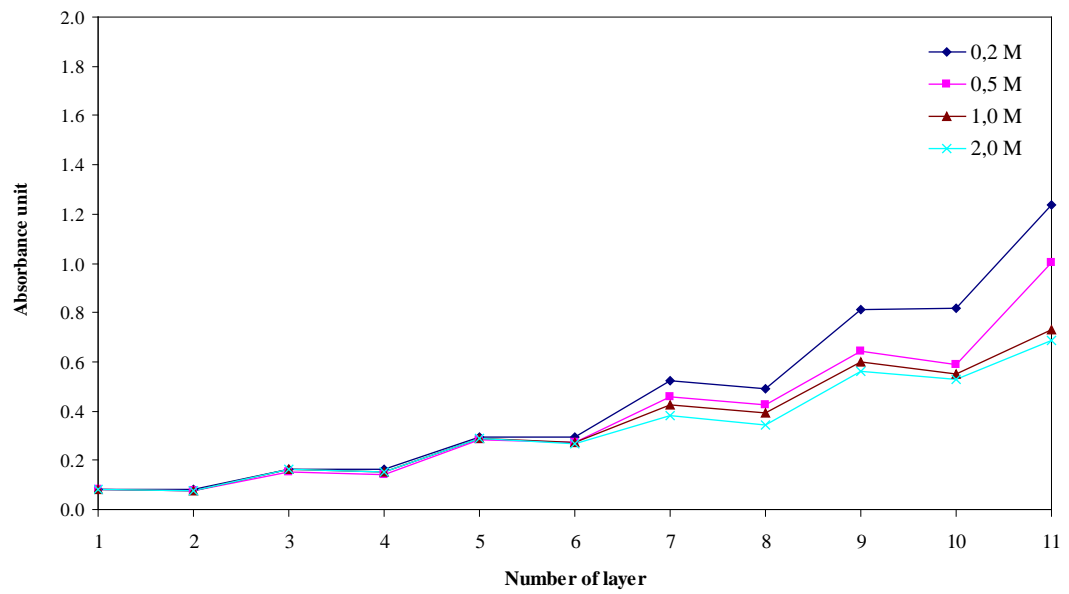


Figure 4.11 Effect of NaCl concentration in 10 mM PDADMAC solution.

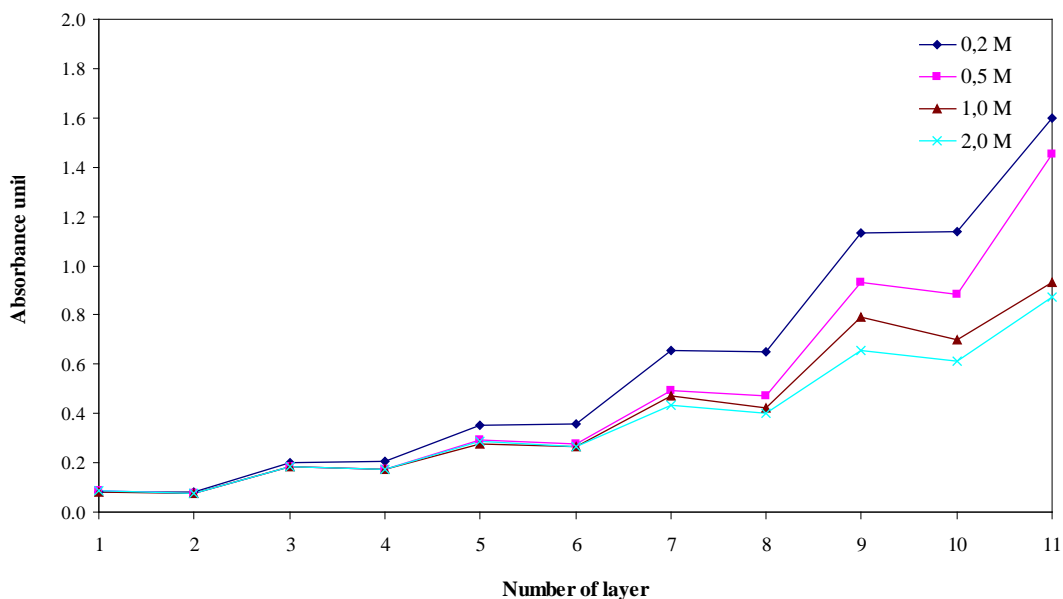


Figure 4.12 Effect of NaCl concentration in 50 mM PDADMAC solution.

Figure 4.10 - 4.12 shown the plot of the change in absorbance of PANi.PSS and PDADMAC thin film by vary the number of layer. Of each PDADMAC concentration, when increase NaCl concentration the polymer films were started to dissociate with the desorption. Loss of an intact multilayer on immersion in 2.0 M NaCl was more rapid. The dissociation of PANi.PSS from PDADMAC is caused by salt ion successfully challenging polymer/polymer segment ion pairs. The degree of extrinsic compensation required for the polymer/polymer interaction to be weakened to the point that the multilayer decomposes is similar to the concept to the minimum charge density on the polyelectrolyte for multilayer formation.

#### 4.2.4 Effect of Aniline:PSS concentration feed ratio for fabricated of polymer multilayer thin films

The different aniline:PSS concentration feed ratio solution of 10:3, 10:5, 10:10, 10:20, 10:50, 10:100, 10:150 and 10:200 mM from interfacial polymerization was used to prepare the polymer thin film. The glass substrate which have 5 layers of positively-charges hydrophilic was immersed into PANi.PSS solution for 5 min/layer. The performance of polymer thin films were investigated by UV-Vis spectroscopy. The absorption spectra for the (PANi.PSS/PDADMAC)<sub>5lys</sub> polymer films was shown in Figure 4.13.

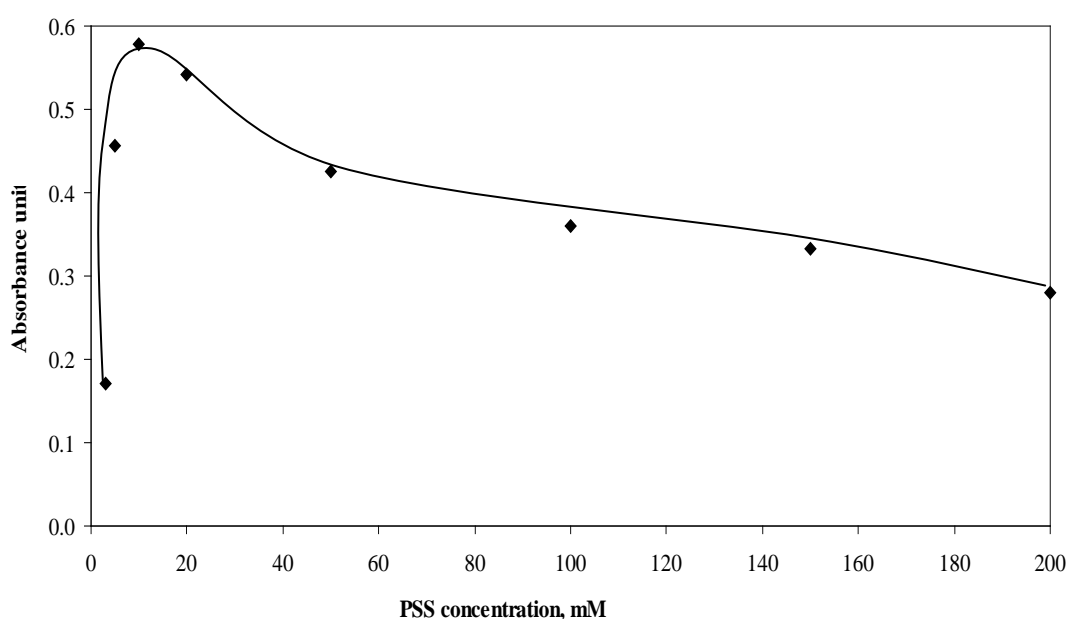


Figure 4.13 The changes in absorbance of (PANi.PSS/PDADMAC)<sub>5lys</sub> multilayer films at various concentration feed ratio of PANi-PSS 10:3, 10:5, 10:10, 10:20, 10:50, 10:100, 10:150 and 10:200 mM.

The clear trend of progressive deposition in each aniline:PSS concentration feed ratio solution is observed. It is interesting to observe that each polymer concentration

feed ratio led to different loading of polymer onto the substrate. Here, the absorption peaks were found increased with increasing the polymer concentration feed ratio from 3 to 10 mM. The maximum absorption peak was found at 10 mM. Then the trend was found to decrease from 20 mM to 200 mM. This difference is mostly due to;

- 1) At the concentration feed ratio of aniline:PSS of 10:3, 10:5 and 10:10 mM, the higher growth rate is due to a strong interpenetration between the oppositely charged polymer layer.
- 2) At the concentration feed ratio of aniline:PSS of 10:20, 10:50, 10:100, 10:150 and 10:200 mM, the appearance of deposition was found to decrease due to the excess of PSS polymer striking onto the surface is probably due to unreacted PSS which were blended in the solution with polyaniline.

In order to confirm the effect of competition of two different polymer species in the solution. This part was studied the effect of competition by: 100 mL of 10:3 PANi.PSS was mixed with the different concentration of PSS from 5, 10, 20, 50, 75 and 100 mM. The solutions were used to fabricate the polymer thin film by immersed the 5 layers of positively-charged hydrophilic primer in the polymer solution. The result was shown in Figure 4.14. The inset shows the plot of the PSS concentration versus the absorbance at  $\lambda_{max}$  of each condition.

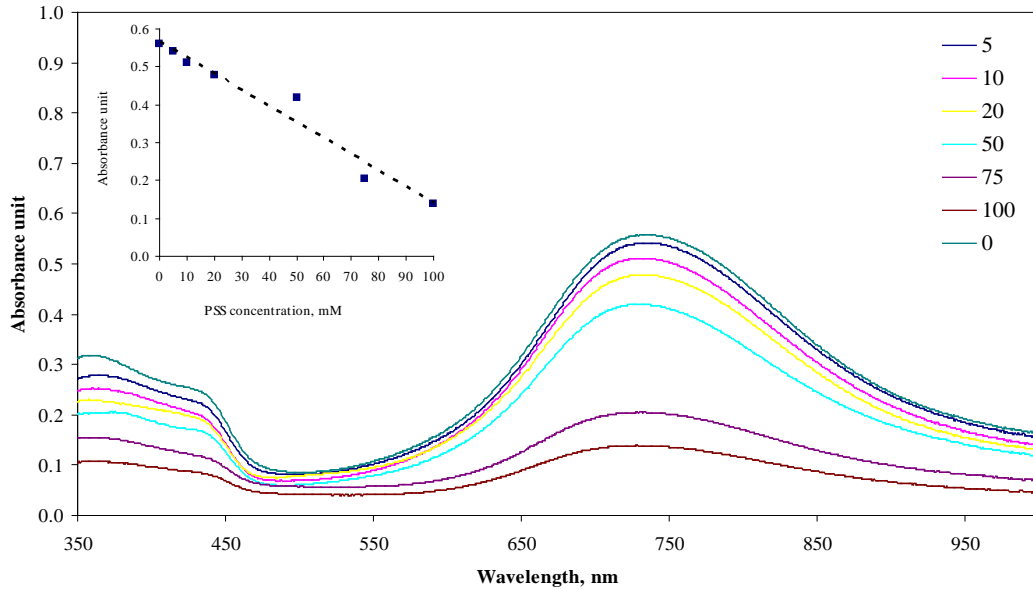


Figure 4.14 Competition study of Layer-by-Layer polymer multilayer thin films

Experiments show that, the trend was found to decrease when increase the PSS concentration. The amount of PSS added was obstructed the polyaniline striking onto the surface of substrate. In the present experiment, one can control the rate of deposition in multilayer film by controlling the amount of polymer excesses into the solution. Figure 4.15 was shown the electrical properties of the PANi.PSS multilayer films. In this experimental, the different PANi-PSS concentration feed ratio of 10:3, 10:5, 10:10, 10:20, 10:50, 10:100, 10:150 and 10:200 mM from interfacial polymerization were used as the sources of anionic polyelectrolyte for film fabrication. The polymer films were fabricated by LbL self assembly by reacting the anionic polyelectrolyte with the PDADMAC cationic polyelectrolyte. The electrical properties was measured by four point probe set-up.

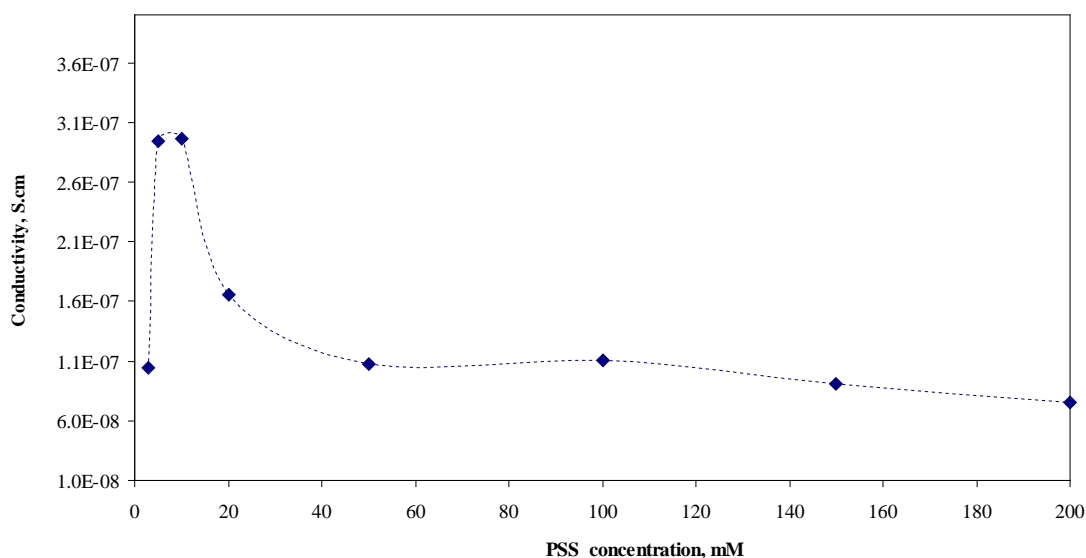


Figure 4.15 The changes in conductivity of (PANI-PSS/PDADMAC)<sub>211ys</sub> multilayer films at various concentration feed ratio of PANi-PSS.

The results showed that, the conductivity of the polyaniline multilayer thin films increase as the PSS concentration is stepped from 3 mM to 10 mM and decrease as the conductivity is stepped of PSS concentration from 20 mM to 200 mM. The conductivity of aniline:PSS concentration feed ratio of 10:5 mM is much highest than the other assemblies. The decrease in conductivity of polymer thin films of aniline:PSS concentration feed ratio of 10: 10 to 10:200 mM is to correlate with the insulated of PSS. Generally, PSS behaves like an electronic insulator, the insulating form of PSS was disrupted, resulting in a decrease conductivity. And moreover, the excess PSS polymer sticking onto the surface is probably due to unreacted polyaniline polymerized which were mixed in the solution with PANi.PSS.

#### 4.2.5 Effect of number of layer onto the film fabrication

One of the simplest methods for the control of the growth of multilayered thin film is to vary the number of layer. In this case the main parameter which are the type

of polyelectrolyte, the ionic strength of solution, the concentration of polyelectrolyte and the dipping time are kept constant. Table 4.2 shown the parameters for polyaniline multilayered thin film fabrication.

Table 4.2 The summarization parameters to fabricate the polyaniline multilayered thin film

No	Parameters	Fixed condition
1.	Polyaniline blend poly(sodium 4-styrene sulfonate)	Aniline:PSS ratio 10:5 mM
2.	PDADMAC concentration	10 mM
3.	NaCl in polyaniline blend poly(sodium 4-styrene sulfonate) solution	2.0 M
4.	NaCl in PDADMAC solution	0.2 M
5.	pH	6
6.	Dipping time	5 min

The increase in absorbance values of (PANi.PSS/PDADMAC)<sub>lys</sub> multilayer films as the function of number of deposition polyaniline blend poly(sodium 4-styrene sulfonate) and PDADMAC layers was shown in Figure 4.16. It can be seen that after the deposition of a few layer (1-13) the increase in absorbance is constant for each deposition step because the amount of polymer being deposited for each dipping cycle is constant. The step increment is the function of the system parameter and is constant if the system parameter are kept constant. This provide a very convenient method to control the thickness of the films.



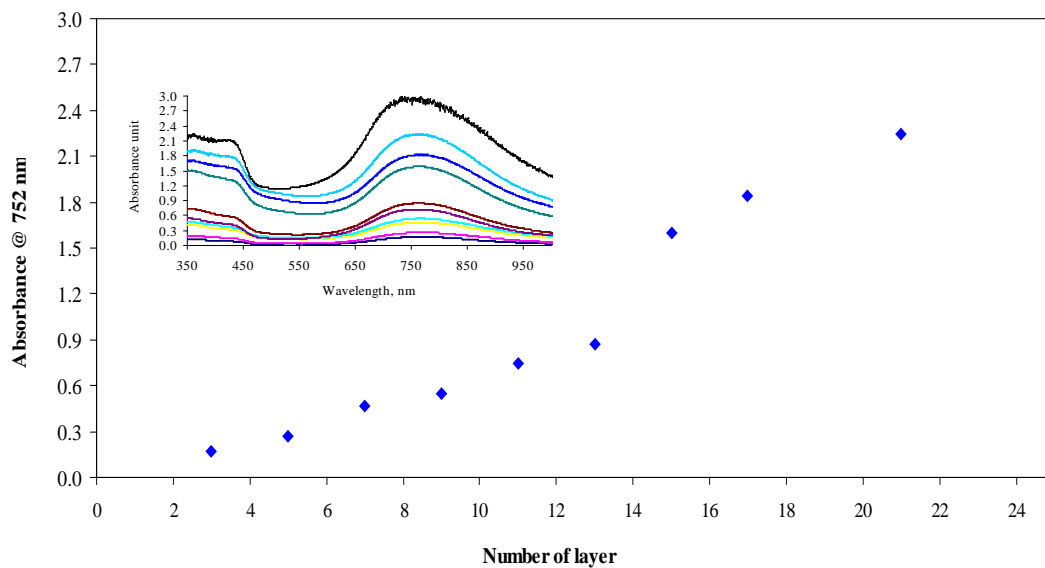


Figure 4.16 The absorbance value as the function of number of (PAni.PSS/PDADMAC)<sub>lys</sub> multilayer films.

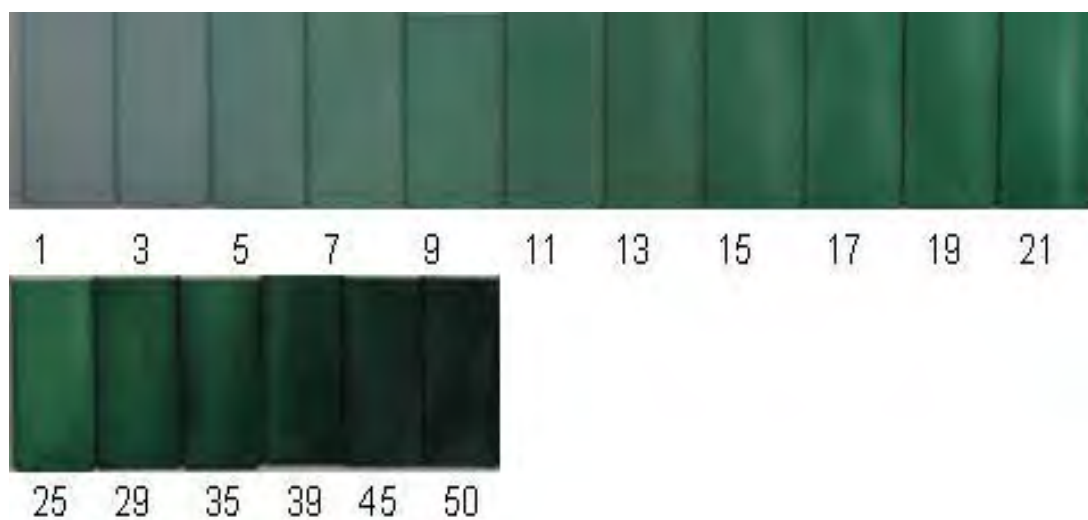


Figure 4.17 Representative digital picture images of assembled (PAni.PSS/PDADMAC)<sub>lys</sub> multilayer films.

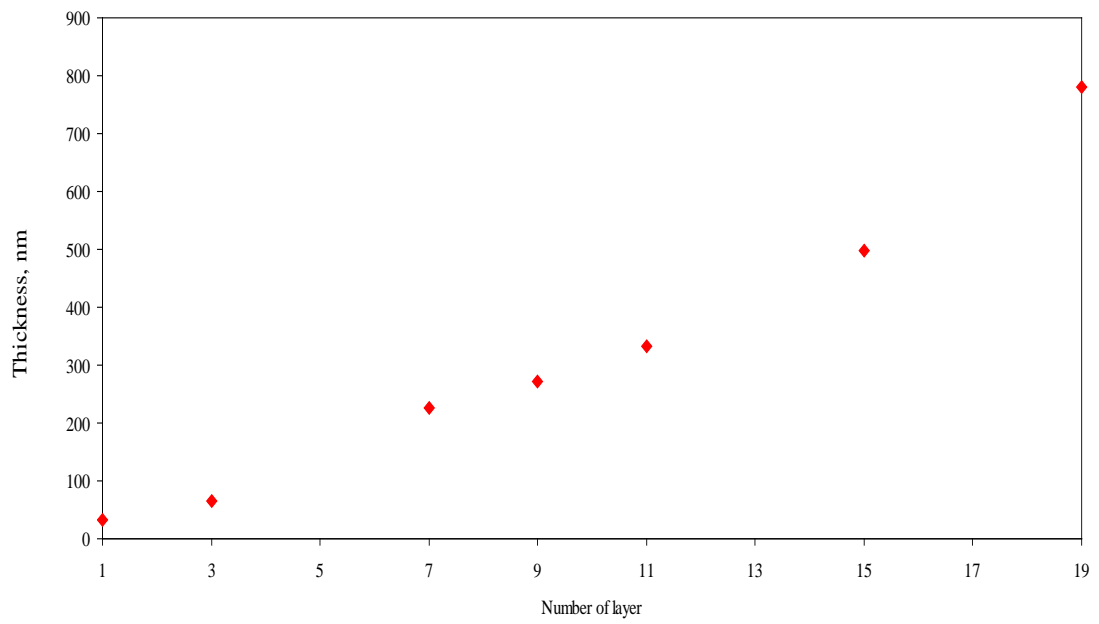


Figure 4.18 Thickness of (PANI.PSS/PDADMAC)<sub>lys</sub> multilayer films

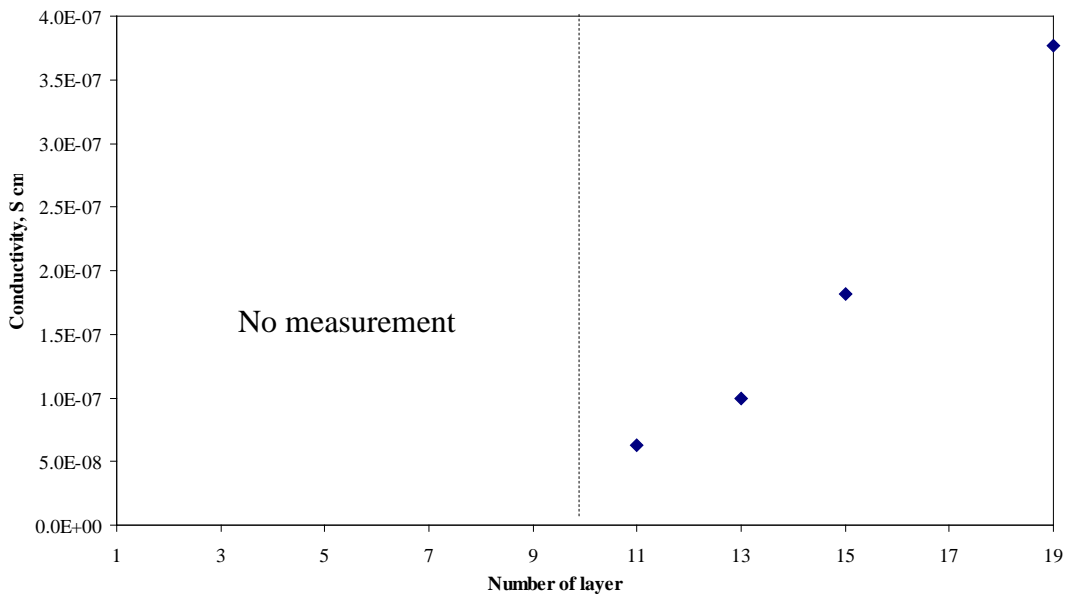


Figure 4.19 Conductivity of the (PANI.PSS/PDADMAC)<sub>lys</sub> multilayer films

Figure 4.18 was shown the thickness of (PANI.PSS/PDADMAC)<sub>lys</sub> multilayer films. It can be seen that the thickness of polymer thin film as the function of number

of layer for (PANI.PSS/PDADMAC)<sub>lys</sub> multilayer deposition on glass substrate. The thickness of multilayer films of polyaniline was found in the range of 50-800 nm when the number of layer varied from 1-19 layers. Figure 4.19 shows the electrical conductivity of doped (PANI.PSS/PDADMAC)<sub>lys</sub> multilayer films. It was indicated that the electrical conductivity of the polymer films increased with increasing the number of layer. The 19 layers had appreciable conductivity  $3.7 \times 10^{-7}$  S/cm after doped with 1.0 M HCl for 2 hours. This was a direct result of the conversion of the emeraldine base form to the emeraldine salt form, which is highly  $\pi$ -conjugated system

#### 4.4 Sensing properties of polyaniline multilayer films and water - soluble polyaniline solution

Recently, polyaniline have been used to prepare optical pH sensors. In this experiment PANI.PSS solution from interfacial polymerization and (PANI.PSS/PDADMAC) multilayer films from layer-by-layer self assembly were used to investigate the optical pH sensors. Figure 4.20 shown the electronic absorption spectra of polyaniline solution in different pH.

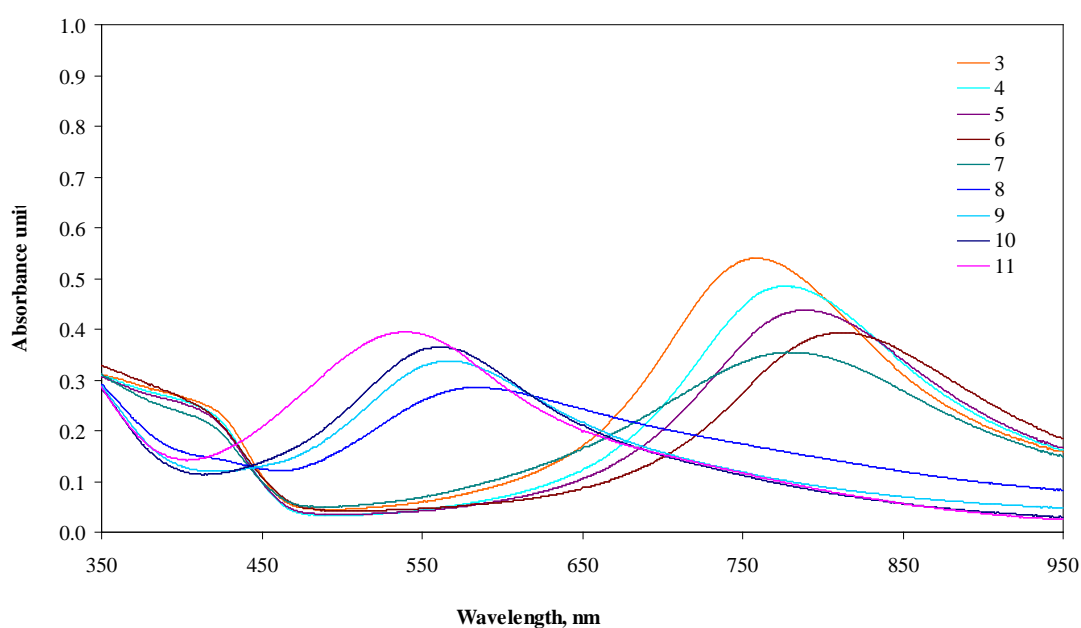


Figure 4.20 Electronic absorption spectra of polyaniline solution in different pH

The effect of pH on the change in electronic spectrum of polyaniline polymer can be explained by the different degree of protonation of the imine nitrogen atoms in the polymer chain. The electronic spectra of polyaniline in different pH are shown in Figure 4.20. The polyaniline solution are rendered fully deprotonated with  $\lambda_{max}$  542 nm (pH 11). When the solution was treated with different pH buffer solution, they are protonated and  $\lambda_{max}$  were shifts to 761 nm (pH 3). During protonated/deprotonated reaction, a reversible color change from green to blue to purpus are observed. This

reversible color change is a typical characteristic of polyaniline solution. Figure 4.21 is a graph of  $\lambda_{\max}$  of polyaniline solution versus pH. In pH range 3-6 and 8-11,  $\lambda_{\max}$  change gradually. However, in pH region of 6-8,  $\lambda_{\max}$  change rapidly with the pH. The wavelength is observed between 3-11; therefore it is possible to measure solution pH by monitoring  $\lambda_{\max}$ .

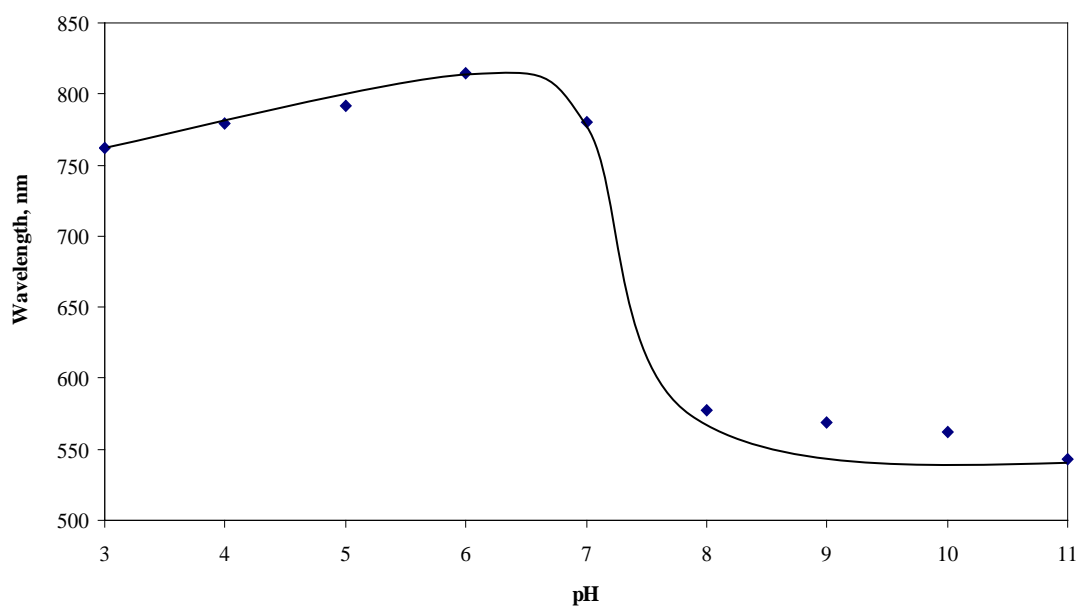


Figure 4.21 The relationship between  $\lambda_{\max}$  and solution pH

Another alternative method of optical pH sensing using polyaniline solution is to monitor absorbance at  $\lambda_{\max}$ . A sigmoidal shape curve is obtained for absorbance change versus pH. Figure 4.22 was shown the absorbance change of polyaniline solution vs pH at 762 and 545 nm. The dynamic range was from 3-11. The appearance pKa is used to describe the sensor response. The appearance pKa is defined as the pH where response is half way between the minimum and maximum values, representing a distribution of pKa's of polyaniline with varied length and different structure. The pKa of water-soluble polyaniline blend poly(sodium 4-styrene sulfonate) solution is 7.73.

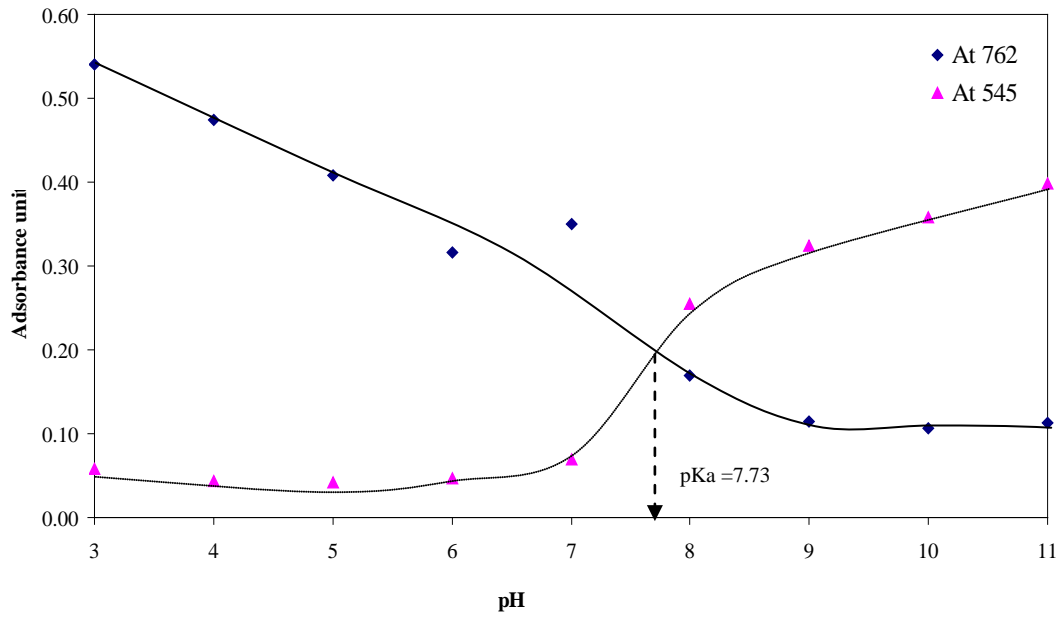


Figure 4.22 The absorbance change of polyaniline solution vs pH at 762 and 545 nm

In order to compare the efficiency of optical pH sensors of polyaniline, the  $(\text{PANi.PSS/PDADMAC})_{15}$  multilayer films were used to investigate the pH sensor performance.

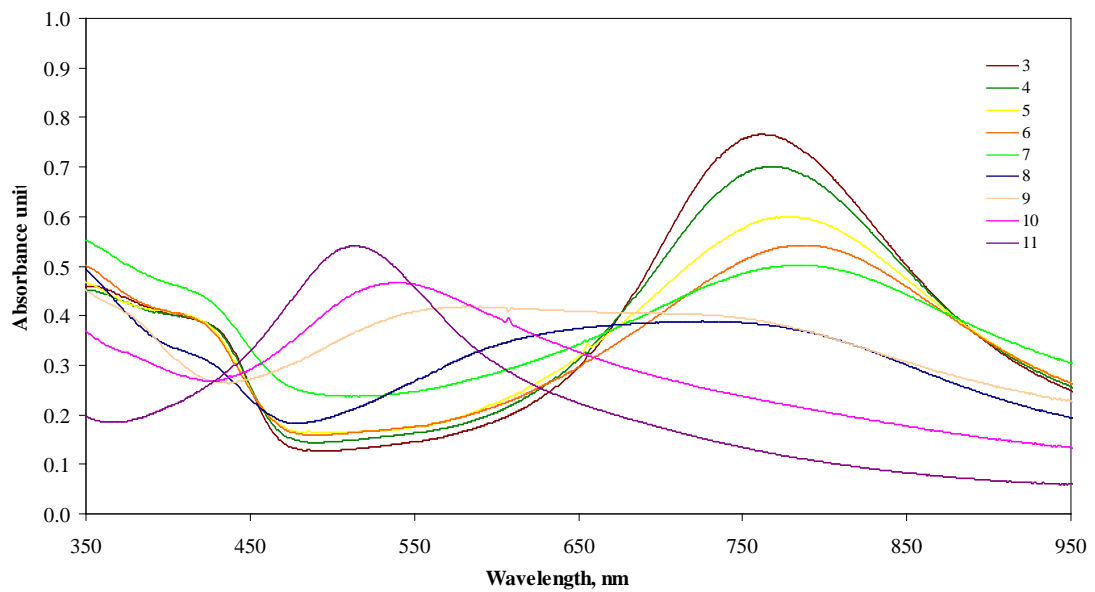


Figure 4.23 Electronic absorption spectra of  $(\text{PANi.PSS/PDADMAC})_{15}$  multilayer in different pH.

The electronic absorption spectra of  $(\text{PANI.PSS/PDADMAC})_{\text{lys}}$  multilayer in different pH was shown in Figure 4.23. The  $(\text{PANI.PSS/PDADMAC})_{\text{n}}$  multilayer film are rendered fully deprotonated with  $\lambda_{\text{max}}$  514 nm (pH 11). When the solution was treated with different pH buffer solution, they are protonated and  $\lambda_{\text{max}}$  were shifts to 765 nm (pH 3). The acid form of this polymer has much higher absorbance than its basic form. This implies that the acid form of the polymer absorbs the emission of the UV light source more efficiently and will give optimal sensitivity for the colorimetric measurement. Figure 4.24 was shown the relationship between  $\lambda_{\text{max}}$  of  $(\text{PANI.PSS/PDADMAC})_{\text{lys}}$  multilayer films vs solution pH. In pH range 3-7 and 10-11,  $\lambda_{\text{max}}$  change gradually. However, in pH region of 7-10,  $\lambda_{\text{max}}$  change rapidly with the pH.

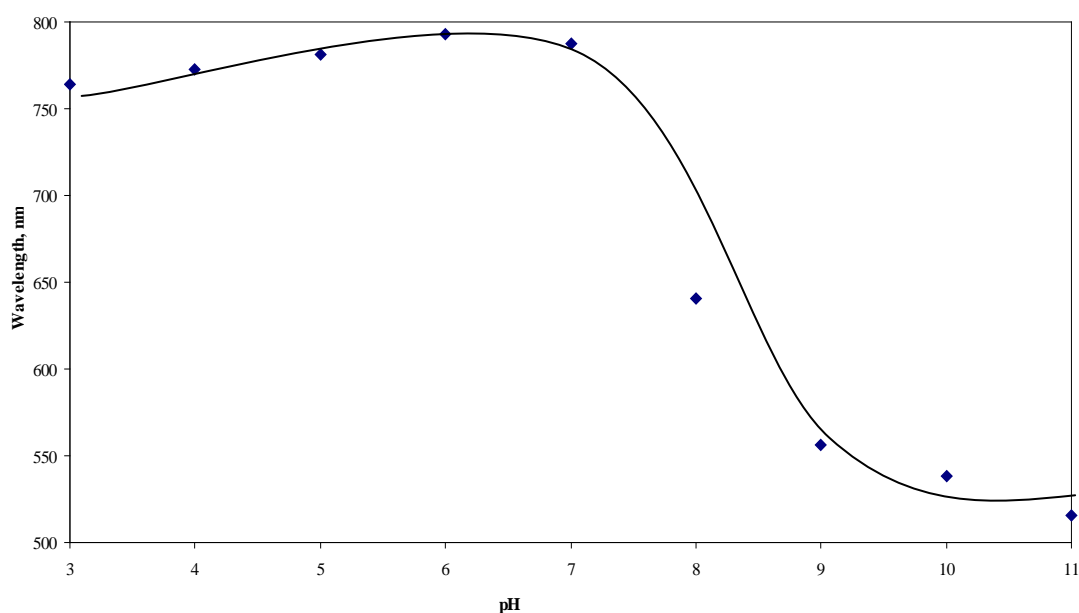


Figure 4.24 The relationship between  $\lambda_{\text{max}}$  and solution pH of  $(\text{PANI.PSS/PDADMAC})$  multilayer

By considering the sigmoidal shape of  $(\text{PANI.PSS/PDADMAC})_{\text{n}}$  multilayer films in Figure 4.24. It can be seen that, the pKa value was found at 8.69.

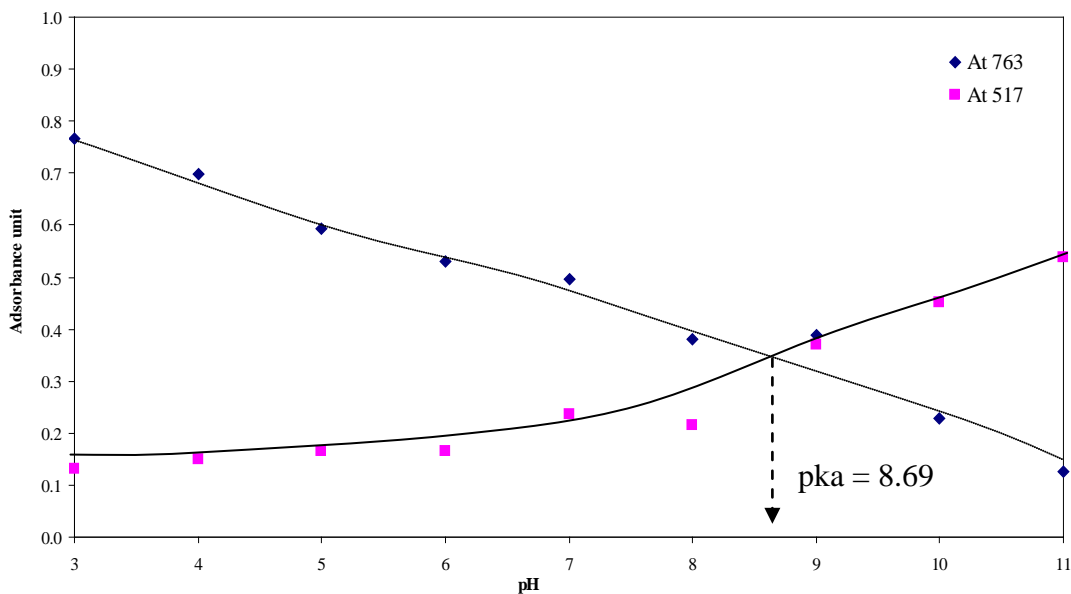


Figure 4.25 The absorbance change of (PANI.PSS/PDADMAC) multilayer vs pH at 763 and 517 nm.

In conclusion, the pH sensing of the water - soluble polyaniline blend poly(sodium 4-styrene sulfonate) solution and (PANI-PSS/PDADMAC)<sub>n</sub> multilayer films were shown the reversible color change from 3 to 11. By monitoring the absorbance at a fixed wavelength or  $\lambda_{max}$ , it is possible to detect pH solution. The different in apparent pKa either in PANI.PSS solution and (PANI-PSS/PDADMAC)<sub>n</sub> multilayer films may be cause from the parameter from thin film formation.



#### **4.4 Dispersion of Multiwall Carbon Nanotubes with Poly(diallyldimethyl ammonium chloride)**

Multiwall Carbon Nanotubes have been of interest since their discovery because their unique architecture and remarkable mechanical, thermal and electronic properties. According to the van der Waals force between nanotubes surface, carbon nanotubes tend to aggregate to each other as a bundle. Therefore, this major problem leads carbon nanotubes hardly dispersed in any kind of solvent and induced the next problem which was how to disperse carbon nanotube before applying in any application. Normally, there are two main approaches for modifying carbon nanotubes surface such as noncovalent and covalent surface modification. In these experiments, PDADMAC was used to disperse MWCNTs by noncovalent surface modification based on the interaction as hydrophobic.

##### **4.4.1 Effect of PDADMAC concentration on the dispersion of MWCNTs**

The pristine MWCNT was dispersed in PDADMAC to the extent of 5 mg/ 100 mL PDADMAC and ultrasonic at 100 KHz for 2 hr. The concentration of PDADMAC has a profound effect on the dispersion of MWCNTs, therefore, different concentrations of PDADMAC (0, 0.01, 0.05, 0.1, 0.2, 0.3, 1.0 and 3.0 mM) were prepared to sonication with MWCNTs. As expected, the pristine MWCNTs could be dispersed.

Figure 4.26 shows the plot of the changes in absorbance of the solution as the function of the added PDADMAC concentration. From the initial solution of aggregated MWCNTs, as PDADMAC concentration is increased from 0.01 to 0.1 mM, the adsorption of the polymer onto MWCNTs leads to dispersion. The increase in absorbance quickly levels off suggesting that all the MWCNTs, present in the

solution have been dispersed. Further increase of the PDADMAC concentration to 3 mM, it does not induce any increase in absorbance.

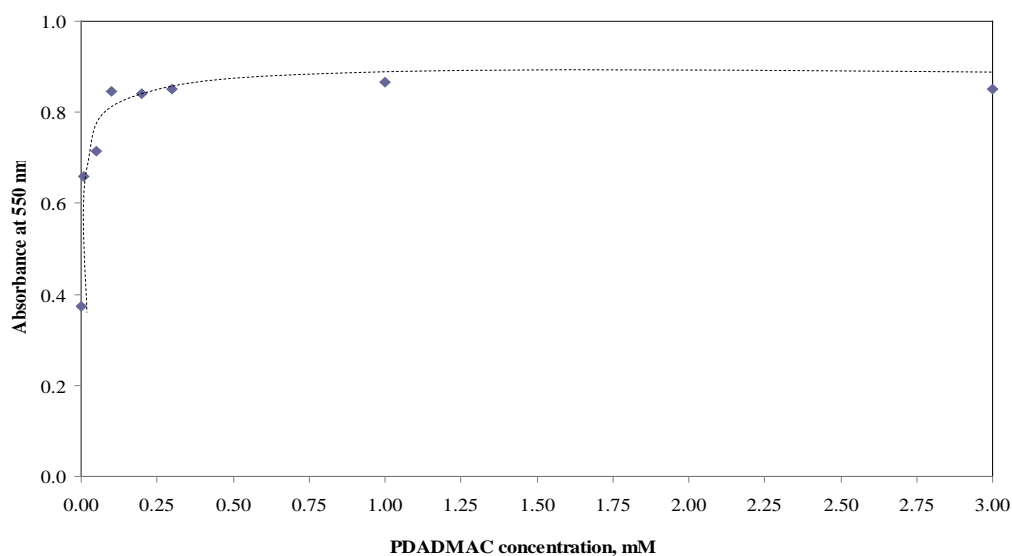


Figure 4.26 Effect of PDADMAC concentration of 0, 0.01, 0.05, 0.1, 0.2, 0.3, 1.0 and 3.0 mM on the dispersion of MWCNTs.

The intermolecular interaction improves the solubility of MWCNTs in water by the quaternary ammonium group of PDADMAC represent the most hydrophobic to be adsorbed and arranged into rolled-up preferentially onto the surface of MWCNTs. The suitable concentration of PDADMAC could account for the stable dispersion of MWCNTs through noncovalent surface modification.

#### **4.4.2 Monolayer of MWCNTs dispersed with the different concentration of PDADMAC**

One of the interesting in the series of PDADMAC polyelectrolyte concentration onto the dispersion of MWCNTs is to explain what concentration of PDADMAC to dispersed in MWCNTs shown the high efficiency to fabrication composite thin film by layer-by-layer self assembly method. The 4 layers of

negatively-charged hydrophilic glass slide substrates were immersed into the MWCNTs-PDADMAC solution. The films were dipped overnight in order to form the monolayer on the substrate surface. The performance of the MWCNTs-PDADMAC monolayer films was characterized by UV-Vis spectrometer. Figure 4.27 shows the monolayer of MWCNTs dispersed with the different concentration of PDADMAC of 0, 0.01, 0.05, 0.1, 0.2, 0.3, 1.0 and 3.0 mM. This can be seen the absorbance monolayer found to increase when increase the concentration of PDADMAC from 0.01 to 0.1 mM. The 0.1 mM PDADMAC dispersed was displayed the high absorbance. Then the absorbance monolayer was found to decrease when increase the concentration of PDADMAC from 0.2 to 1.0 mM. The deposition was found to decrease due to the excess of unreacted PDADMAC stuck onto the surface of the substrate. So from this experiment 0.1 mM PDADMAC was used to disperse MWCNTs.

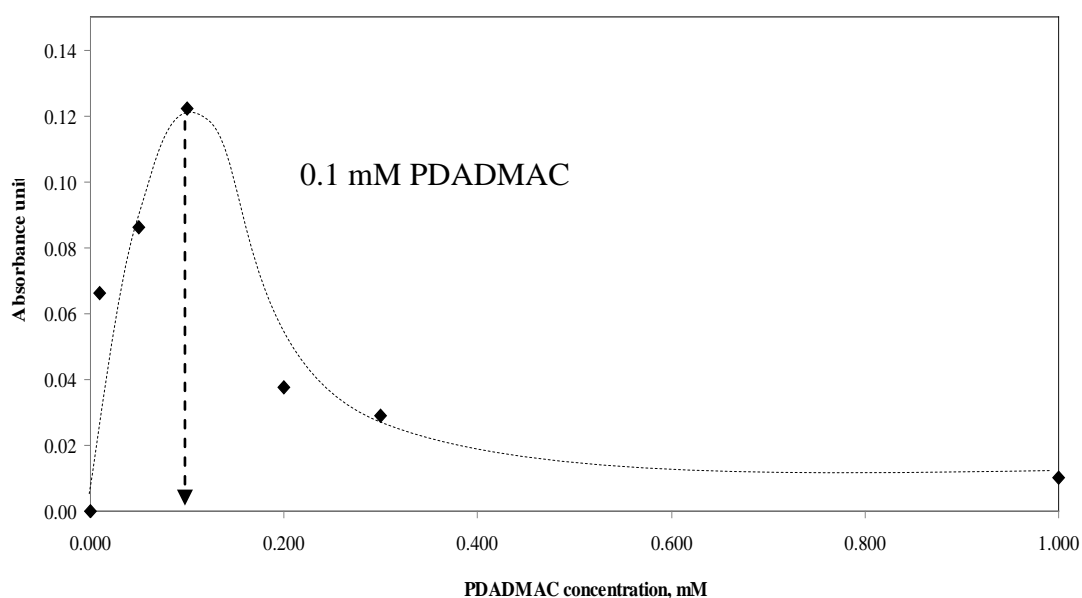


Figure 4.27 Monolayer of MWCNTs dispersed with the different concentration of PDADMAC of 0, 0.01, 0.05, 0.1, 0.2, 0.3 and 1.0 mM.

#### 4.4.3 Effect of sonication times on MWCNTs dispersed with PDADMAC

Sonication time is also an important influence factor to disperse MWCNTs with PDADMAC. The sonication process was necessary step to temporarily dispersed MWCNTs in PDADMAC solution. Although the MWCNTs was sonicated, but it still hardly dispersed in solution because of the strong hydrophobic properties. So this studied was carried out by mixing 5 mg of MWCNTs with 0.1 mM PDADMAC solution. The dispersion was investigates in the time intervals ranging from 0.15, 0.30, 1.0, 1.5, 2.0 and 3.0 hours. The mixture solution was stored at room temperature for 24 hours and measured the turbidity by UV-Vis spectroscopy. Figure 4.28 was shown the effect of sonication time onto the dispersion. It shows that the absorbance response of MWCNTs-PDADMAC were highly dependent on the sonication time. The absorbance was found to increase as the sonication time increased from 0.15, 0.30 hour and then stable with further sonication time. It can be seen that the MWCNTs are totally dispersed at sonication time 0.30 hour.

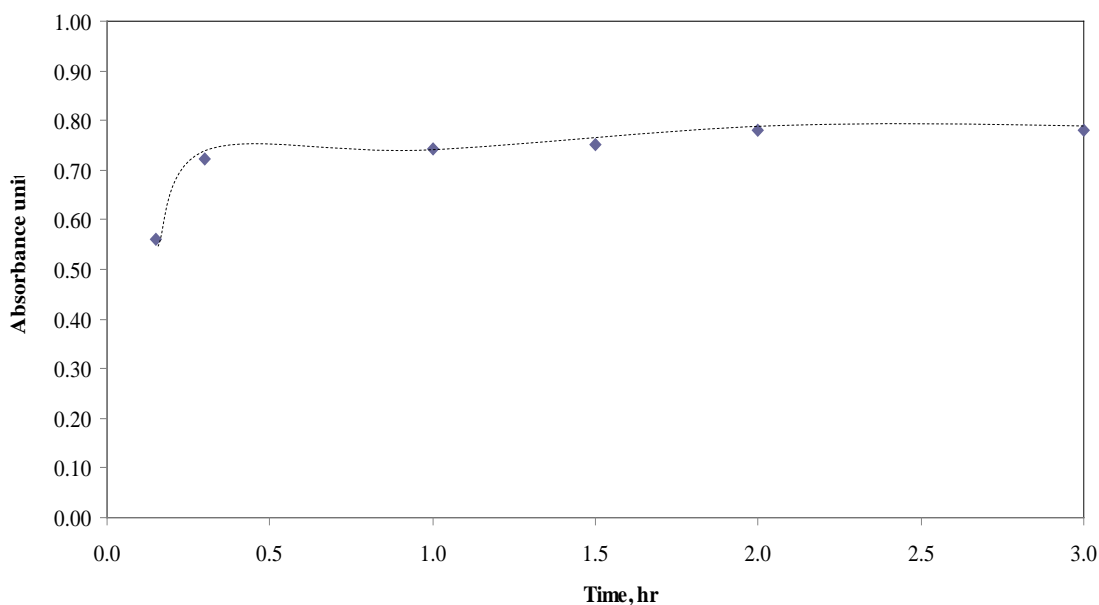


Figure 4.28 Effect of sonication time onto the dispersion of MWCNTs with PDADMAC

#### **4.4.4 Stability of MWCNTs dispersed with PDADMAC**

It is well known that noncovalent functionalization of MWCNTs using polymer, surfactant and biomolecule provided the weak interaction between the hydrophobic backbone of the dispersing agent and hydrophobic nanotubes surface. Therefore, in order to know the stability of MWCNTs dispersed with PDADMAC solution. The effect of functionalization times, salt types, salt concentration and pH were investigated.

##### **4.4.4.1 Effect of functionalization times on the stability of MWCNTs**

This experiment was carried out by dispersing 5.0 mg of MWCNTs in 0.1 mM PDADMAC solution. The solution was sonicated by probe sonicator for 2 hours in order to form the dispersion of MWCNTs. The mixture solutions were kept for 24 hours and measure the performance of each mixture solution by UV-Vis spectrometer. Figure 4.29 was shown the stability of noncovalent surface modification of MWCNTs dispersed with PDADMAC, as the function of time. The dispersion was stable up to 2 weeks.

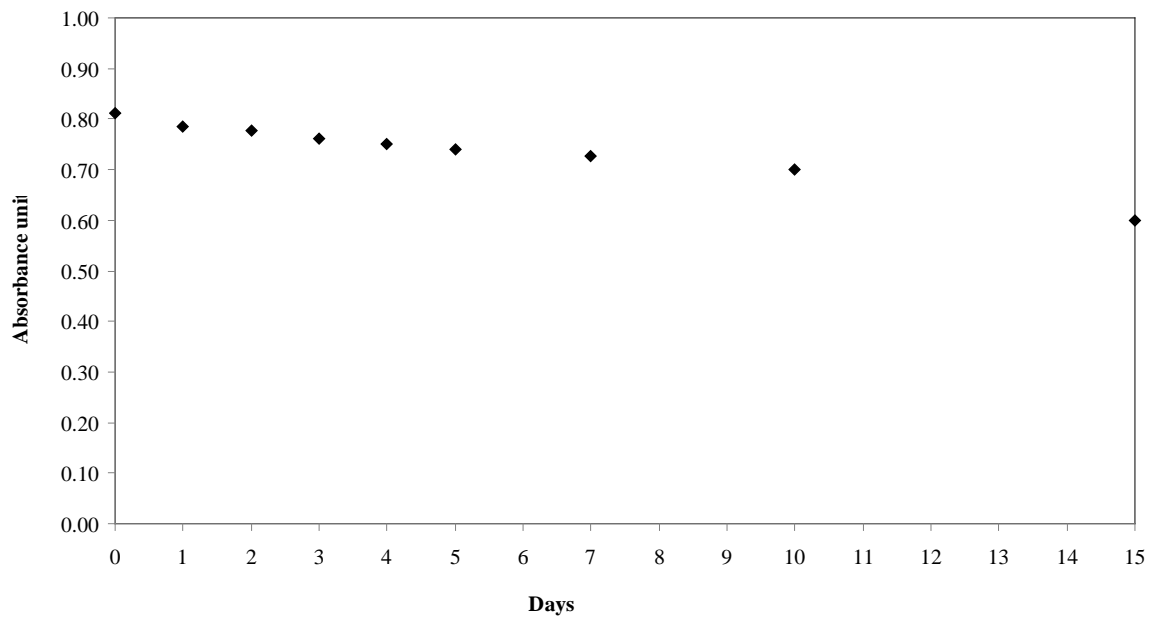


Figure 4.29 Stability of noncovalent surface modification of MWCNTs dispersed with PDADMAC, as the function of time.

The obtained stability was highly homogeneous and showed drastically improved stable properties of MWCNT dispersed with PDADMAC as compared to other prepared by same method.

#### 4.4.4.2 Effect of ionic interaction on the stability of MWCNTs

It is well known that noncovalent surface modification of MWCNTs is not straightforward for the stability because its provided the weak interaction between the dispersing species and MWCNTs surface. In this part the stability in term of salt type and salt concentration were investigated. Figure 4.44 shown the stability of noncovalent surface modification of MWCNTs dispersed with PDADMAC, as the function of salt type (NaCl, Na<sub>2</sub>SO<sub>4</sub> and Na<sub>3</sub>HPO<sub>4</sub>) and salt concentration.

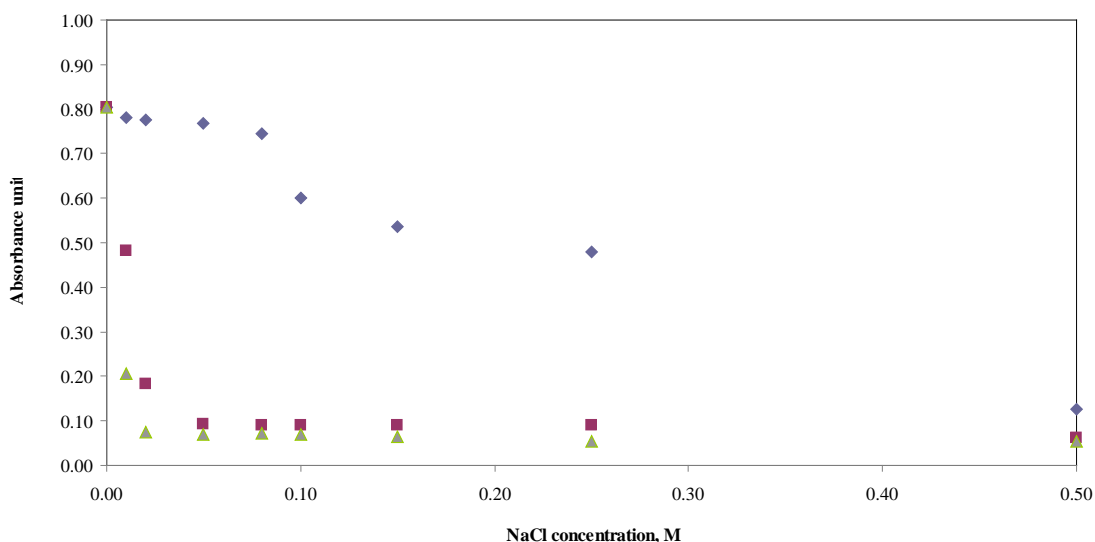


Figure 4.30 Stability of noncovalent surface modification of MWCNTs dispersed with PDADMAC, as the function of salt type and salt concentration: where  $\blacklozenge$  = NaCl,  $\blacksquare$  = Na<sub>2</sub>SO<sub>4</sub> and  $\blacktriangle$  = Na<sub>3</sub>HPO<sub>4</sub>)

The influences of Cl<sup>-</sup>, SO<sub>4</sub><sup>2-</sup> and HPO<sub>4</sub><sup>3-</sup> on the stability of MWCNTs dispersed with PDADMAC were investigated. The SO<sub>4</sub><sup>2-</sup> and HPO<sub>4</sub><sup>3-</sup> ions produced a similar shape of precipitation curve of the dispersed MWCNTs in PDADMAC solution. MWCNTs dispersed was precipitated quickly when the di-, and tri- valent salt added. . The precipitation could be attributed to the depressed of hydrophobic interaction by the added ions, which could lower the electrostatic repulsion between MWCNTs and thus lead to the aggregation and sedimentation of MWCNTs On the other hand mono valent, Cl<sup>-</sup> was shown the slowly precipitation. At low NaCl concentration, NaCl could screen the MWCNTs surface, but the hydrophobic properties was still higher than the van der Waals attractive force of MWCNTs, hence it was shown the high stability more than high concentration added.

#### 4.4.4.3 Effect of pH on MWCNTs dispersed with PDADMAC

To investigate the influence of the pH on the stability of MWCNTs dispersed with PDADMAC, MWCNTs dispersed with PDADMAC was conducted in buffers with the variable of pH. A curve obtained at different pH varied from 3-11 is depicted in Figure 4.31. From the graph, it is clearly seen that the absorbance curve stable in all pH. pH solution can control the dissociation of PDADMAC. Normally PDADMAC is a strong polyelectrolyte which can play the positive charges in all the pH. So MWCNTs can be stable in all aqueous solution

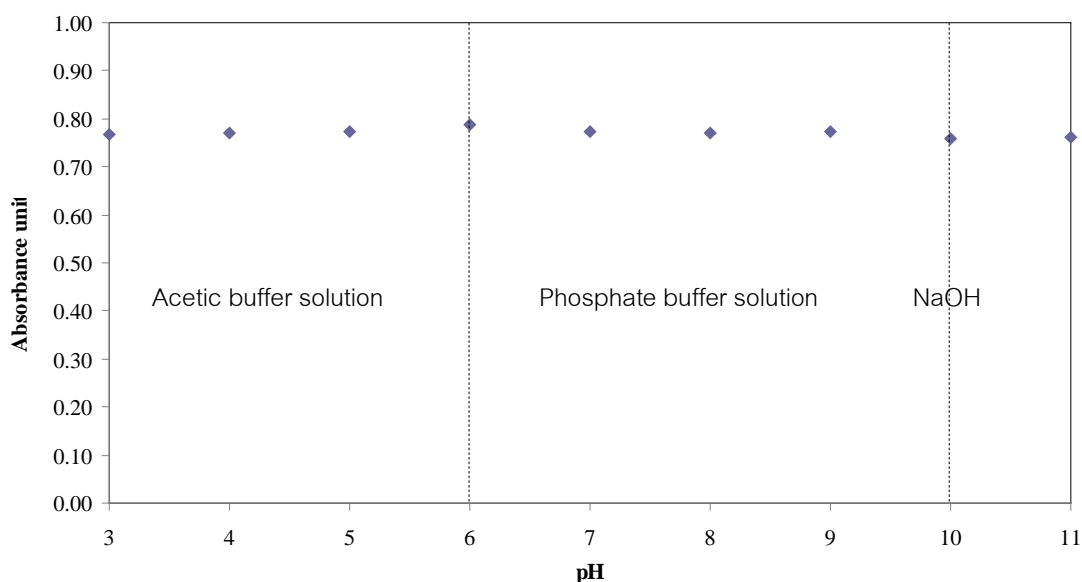


Figure 4.31 Stability of noncovalent surface modification of MWCNTs dispersed with PDADMAC, as the function of pH

The dispersion of MWCNTs was also investigated using TEM. The TEM images taken after dispersed 5 mg MWCNTs with 0.1 mM PDADMAC and wait it stable before 24 hours. Figure 4.32 shown TEM nanograph in different scale bar. The noncovalent surface modification MWCNTs with PDADMAC were seen to be



dispersed. The observation presented in Figure 4.32 (a) display that most of the individual nanotubes are uniform. The calculated thickness of the dispersion of MWCNTs was 14 nm.

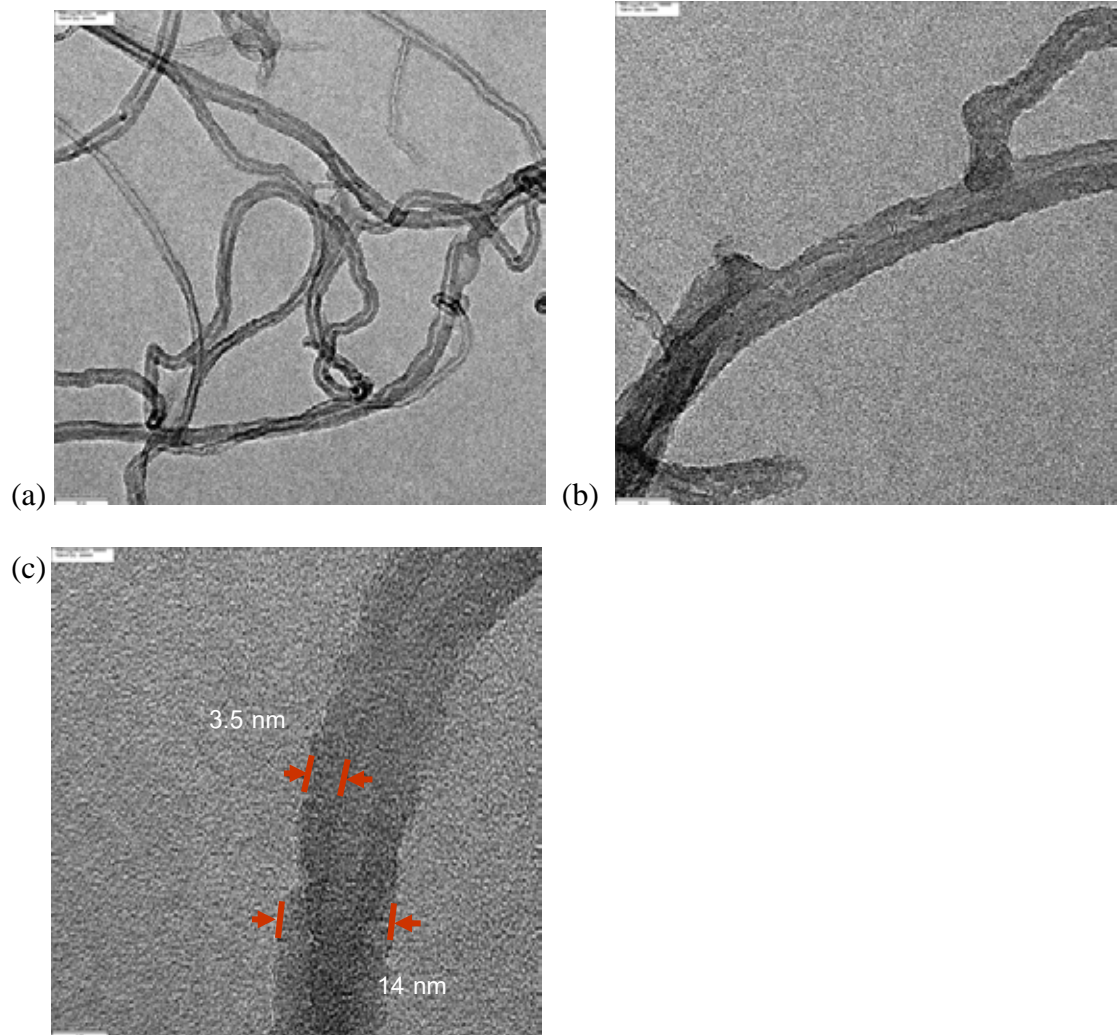


Figure 4.32 TEM micrograph of MWCNTs dispersed in PDADMAC (a) scale bar 50 nm, (b) scale bar 20 nm and (c) scale bar 7 nm.

## **4.5 Dispersion of Multiwall Carbon Nanotubes with polyaniline blend poly(sodium 4-styrenesulfonate, PANi.PSS)**

Our hypothesis was that the used of conducting polymer as the dispersing agent to disperse MWCNTs might allow better conductivity. In this experiment, PANi.PSS was used as the dispersing agent for MWCNTs. This part was discussed the effect of polymer concentration, pH onto the dispersion of MWCNTs and the stability of the solution only.

### **4.5.1 Effect of PANi.PSS concentration on the dispersion of MWCNTs**

The concentration of PANi.PSS has a profound effect on the dispersion of MWCNTs, therefore, different concentration of PANi.PSS were prepared to sonication with MWCNTs. The 5.0 mg pristine MWCNT was dispersed in 100 mL of pH 6 PANi.PSS. The polymer concentration was varied from 0.01. to 0.15 %.weight. Figure 4.33 shown the plot of the changes in absorbance of the solution as the function of the added PANi.PSS concentration. The absorbance of the mixture solution starts increasing at the polymer concentration from 0.01 to 0.05 % weight and turn to stable when polymer concentration increase from 0.05 to 0.15 % weight. During the dispersing process, intermolecular interaction improves the solubility of MWCNTs in PANi.PSS by the planar aromatic species of polyaniline have been found to adhere tightly to the side wall of carbon nanotube surface via  $\pi$ - $\pi$  stacking. It was suggested that the  $\pi$ - $\pi$  stacking interactions generated the dispersing of MWCNTs

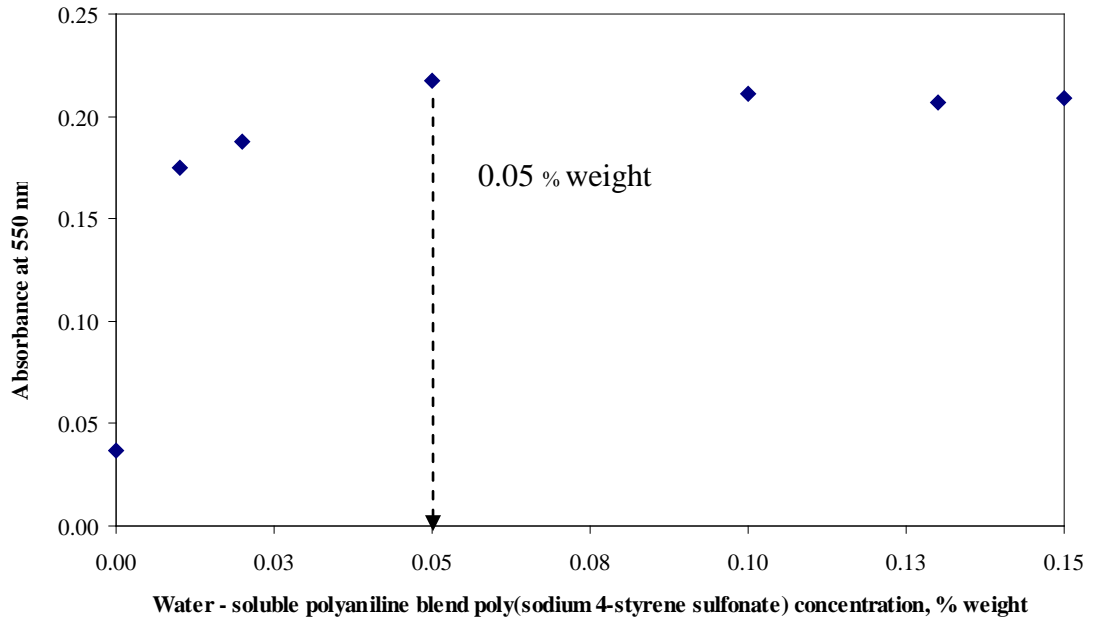


Figure 4.33 Effect of PANi.PSS concentration (0, 0.01, 0.02, 0.05, 0.1, 0.13 and 0.15 % weight) onto the dispersion of MWCNTs.

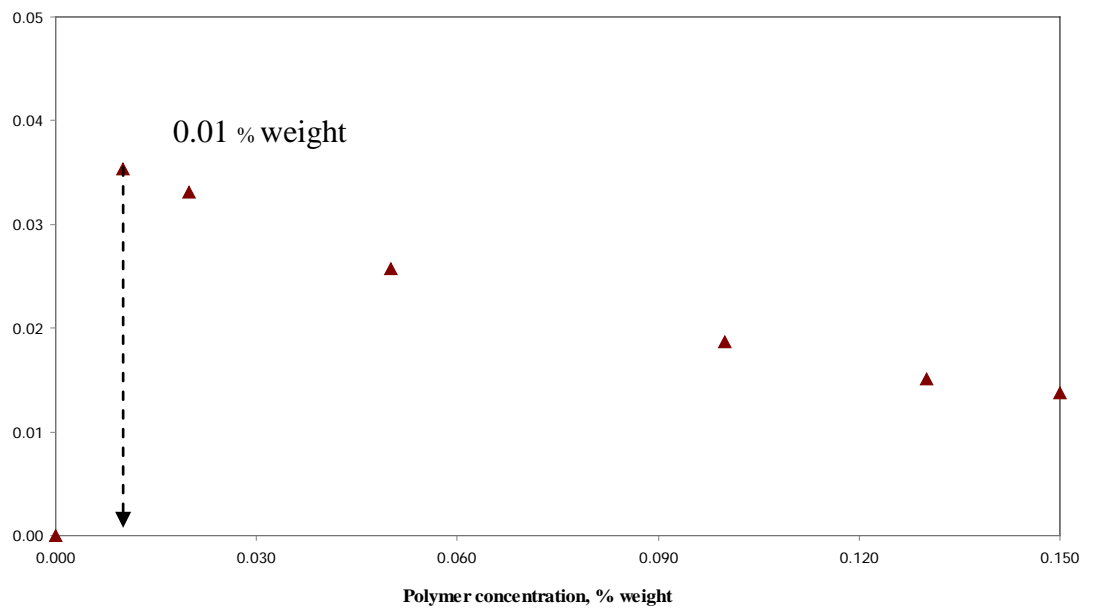


Figure 4.34 Monolayer of MWCNTs dispersed with the different concentration of PANi.PSS (0, 0.01, 0.02, 0.05, 0.1, 0.13 and 0.15 % weight) on glass substrate.

The monolayer of MWCNTs dispersed with the different concentration of PANi.PSS of 0, 0.01, 0.02, 0.05, 0.1, 0.13 and 0.15 % weight was shown in Figure 4.34. The absorbance of the monolayer was displayed maximum at the polymer concentration of 0.01 % weight. Then the absorbance monolayer was found to decrease when increase the concentration of PDADMAC from 0.02 to 0.15 % weight. The deposition of the monolayer was found to decrease due to excess of unreacted PANi.PSS stricked onto the surface of the substrate.

#### 4.5.2 Effect of pH on the dispersion of MWCNTs

This experiment was conducted by varied the pH of the PANi.PSS and fixing the concentration of the polymer constantly. The 5.0 g of MWCNTs was mixed with different pH of polymer solution under the sonication process. The mixture solutions was kept for 1 day in room temperature and measure the turbidity of the solution by UV-Vis spectroscopy at the wavelength of 550 nm.

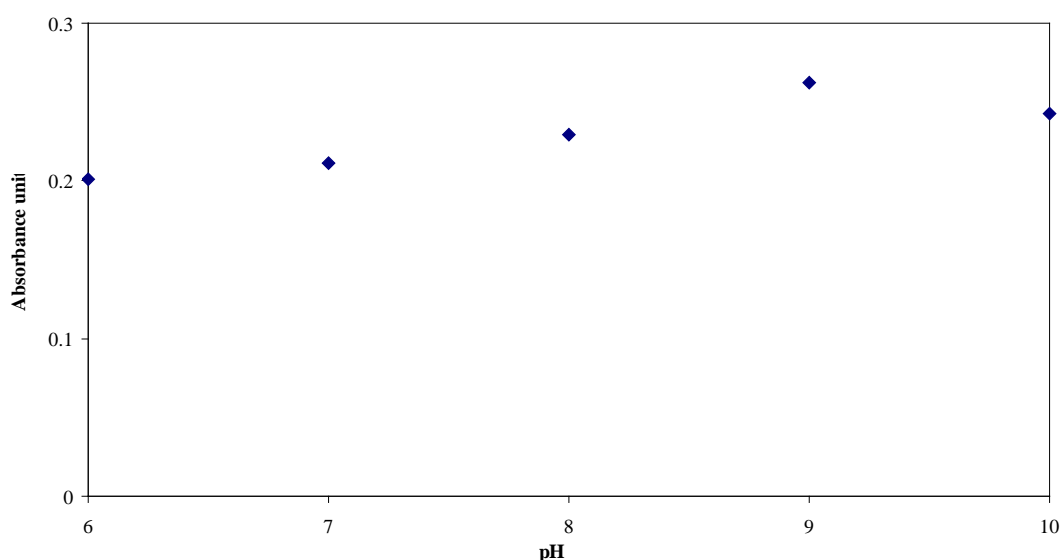


Figure 4.35 Effect of pH of PAN.PSS onto the dispersion of MWCNTs.

Figure 4.35 shown pictures of solution corresponding to MWCNTs dispersed with the various pH of PANi.PSS. It can be seen that when increasing the pH of polymer solution from 6 to 10, there is no change in the absorbance of mixture solution. The intermolecular interaction of the noncovalent surface modification of MWCNTs was shown the role of  $\pi$ - $\pi$  stacking interaction with PANi.PSS at all pH range.

#### 4.5.3 Stability of MWCNTs dispersed with PANi.PSS: functionalization times

In order to optimize the stability of MWCNTs dispersed with PANi.PSS, the effect of functionalization times of the mixture solution was evaluated. The 5.0 mg MWCNT was mixed with 0.01 % PANi.PSS solution under the sonication process for 2 hours. The performance of the mixture solution was measured the characteristic by UV-Vis spectrometer for the half of month. The result was shown in Figure 4.36.

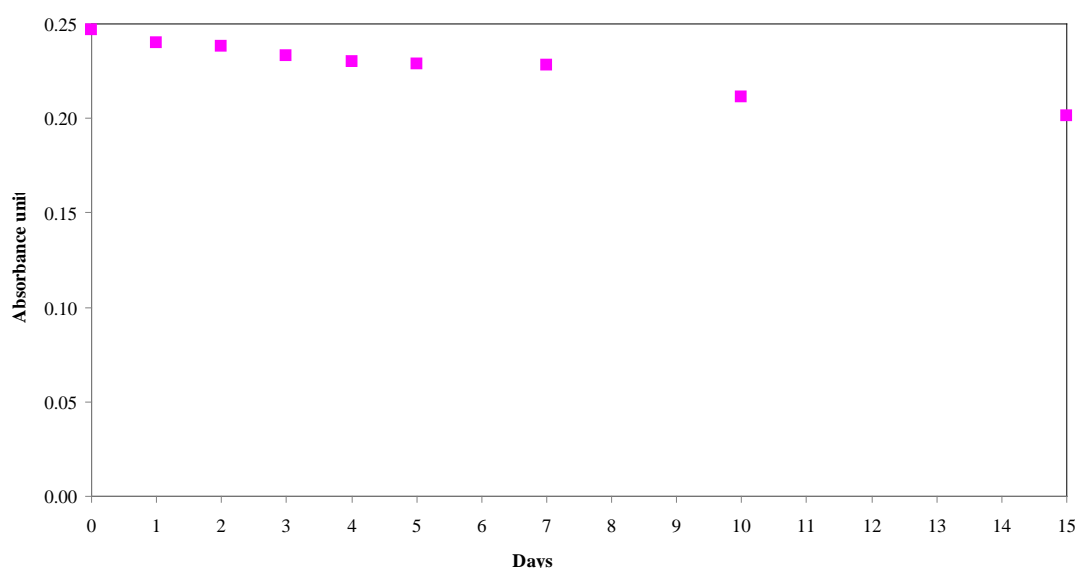


Figure 4.36 Stability of noncovalent surface modification of MWCNTs dispersed with water - soluble polyaniline blend poly(sodium 4-styrenesulfonate, PSS), as the function of time.

The stability of noncovalent surface modification of MWCNTs dispersed with PANi.PSS as the function of time was found to stable more than 2 weeks. The  $\pi$ - $\pi$  noncovalent surface modification was found much stronger than a simple hydrophobic association.

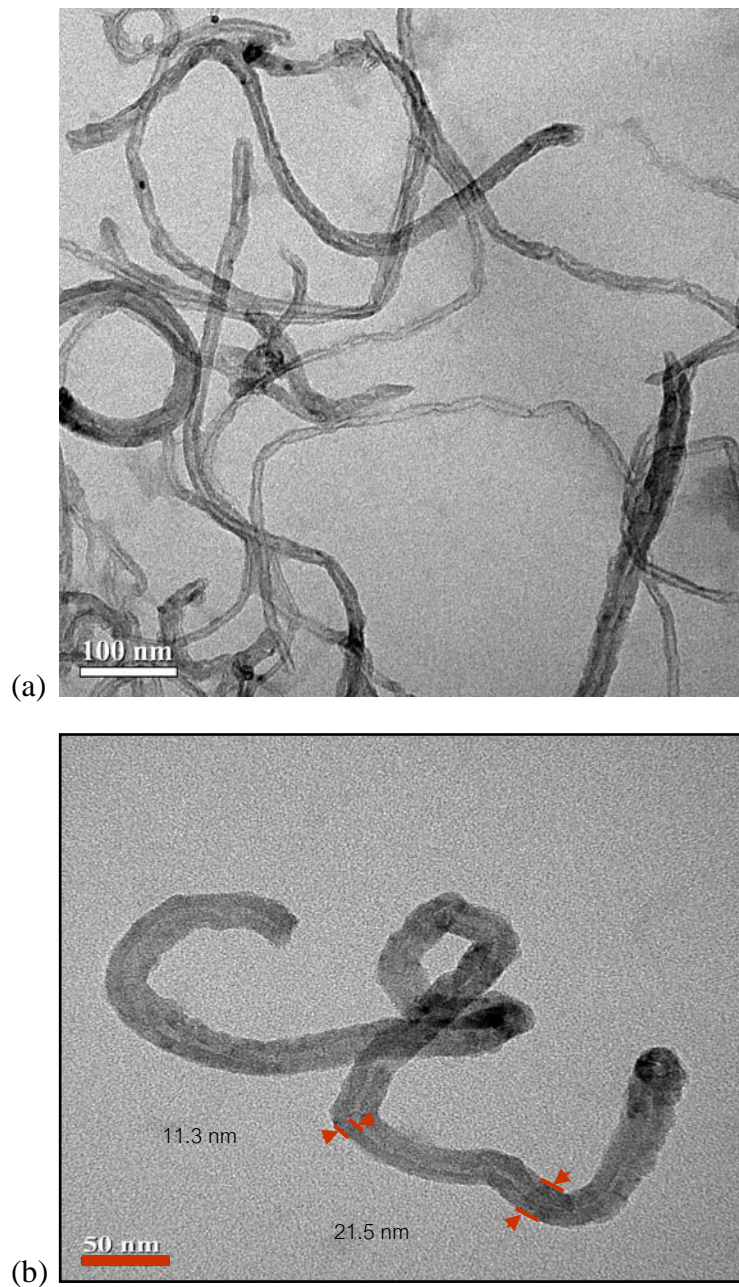


Figure 4.37 TEM micrograph of MWCNTs dispersed in PANi.PSS (a) scale bar 100 nm and (b) scale bar 50 nm.

In order to confirm the dispersion efficiency of noncovalent surface modification of MWCMTs dispersed in PANi.PSS, TEM was used to investigate. It is clearly observed that the noncovalent surface modification of MWCMTs dispersed well in the PANi.PSS solution implying that PANi.PSS is better dispersion medium for MWCNTs. The observation presented in Figure 4.37 (a) and (b) display that most of the individual nanotubes are uniform. The calculated thickness of the dispersion of MWCNTs was 21.5 nm.

#### **4.6 Layer-by-layer self assembly of MWCNTs**

In this section, the LbL self assembled method was used to prepare the different composite multilayer films by the different series of polyanion and polycation and the properties of the obtained composite multilayer films were examined by measure the electrical conductivity, thickness and surface morphology.

##### **4.6.1 Layer-by-layer self assembly of MWCNTs dispersed with poly(diallyldimethyl ammonium chloride) / poly(sodium 4-styrene sulfonate); (MWCNTs.PDADMAC)/PSS.**

Our initial approach was to study the incorporation of MWCNTs dispersed with PDADMAC into the PSS polymer. The polyanionic and polyionic with the best stability and solubility were chosen for the multilayer fabrication. In these case polycationic which was dispersed 5 mg MWCNTs with 0.1 mM PDADMAC were used for film fabrication. These MWCNTs dispersed with PDADMAC have a linear ionic charge density similar to that of common highly charged polyelectrolyte such as PDADMAC. The deposition conditions for the polyelectrolyte were used as 10 min

dipping time. The mechanism of layer-by-layer self assembly of (MWCNTs.PDADMAC)/PSS multilayer thin films was shown in Figure 4.38.

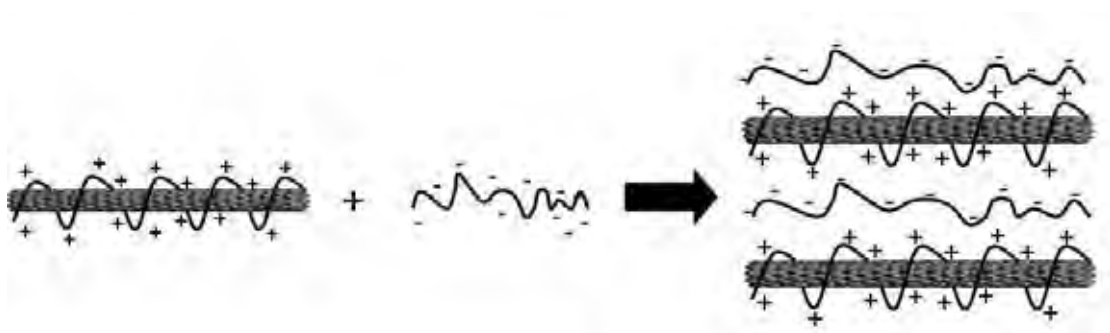


Figure 4.38 Schematic mechanism of layer-by-layer self assembly of (MWCNTs.PDADMAC)/PSS multilayer thin films.

The composite thin film was fabricated by the electrostatic interaction between the sulfonic group of PSS and quaternary ammonium group of MWCNTs dispersed with PDADMAC. The progress of film formation in the term of increasing in number of layer were shown in Figure 4.39 and 4.40. The data was reported as the function of absorbance and thickness, respectively.

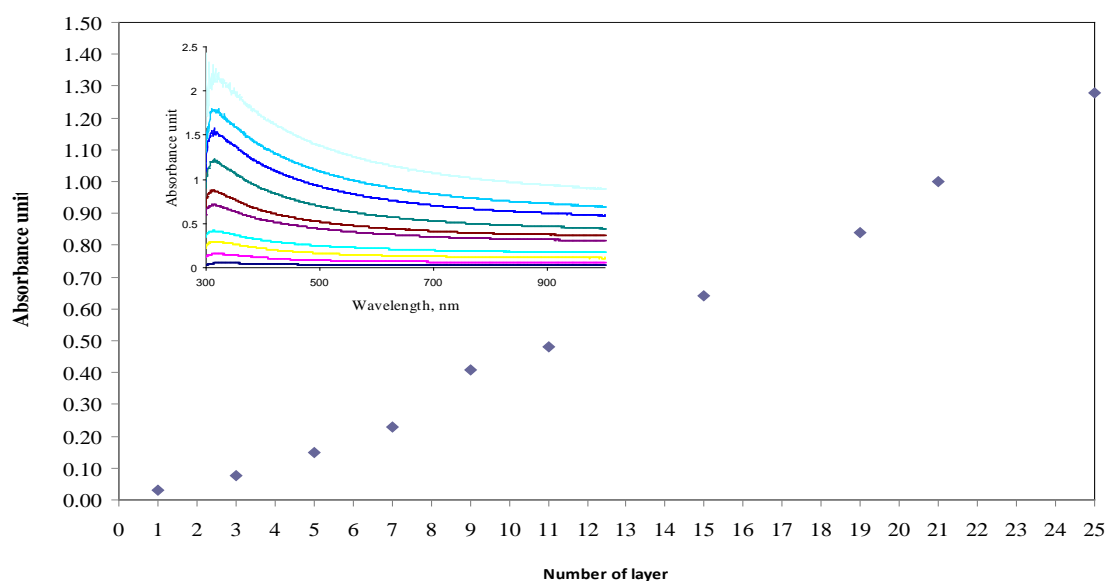


Figure 4.39 Plot of the changes in absorbance of Layer-by-layer self assembly of (MWCNTs.PDADMAC)/PSS



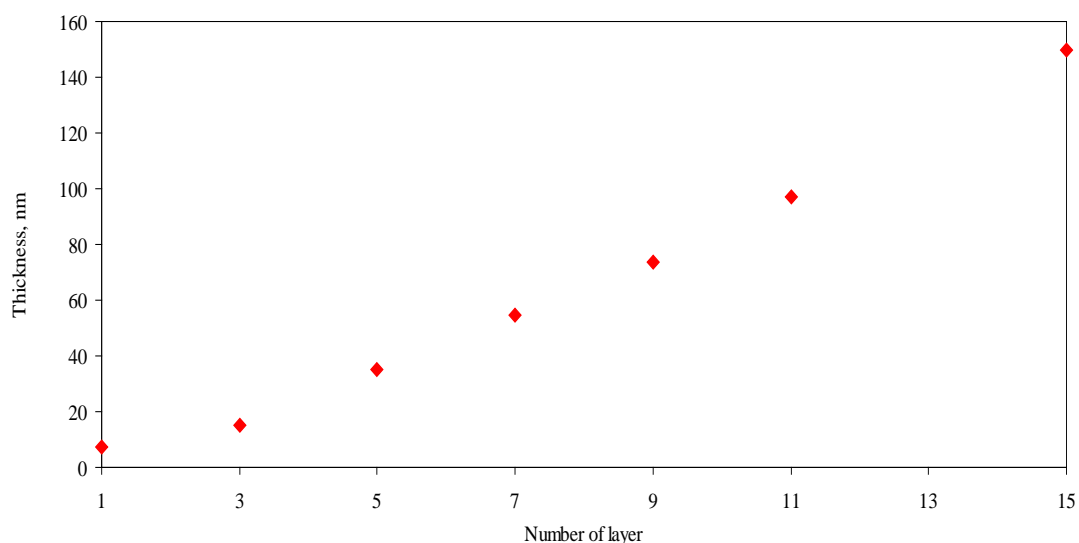


Figure 4.40 Thickness of (MWCNTs.PDADMAC) / PSS multilayer thin films.

Figure 4.39 shows the absorbance of MWCNTs.PDADMAC)/PSS multilayer thin films as the function of number of layer. The absorbance was found to increase when increase the number of layer. The multilayer growth was found linear due to each adsorbed layer imparts a constant amount of charge to the growing films. This reason could be confirmed by measure the thickness of the films by AFM. The thickness was found to increase when increase the number of layer (Figure 4.40).

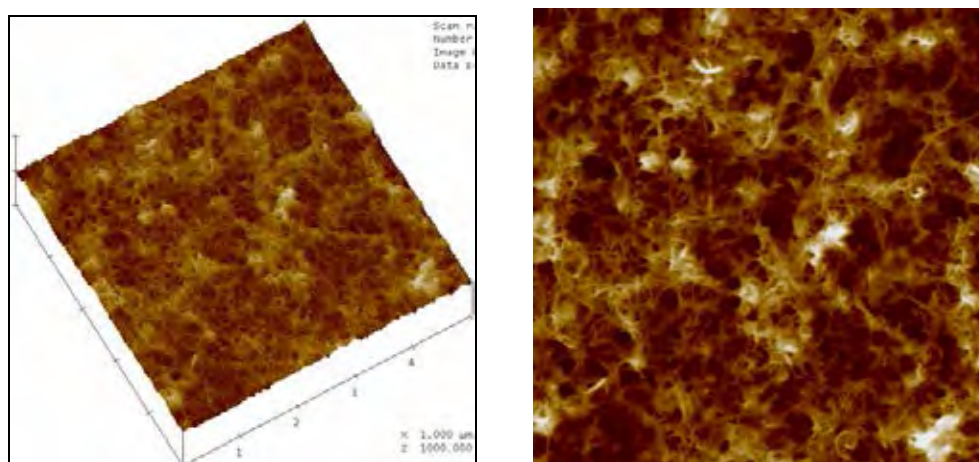


Figure 4.41 AFM pictures for the (MWCNTs.PDADMAC)/PSS 15 layers.

The AFM images of (MWCNTs.PDADMAC)/PSS multilayer thin films at number of layer 15 were investigated. It was found that the MWCNTs thin film have an interconnected network structure with have an average diameter of  $15\pm 5$  nm. The electrical conductivity of (MWCNTs.PDADMAC)/PSS multilayer thin films was shown in Figure 4.42. It can be seen that the electrical conductivity of the multilayer films increased with increasing number of layer. The 15 layers of multilayer films had the conductivity up to  $8.54 \times 10^{-5}$  S/cm.

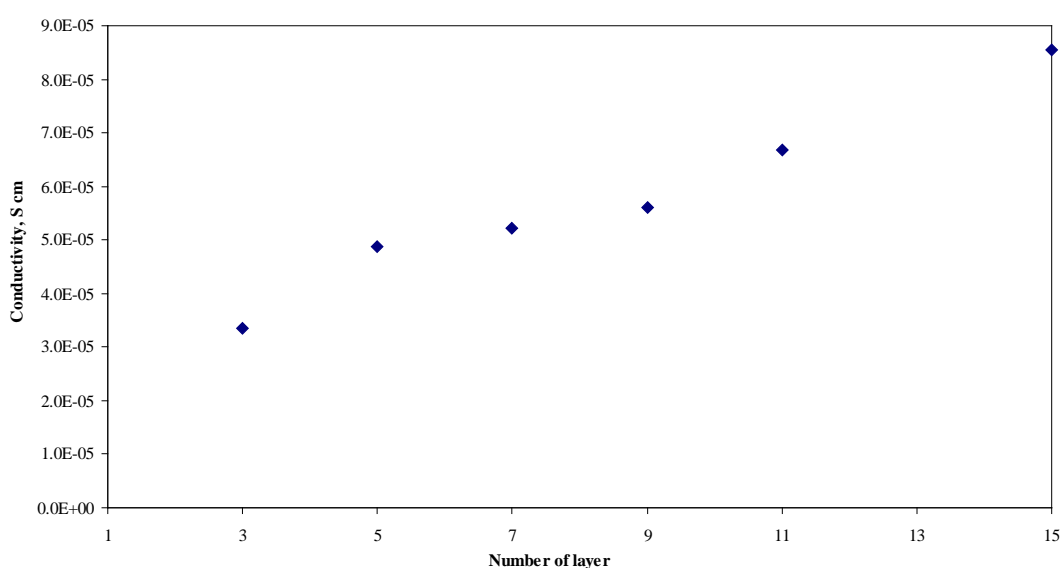


Figure 4.42 Conductivity of (MWCNTs.PDADMAC)/PSS multilayer thin films by varying number pf layer.

In order to investigate the optical and electrical properties of (MWCNTs.PDADMAC)/PSS multilayer thin films in term of pH changes, the 15 layers of composite films were dipped into the different pH buffer solution for 2 hours. The optical and electrical properties were measured by UV-Vis spectrophotometer and 4 point probe, respectively. The results were shown in Figure 4.43-4.44.

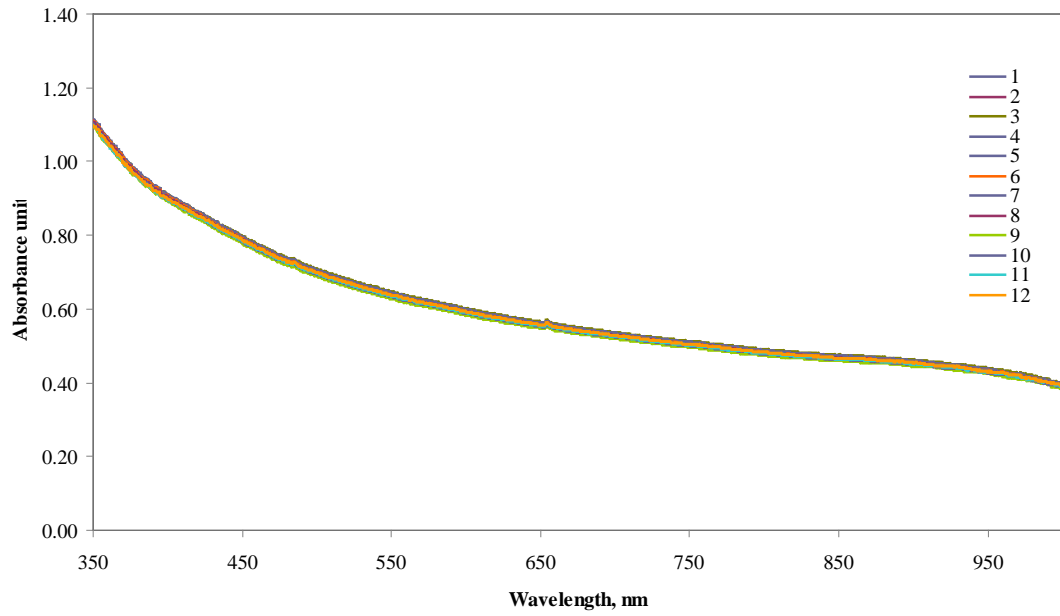


Figure 4.43 The UV-Vis spectra of 15 layers (MWCNTs.PDADMAC)/PSS multilayer thin films at pH 1 to 12.

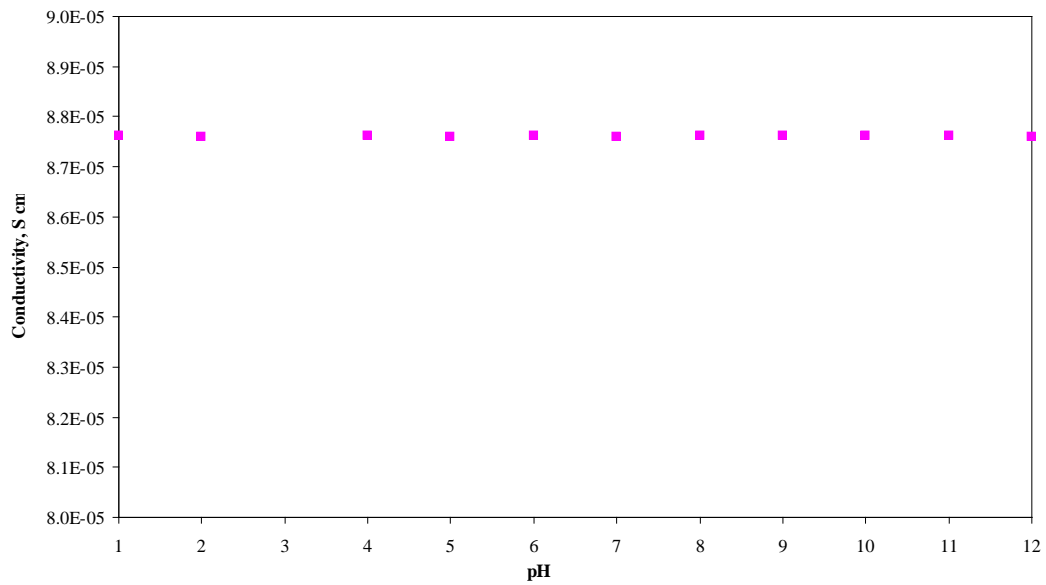


Figure 4.44 Conductivity of 15 layers (MWCNTs.PDADMAC)/PSS multilayer thin films by varying pH.

Figure 4.43 and 4.44 shows the optical and electrical properties of (MWCNTs.PDADMAC)/PSS multilayer thin films in term of pH changes. It was already mentioned that the optical and electrical properties of (MWCNTs.PDADMAC)/PSS multilayer thin films are not pH dependent. The optical properties were found very stable. At the same time, almost no changes are observed in the specific conductivity curve of 15 layers (MWCNTs.PDADMAC)/PSS multilayer thin films by varying pH. All this indicates that the (MWCNTs.PDADMAC)/PSS multilayer thin films are very stable in term of optical and electrical properties in all pH.

#### **4.6.2 Layer-by-layer self assembly of MWCNTs dispersed with poly(diallyldimethyl ammonium chloride / water - soluble polyaniline blend poly(sodium 4-styrenesulfonate); (MWCNTs.PDADMAC)/PANi.PSS**

The key approach to provide the best conductivity of composite thin films is to use the conducting polyelectrolyte as the layer film. In this part, PANi.PSS was used as the anionic polyelectrolyte for fabricate the composite thin films of (MWCNTs.PDADMAC). The electrostatic interaction between sulfonic group (of PANi.PSS and quaternary ammonium group of MWCNTs dispersed with PDADMAC was displayed for film fabrication (Figure 4.45).

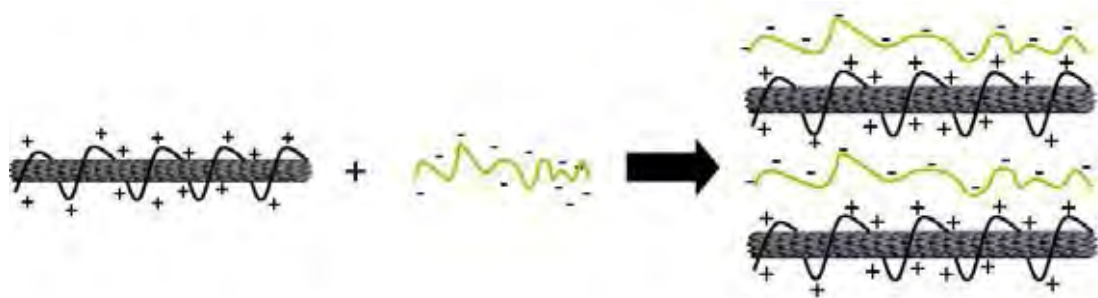


Figure 4.45 Schematic mechanism of layer-by-layer self assembly of (MWCNTs.PDADMAC)/ PANi.PSS multilayer thin films.

The progress of composite film fabrication can be seen in Figure 4.46. When increase the number of layer the absorbance was found to increase. The multilayer growth of (MWCNTs. PDADMAC)/ PANi.PSS multilayer thin films was found linear due to each adsorbed layer imparts a constant amount of charge to the growing films.

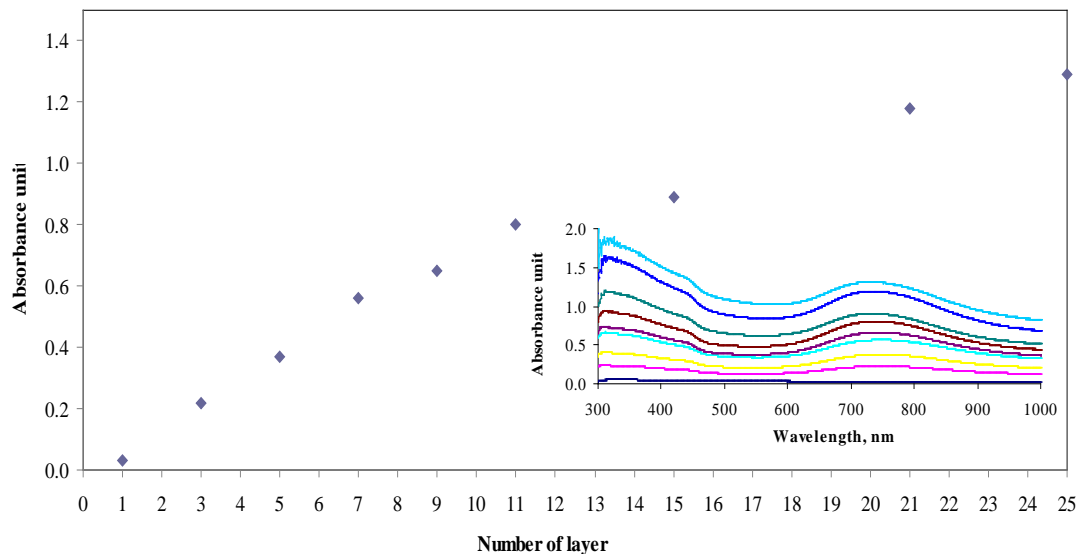


Figure 4.46 Plot of the changes in absorbance of Layer-by-layer self assembly of MWCNTs. PDADMAC / PANi.PSS multilayer thin films.

Figure 4.47 was shown the thickness of the composite films. By considering the comparison of the thickness of the (MWCNTs.PDADMAC)/PSS multilayer thin films (Figure 4.40) and (MWCNTs.PDADMAC)/PANi.PSS multilayer films (Figure 4.47), it can be seen that the thickness of MWCNTs.PDADMAC/PANi.PSS has thicker. It could be concluded that, the ionic surface charges density of PANi.PSS is greater than that of PSS. The AFM images of (MWCNTs.PDADMAC)/PANi.PSS multilayer thin film (Figure 4.48) show more densely packed MWCNTs network structure.

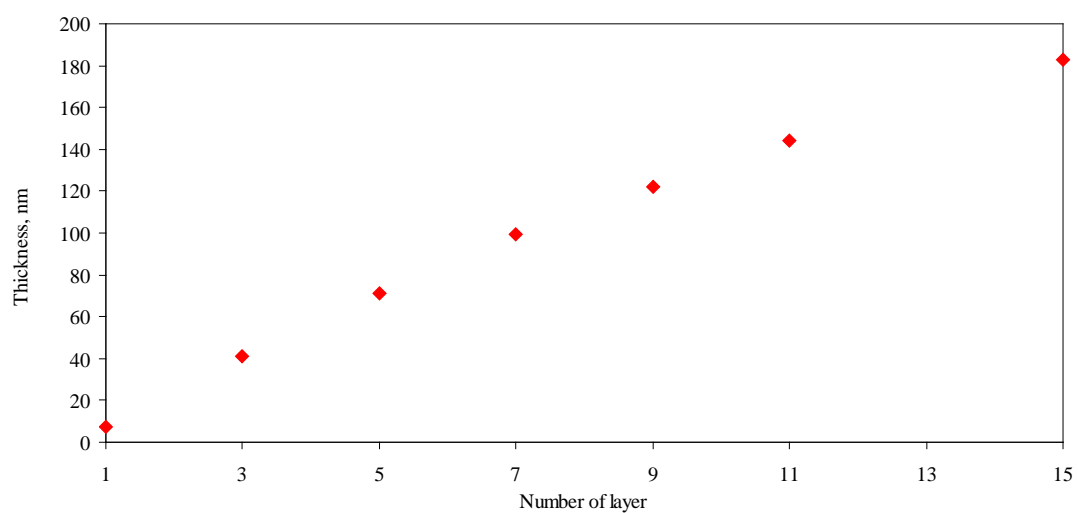


Figure 4.47 Thickness of (MWCNTs. PDADMAC) / PANi.PSS multilayer thin films.

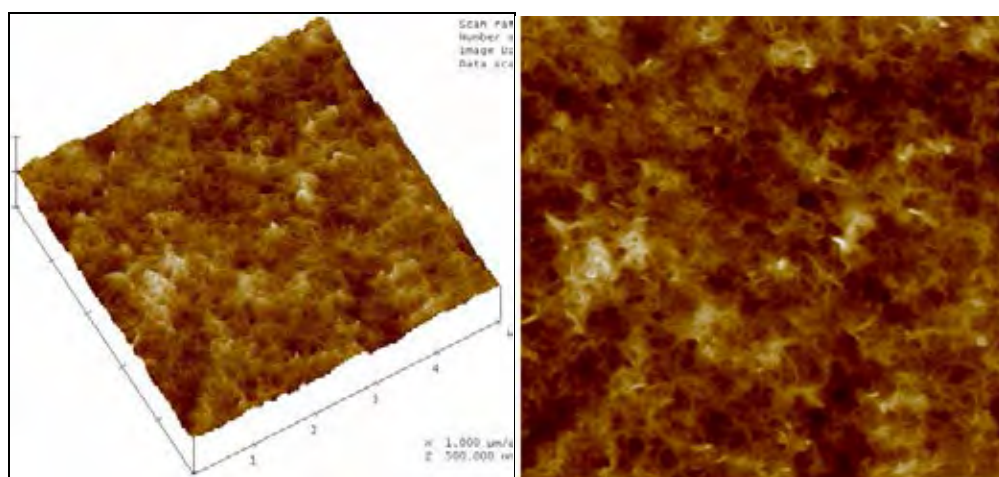


Figure 4.48 AFM pictures for the (MWCNTs. PDADMAC) / PANi.PSS multilayer thin films, at 15 layers.

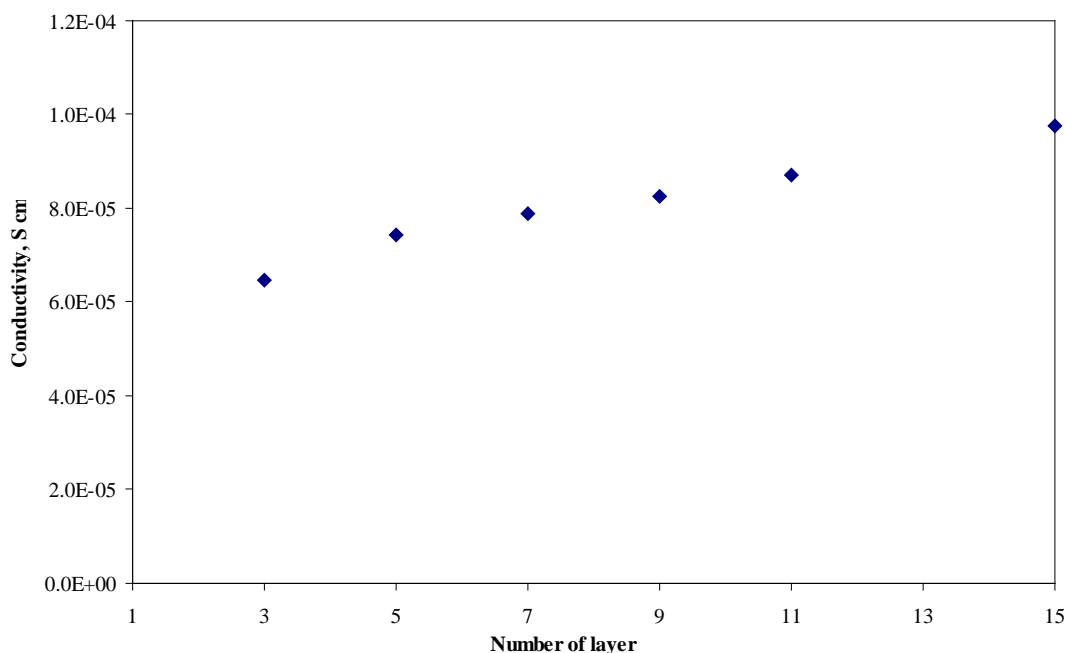


Figure 4.49 Conductivity of MWCNTs. PDADMAC / PANi.PSS multilayer thin films

The effect of PANi.PSS as the polyanion to fabricate the multilayer films with (MWCNTs.PDADMAC) as the function of electrical conductivity was shown in Figure 4.49. It was found that the electrical conductivity of the multilayer films increased when increasing the number of layer. The 15 layers of composite films were shown the electrical conductivity  $9.77 \times 10^{-5}$  S/cm. The conductivity of MWCNTs.PDADMAC/PANi.PSS multilayer films was shown the high electrical conductivity when compare with MWCNTs.PDADMAC/PSS multilayer thin films due to the effect of polyanion conducting polymer. The emeraldine salt form of PANi.PSS was shown the conducting layer for film fabrication.

Figure 4.50 and 4.51 shows the optical and electrical properties of 15 layers (MWCNTs. PDADMAC) / PANi.PSS multilayer thin films at pH 1 to 12. It was found that the color of (MWCNTs. PDADMAC) / PANi.PSS multilayer thin films

change with pH, which is the basic for an all optical pH sensor based on PANi. The effect of pH on the change in electronic spectra of (MWCNTs. PDADMAC) / PANi.PSS multilayer thin films can be explained by the different degree of protonation of the imine nitrogen atoms in the PANi polymer chain.

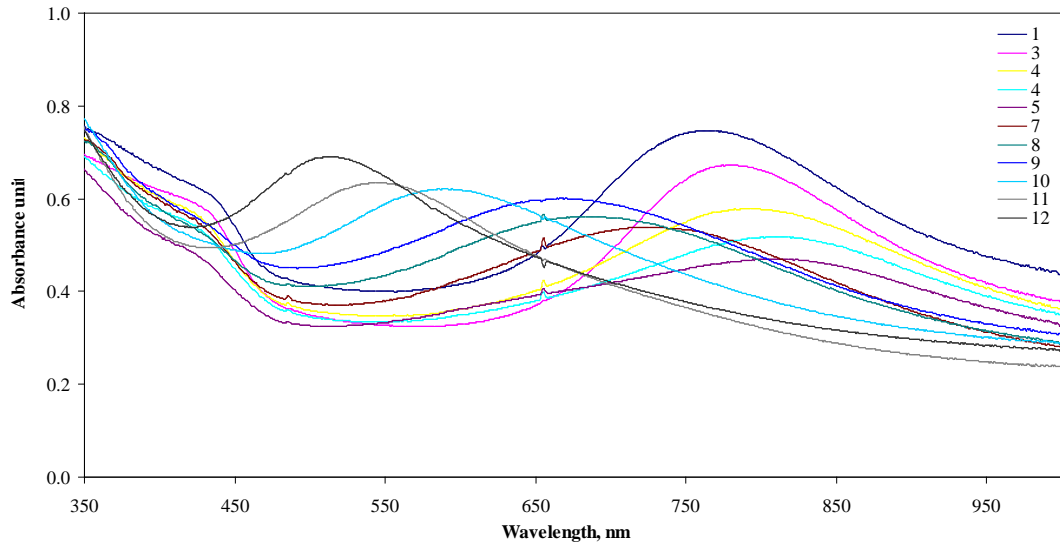


Figure 4.50 The UV-Vis spectra of 15 layers (MWCNTs. PDADMAC) / PANi.PSS multilayer thin films at pH 1 to 12.

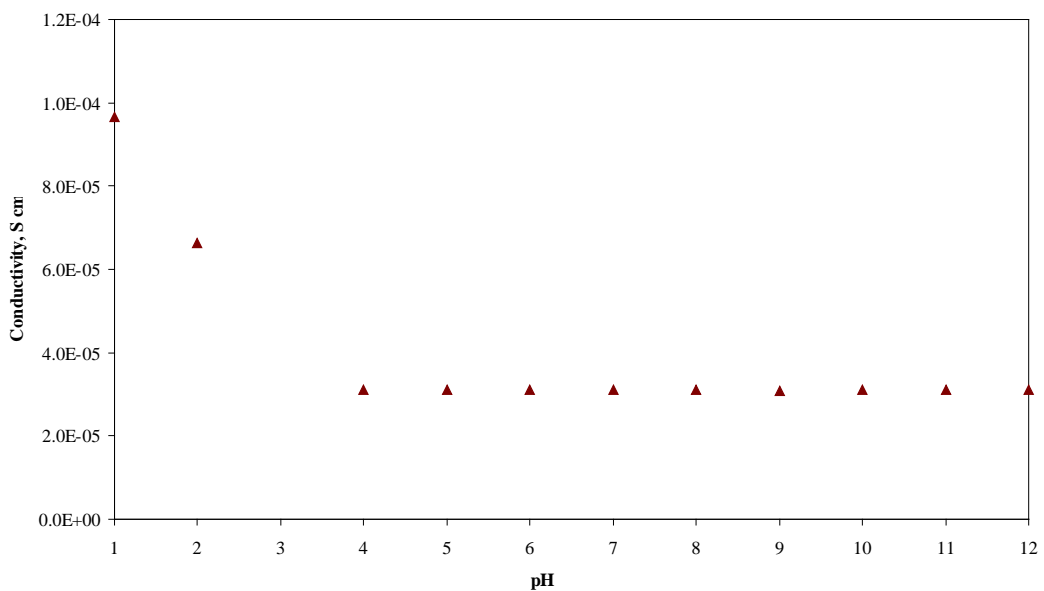


Figure 4.51 Conductivity of 15 layers (MWCNTs. PDADMAC) / PANi.PSS multilayer thin films by varying pH from 1-12.



It has been demonstrated previously that the electrical properties of PANi thin films depends strongly on its environmental pH. So the electrical properties of 15 layers (MWCNTs. PDADMAC) / PANi.PSS multilayer thin films should also be studied by a change of pH. Shown in Figure 4.51 is the conductivity of 15 layers (MWCNTs. PDADMAC) / PANi.PSS multilayer thin films by varying pH from 1-12. It is clear that the electrical properties shows different potential response in different pH solution. The electrical conductivity of the composite films decreased when pH increased from 1 to 12. The pH 1 had appreciable highest conductivity around  $9.654 \times 10^{-5}$  S/cm. On the other hand, after the composite thin films were dipped into the high pH 2-12, the electrical conductivity of the films decreased and stable at pH 4-12. This was a direct result of the conversion of emeraldine salt form to emeraldine base form. At pH 4-12, the electrical conductivity of the composite films were shown only the conductivity of MWCNTs.

#### **4.6.3 Layer-by-layer self assembly of MWCNTs dispersed with water - soluble polyaniline blend poly(sodium 4-styrenesulfonate) / poly(diallyldimethyl ammonium chloride) multilayer thin films; (MWCNTs.PANi.PSS)/PDADMAC**

The layer-by-layer deposition can also carried out with anionic MWCNTs and polycation, e.g. with PDADMAC. So in this part the PANi.PSS was used as the noncovalent surface charge modification of MWCNTs in order to promote anionic MWCNTs for polyelectrolyte multilayer deposition. 5 mg of MWCNTs was dispersed with the 0.01 % PANi.PSS concentration The intermolecular interaction improves the solubility of MWCNTs in water by the  $\pi$ - $\pi$  interaction of PANi.PSS and MWCNTs backbone. The composite thin films was fabricated by the electrostatic interaction between sulfonic group of MWCNTs dispersed with PANi.PSS and quaternary

ammonium group of PDADMAC. The possible mechanism was shown in Figure 4.52.

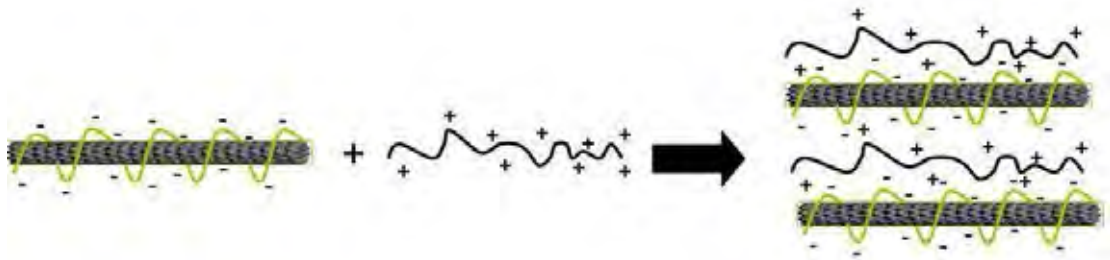


Figure 4.52 Schematic mechanism of layer-by-layer self assembly of (MWCNTs.PANi.PSS)/PDADMAC multilayer thin films.

Working with anionic MWCNTs is straightforward as with cationic one. Because cationic MWCNTs were easily precipitate during substrate incubation, probably due to the negatively charged substrate. Figure 4.53 shows the absorbance of the composite thin film of (MWCNTs.PANi.PSS<sub>0.01% weight</sub>)/PDADMAC when the number of layer was varied. All (MWCNTs.PANi.PSS)/PDADMAC multilayer thin films growth are linear although less irregular than that of cation MWCNT multilayer, perhaps due to low density charge. The absorbance of (MWCNTs.PANi.PSS<sub>0.01% weight</sub>)/PDADMAC multilayer thin films was shown the highest absorbance. The high growth rate of (MWCNTs.PANi.PSS<sub>0.01% weight</sub>)/PDADMAC multilayer thin films was found to increase due to the strong interpenetration between oppositely charged electrolyte.

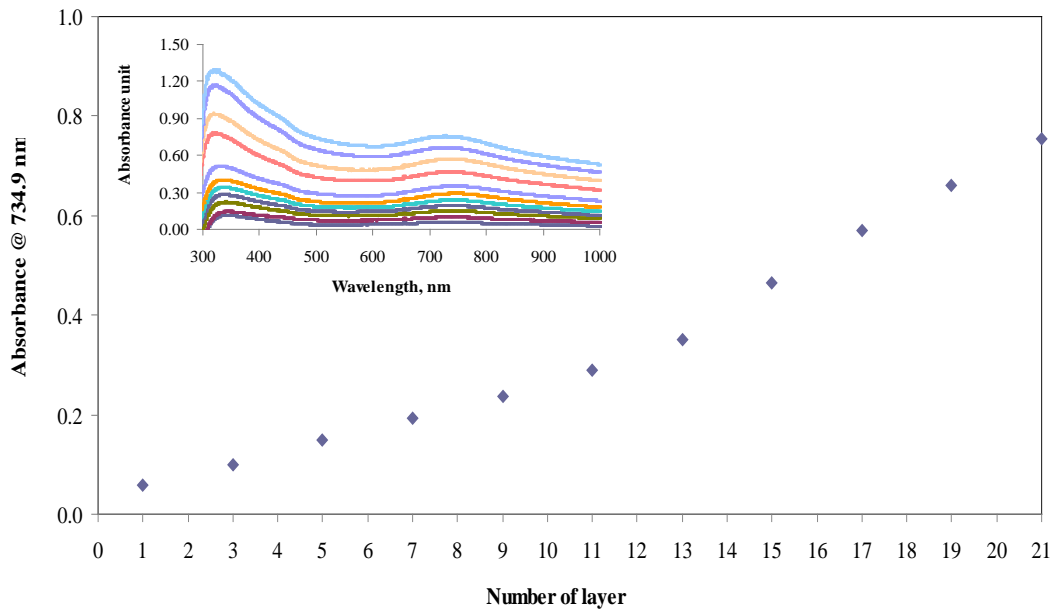


Figure 4.53 Plot of the changes in absorbance of Layer-by-layer self assembly of (MWCNTs.PANi.PSS<sub>0.01% weight</sub>) / PDADMAC multilayer thin films.

The thickness of (MWCNTs.PANi.PSS<sub>0.01% weight</sub>) /PDADMAC multilayer thin films was shown in Figure 4.54. The first layer of the composite film was found to increase when increase the number of layer. The first number of layer was shown the thickness around 5.367 nm. Moreover Figure 4.55 shows AFM pictures for the composite one by vary the number of layer. The network structure of the LbL assembled MWCNTs thin films can be observed with the first number of layer. All AFM images clearly show that MWCNTs thin films have an interconnected network structure and shown more densely packed MWCNTs network structure when increasing the number of layer.

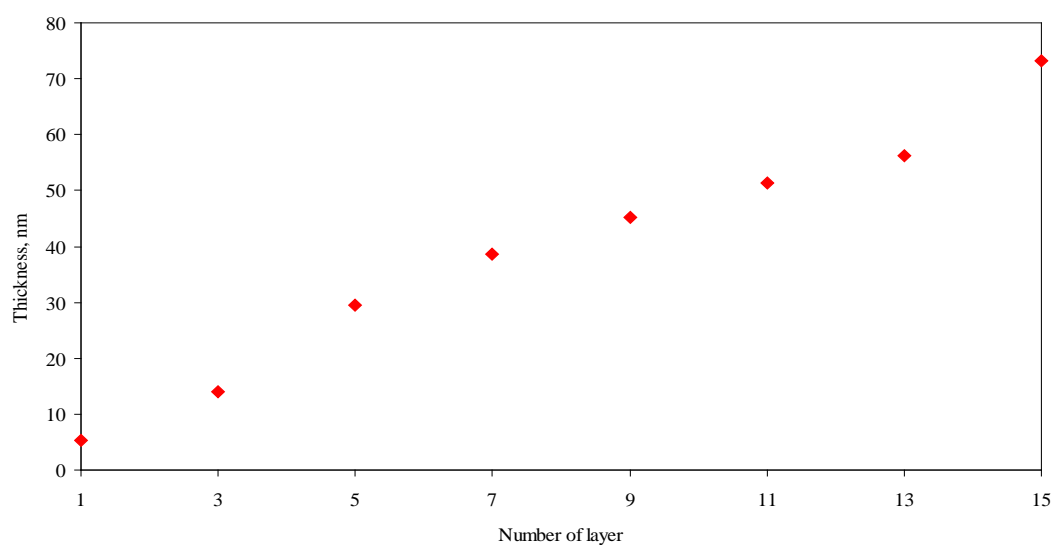


Figure 4.54 Thickness of (MWCNTs.PANi.PSS<sub>0.01%</sub> weight) /PDADMAC multilayer thin films.

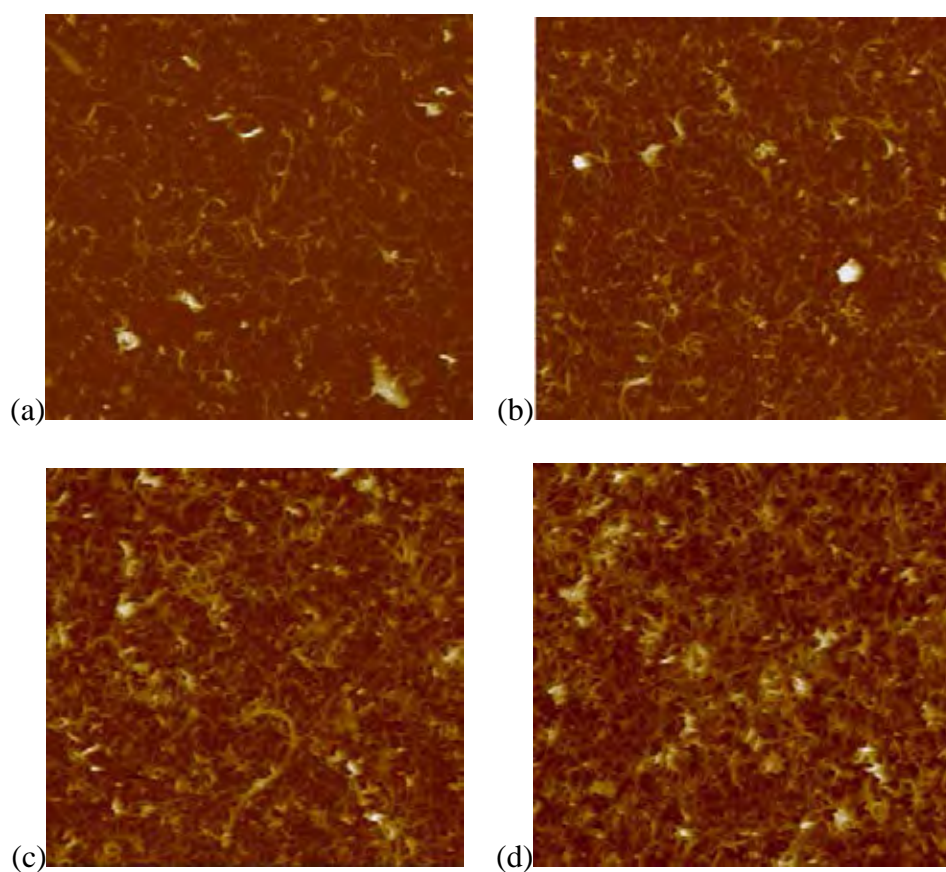


Figure 4.55 AFM pictures for the (MWCNTs.PANi.PSS<sub>0.01%</sub> weight) /PDADMAC multilayer thin films at (a) 1, (b) 3, (c) 9 and (d) 15 layers.

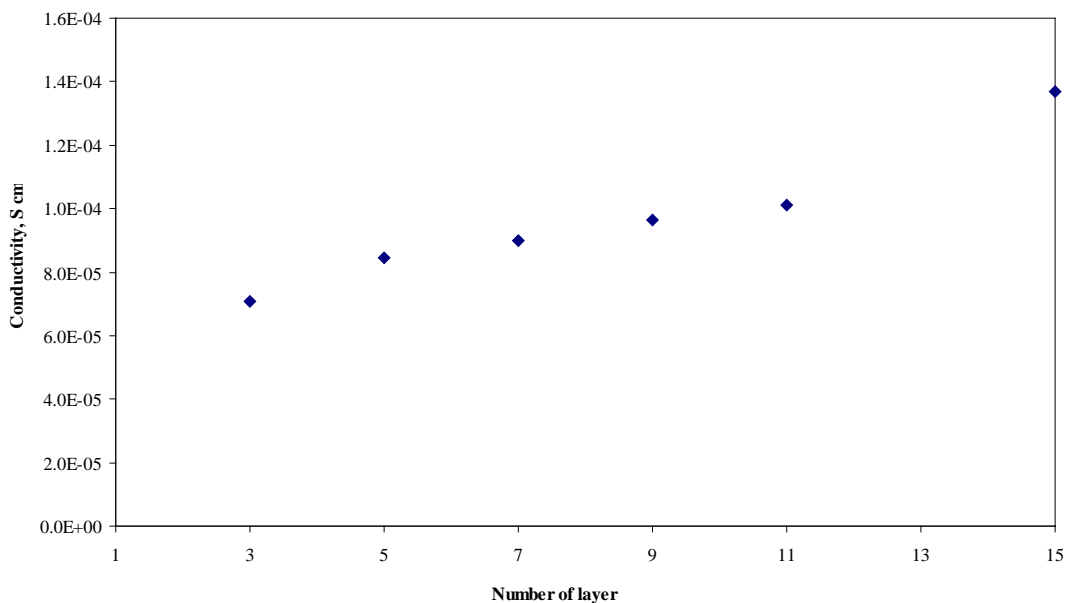


Figure 4.56 Conductivity of (MWCNTs.PANi.PSS<sub>0.01% weight</sub>) /PDADMAC multilayer thin films

Figure 4.56 shows the electrical conductivity of (MWCNTs.PANi.PSS<sub>0.01% weight</sub>) /PDADMAC multilayer thin films as the function of number of layer. The films were doped with 1 M HCl for 2 hours, the electrical conductivity of the multilayer films increased significantly with increasing the number of layer. The films of 15 layer had appreciable conductivity  $1.36 \times 10^{-4}$  S/cm.

Figure 4.57 and 4.58 shows the optical and electrical properties of 15 layers (MWCNTs.PANi.PSS<sub>0.01% weight</sub>) /PDADMAC multilayer thin films at pH 1 to 12. The optical properties of the (MWCNTs.PANi.PSS<sub>0.01% weight</sub>) /PDADMAC multilayer thin films at pH 1 to 12 were not observed changes in optical spectra suitable for pH sensor. It is clear that the former is much weaker than the previous composite materials. The main reason for this is that the MWCNTs networks have a negligible

effect on the optical properties of the PANi. The MWCNTs networks were shown more featureless spectra in the visible range.

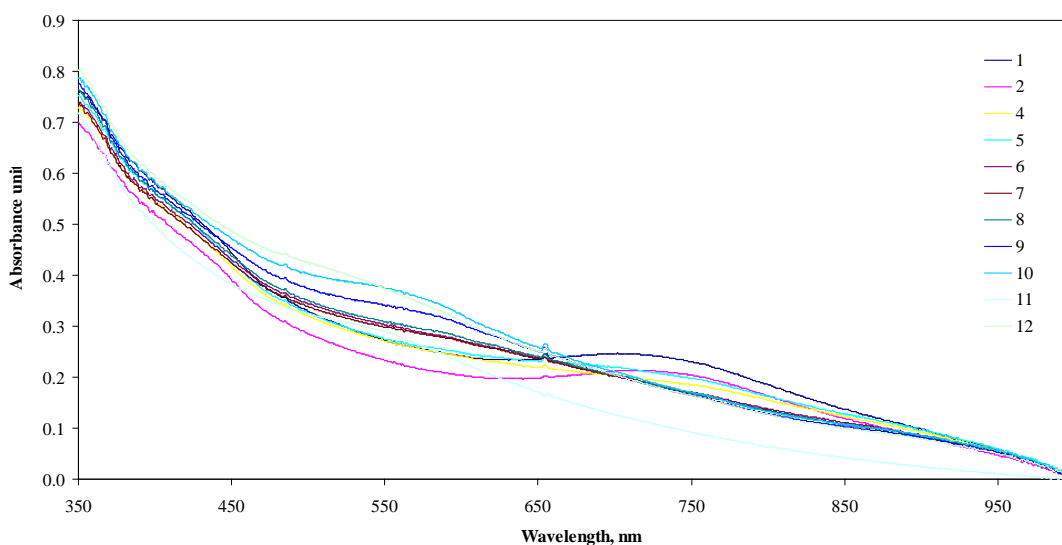


Figure 4.57 The UV-Vis spectra of 15 layers (MWCNTs.PANi.PSS<sub>0.01%</sub> weight) /PDADMAC multilayer thin films at pH 1 to 12.

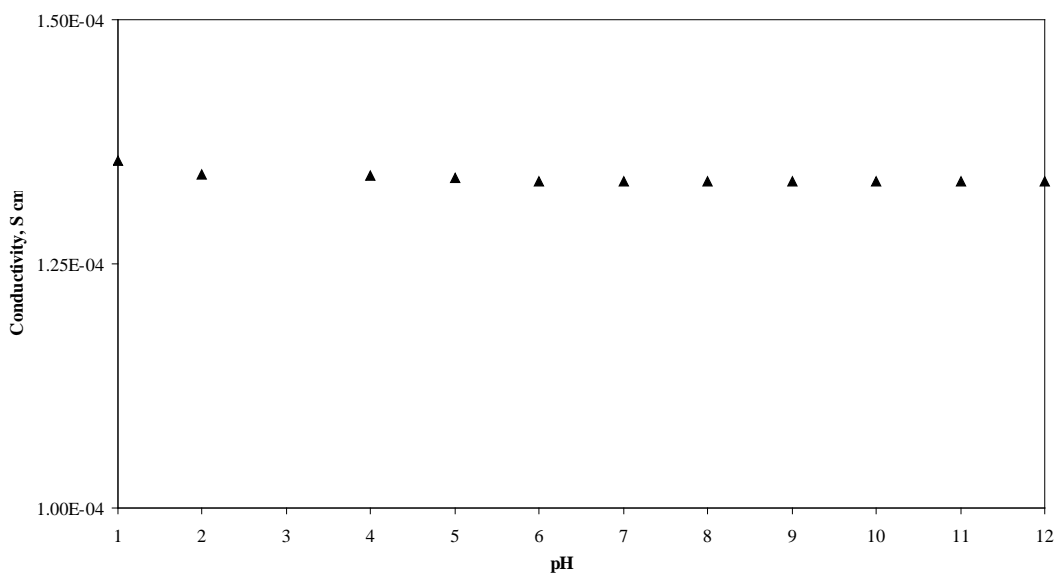


Figure 4.58 Conductivity of 15 layers (MWCNTs.PANi.PSS<sub>0.01%</sub> weight) /PDADMAC multilayer thin films by varying pH from 1-12.

Figure 4.58 shows the electrical conductivity of 15 layers (MWCNTs.PANi.PSS<sub>0.01%</sub> weight) /PDADMAC multilayer thin films as the function of pH. The result was indicated that the electrical conductivity of the composite films were found stable in all pH. The stable electrical conductivity of (MWCNTs.PANi.PSS<sub>0.01%</sub> weight) /PDADMAC multilayer thin films in all pH may be due to the main electrical conductivity of MWCNTs in composite films.

#### **4.6.4 Layer-by-layer self assembly of MWCNTs dispersed with poly(diallyldimethyl ammonium chloride) / MWCNTs dispersed water - soluble polyaniline blend poly(sodium 4-styrenesulfonate) multilayer thin films; (MWCNTs.PANi.PSS)/(MWCNTs.PDADMAC)**

This experimental the anionic and cationic of MWCNTs polyelectrolytes were used to prepared composite thin films. The anionic and cationic of MWCNTs polyelectrolyte were prepared by noncovalent surface charge modification with PANi.PSS and PDADMAC, respectively which offer a possibility to construct pure nanotube multilayers in a controlled fashion. To demonstrate this, we have fabricated (MWCNTs/MWCNTs) multilayers using oppositely charged nanotubes by their alternate adsorption. The possible mechanism of film formation was shown in Figure 4.59. The films were fabricate by the electrostatic interaction between sulfonic group of (MWCNTs.PSS) and quaternary ammonium group of (MWCNTs.PDADMAC). Without any added electrolyte in the nanotube solutions, the growth of multilayer films were shown in Figure 4.60. The trend of deposition was found to increase when increase the number of layer.



Figure 4.59 Schematic mechanism of layer-by-layer self assembly of (MWCNTs.PDADMAC) / (MWCNTs.PANi.PSS) multilayer thin films

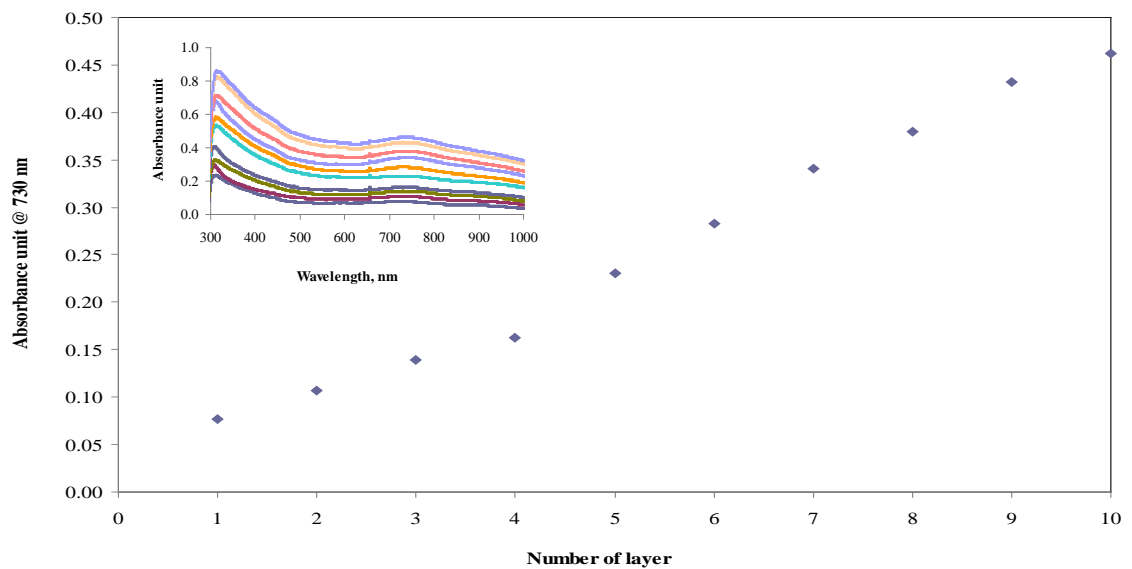


Figure 4.60 Plot of the changes in absorbance of Layer-by-layer self assembly of (MWCNTs.PDADMAC) / (MWCNTs.PANi.PSS) multilayer thin films.



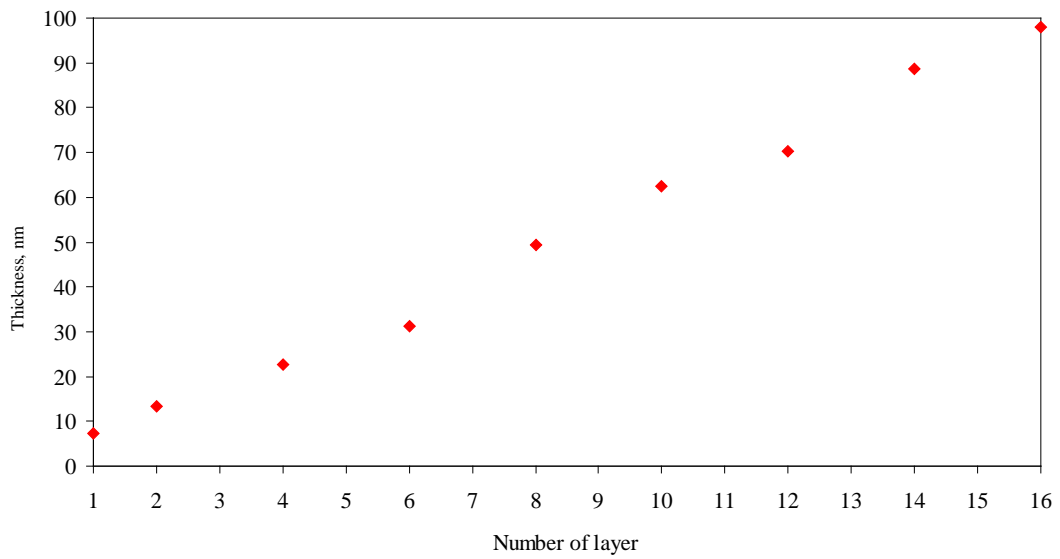


Figure 4.61 Thickness of (MWCNTs.PDADMAC)/ (MWCNTs.PANi.PSS) multilayer thin films.

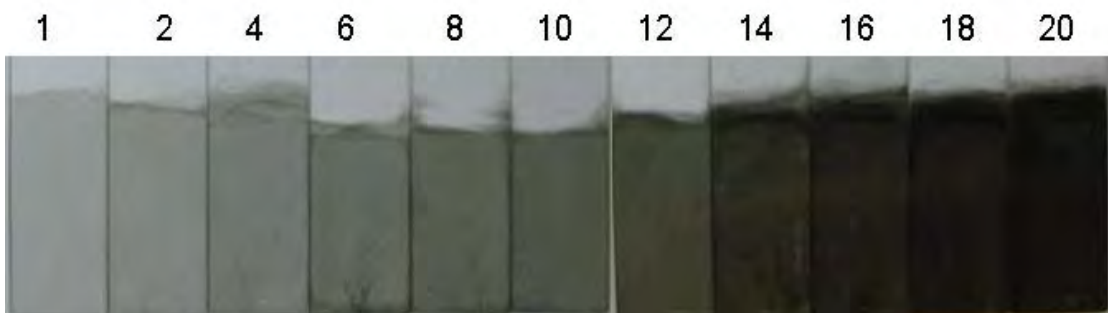


Figure 4.62 Representative digital picture images of assembled (MWCNTs PDADMAC) / (MWCNTs.PANi.PSS) multilayer thin films.

Figure 4.61 and 4.62 shows the thickness and digital picture images of assembled of (MWCNTs.PDADMAC) / (MWCNTs.PANi.PSS) multilayer thin films at various number of layers. The films darken with increasing the number of layer and appear at a thickness greater than 50-100 nm when the number of layer varied from 10-16, which could also lead to thinner films with somewhat denser packing between nanotubes. The trend of film growth was found to linear when increase the number of layer.

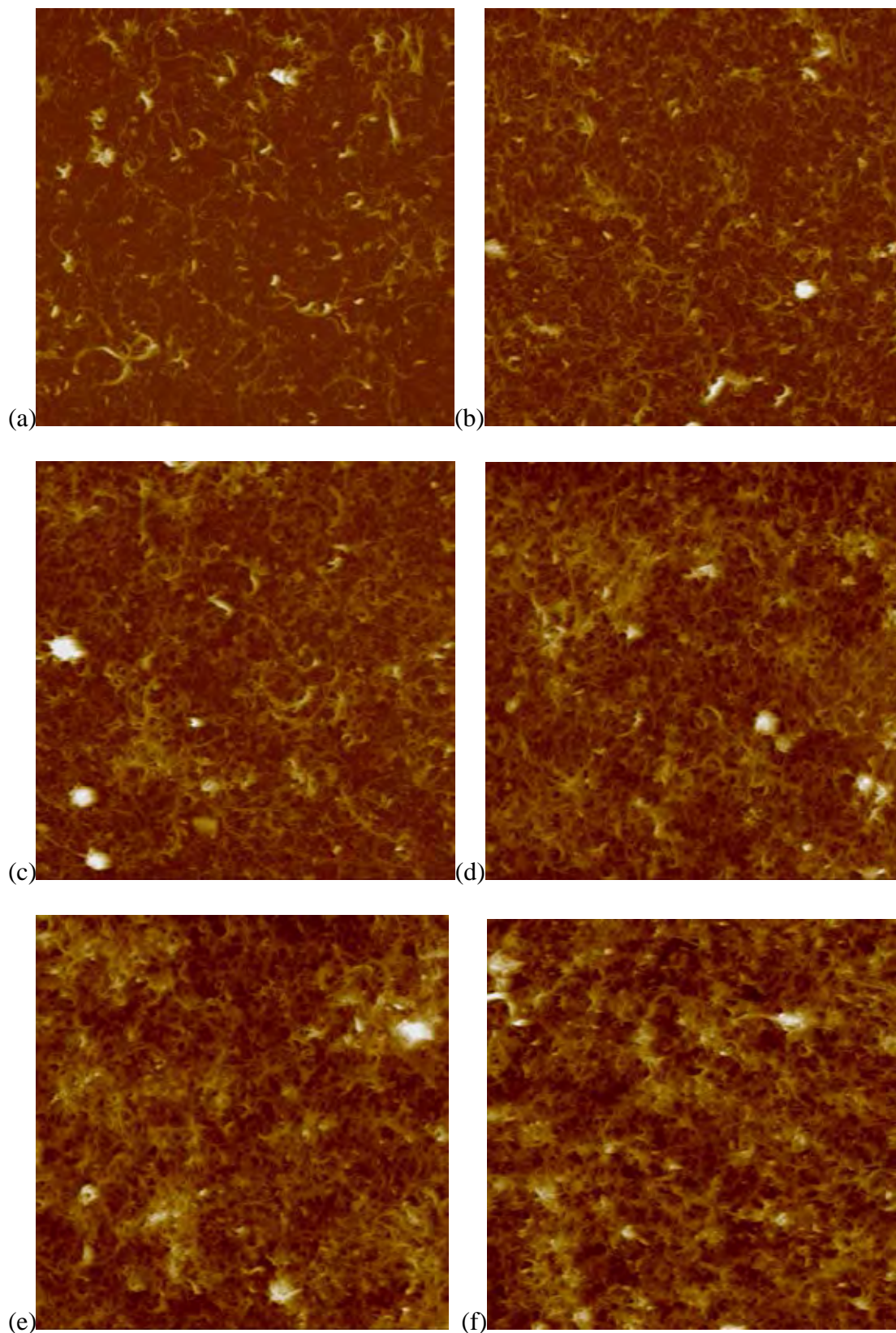


Figure 4.63 AFM pictures for the (MWCNTs.PDADMAC) / (MWCNTs.PANi.PSS) multilayer thin films at (a) 2, (b) 4, (c) 6, (d) 8 , (e) 10 and (f) 16 layers

Figure 4.63 shows tapping mode AFM images of (MWCNTs.PDADMAC) / (MWCNTs.PANi.PSS) multilayer thin films assembled at different number of layer. All AFM images clearly show that MWCNTs thin films have an interconnection network structure with separated individual MWCNTs. The LbL films shows the separated individual MWCNTs due to the electrostatic repulsion between nanotubes that act against van der Waals interactions that yield close packed aggregate, as well as electrostatic cross-linking between positively and negatively charge MWCNTs during the LbL process that lead to randomly oriented, kinetically driven CNT arrangements in the film.

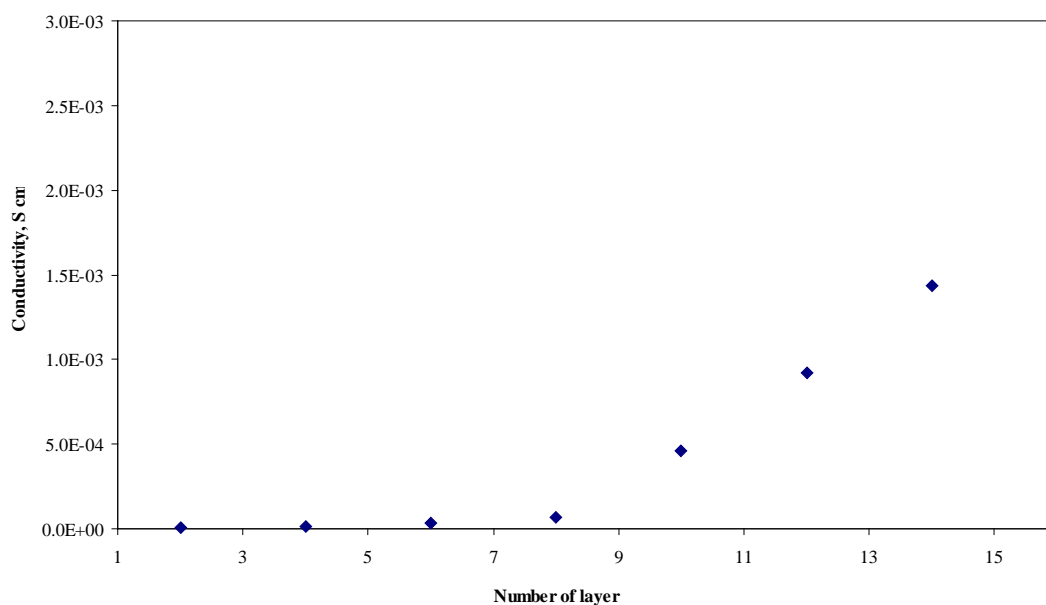


Figure 4.64 Conductivity of (MWCNTs.PDADMAC)/(MWCNTs.PANi.PSS) multilayer thin films.

Figure 4.64 shows the electrical conductivity of (MWCNTs.PDADMAC) / (MWCNTs.PANi.PSS) multilayer thin films as the function of number of layer. The films were doped with 1 M HCl for 2 hours, the electrical conductivity of the

multilayer films increased significantly with increasing the number of layer. The films of 16 layer had appreciable conductivity  $2.39 \times 10^{-3}$  S/cm.

Figure 4.65 and 4.66 shows the optical and electrical properties of 16 layers (MWCNTs.PDADMAC) / (MWCNTs.PANi.PSS) multilayer thin films at pH 1 - 12. The optical properties of the (MWCNTs.PDADMAC) / (MWCNTs.PANi.PSS) multilayer thin films at pH 1 - 12 were found the same trend like the (MWCNTs.PANi.PSS<sub>0.01% weight</sub>) / PDADMAC multilayer thin films. When the (MWCNTs.PDADMAC) / (MWCNTs.PANi.PSS) composite thin films were treated with different pH buffer solution, the spectra of composite thin films were changed to the different form due to the protonated-deprotonated phenomena of PANi..

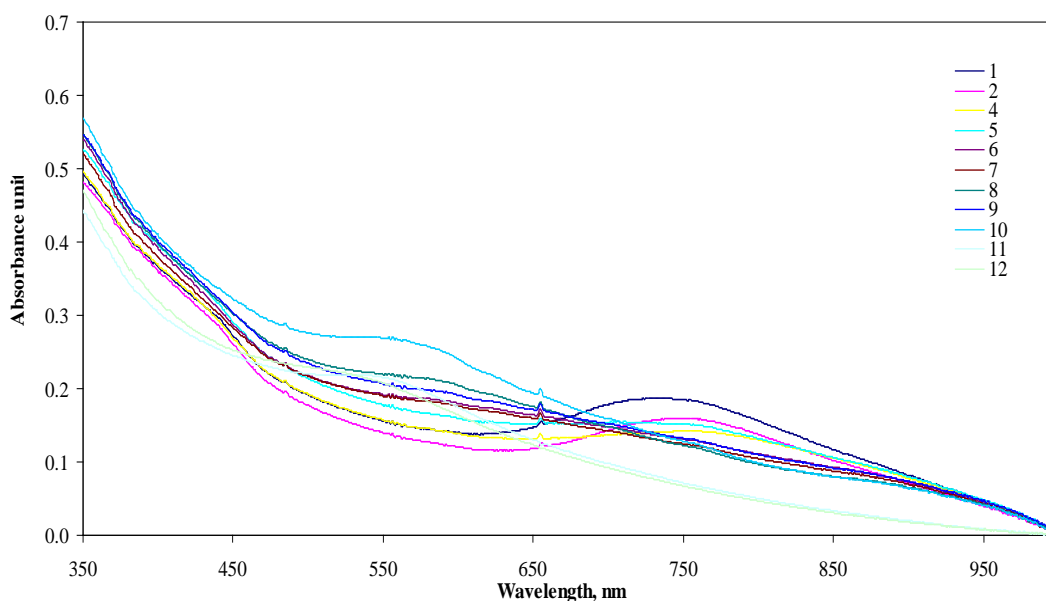


Figure 4.65 The UV-Vis spectra of 16 layers (MWCNTs.PDADMAC) / (MWCNTs.PANi.PSS) multilayer thin films at pH 1 to 12.

The electrical conductivity of (MWCNTs.PDADMAC) / (MWCNTs.PANi.PSS) multilayer thin films as the function of pH was shown in Figure 4.82. The electrical

conductivity of composite films were found to stable in all pH due to the main electrical conductivity of composite films depend on the MWCNTs behavior.

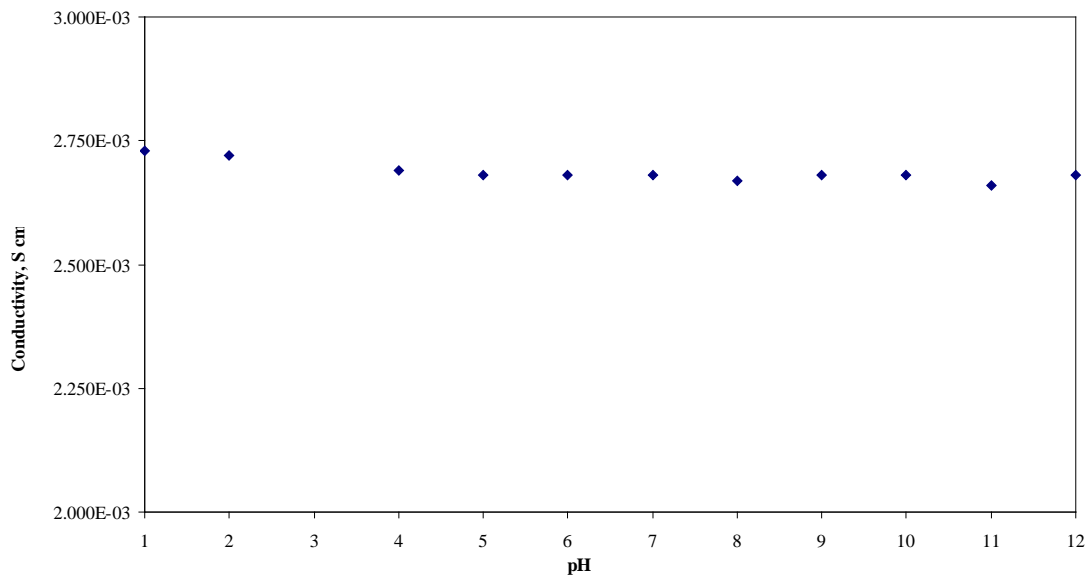


Figure 4.66 Specific conductivity of 16 layers (MWCNTs.PDADMAC)/(MWCNTs.PANi.PSS) multilayer thin films by varying pH from 1-12.

*In conclusions:* This research demonstrated the penetration of MWCNTs in already-prepared LbL films. The noncovalent surface modification of MWCNTs using the different polyanionic and polycationic such water - soluble polyaniline in the presence of poly(sodium 4-styrenesulfonate) and poly(diallyldimethylammonium chloride) can be used for preparation of thin films by LbL self assembly method. All the prepared MWCNTs multilayers films are shown a very stable.

## 4.7 Gas sensing

### 4.7.1 Dependence of the sensors response on NH<sub>3</sub> concentration

In this section, (MWCNTs.PDADMAC)/ (MWCNTs.PANi.PSS) multilayer thin films was used to study the response of NH<sub>3</sub> gas. The activity of (MWCNTs.PDADMAC)/ (MWCNTs.PANi.PSS) multilayer thin films based sensor had been investigated by measuring the changes of sensor electrical responsivity. The composite films based sensor were exposed to ammonia gas with concentration of 100, 50, 10 and 5 ppm. Typical change of basic resistance of composite films based sensor with ammonia concentration were illustrated in Figure 4.67.

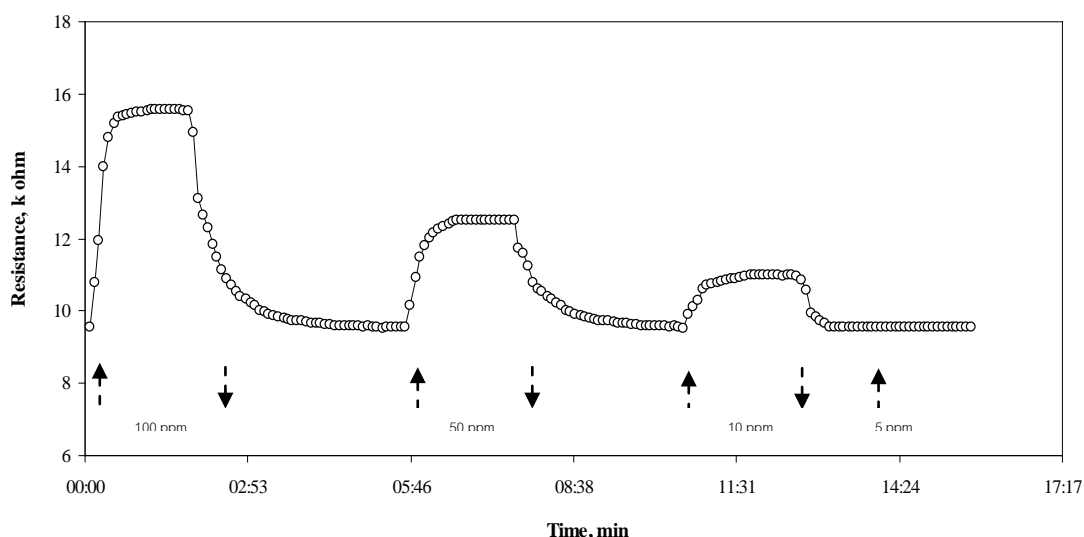


Figure 4.67 Relative resistance variation of (MWCNTs.PDADMAC) / (MWCNTs.PANi.PSS) multilayer thin films based sensor versus time exposed to

The onset of stable response was defined as the response time of sensor. For NH<sub>3</sub> concentration of 100, 50 and 10 ppm, the response time of all sensors were shown 30, 50 and 61 sec, respectively. It can be inferred that the (MWCNTs.PDADMAC) / (MWCNTs.PANi.PSS) multilayer thin films based sensor could detect NH<sub>3</sub> concentration level as low as sub-ppm at room temperature. The

increase of  $\text{NH}_3$  concentration enhances the rate of diffusion of ammonia molecules towards and into the composite polymer thin films. The number of molecules that achieve contact with the sensing sites on the film in a giving time increases and therefore the response time decreases.

Figure 4.68 shows the

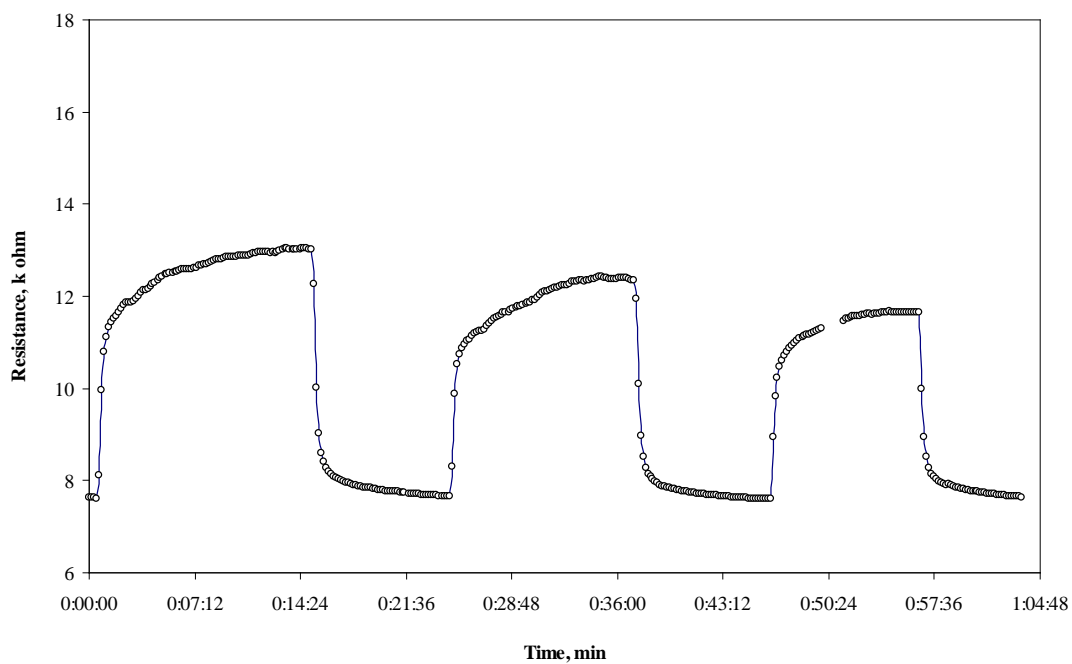


Figure 4.68 Relative resistance variation of (MWCNTs.PDADMAC) / (MWCNTs.PANi.PSS) multilayer thin films based sensor versus time exposed to moist at room temperature.

## CHAPTER V

### CONCLUSIONS

Water-soluble polyaniline were synthesized via the aqueous/ organic interfacial polymerization route with the aid of PSS. Using different concentration of PSS had a strong effect on the solubility efficiency of polyaniline. The aniline monomers can be absorbed completely through the electrostatic interaction onto the negatively charged sulfonic groups of PSS during the polymerization, leading to the alignment in the conjugation of the polyaniline backbone. The PSS with the concentration higher than 3 mM also displayed the good dispersion when 10 mM of aniline monomer and 5 mM ammonium persulfate were fixed. As for the polyaniline multilayer films were successfully prepared via the LbL method. The obtained multilayer thin films were very stable and conductive in the protonated form of polyaniline. They also showed a stable toward the deprotonated form of polyaniline, which make it a good candidate as the pH sensor. The polyaniline multilayer films show reversible color change in the pH region of 3 to 11, the strong color shift from green-blue-purple. The pH sensing can be monitored by observed the absorbance change when fixed wavelength or  $\lambda$  max of the sensing devices. It is possible to used the polyaniline multilayer films for pH sensing because the films have an apparent pKa around 8.69 which have the accurate pH measurement around 3-11.

The noncovalent surface modification of MWCNTs carrying anionic and cationic group such as water - soluble polyaniline blend poly(sodium 4-styrenesulfonate) and poly(diallyldimethylammonium chloride), respectively. MWCNTs polyelectrolyte can be used for the preparation of composite thin films by the layer-by-layer self assembly technique in an aqueous media. This is very general and powerful technique for the



fabrication of thin carbon nanotubes films of arbitrary composition and architecture. The charge compensation in these MWCNTs multilayer is intrinsic, which shows that the electrostatic interaction mainly responsible for the multilayer buildup. Interpenetrating MWCNTs in the assembly make networks that can achieve high electronic conductivity. The electrostatic layer-by-layer self assembly of MWCNTs is a feasible method to fabricate MWCNTs films with thickness from a few nanometers to ten or hundred of nanometers. The incorporation of other components can be done as easily as with other polyelectrolyte multilayers. The process is carried out entirely in aqueous medium, which is important for biocompatibility and offers, therefore, a possibility for an environmental-friendly, solvent-free method for the fabrication of carbon nanotubes films and composite. The ammonia sensing capability of the thin films are investigated and the optimal film characteristics are established. A 15 layers of LbL films is found to be the most suitable system. The MWCNTs composite multilayers based sensor films exhibits stable, reproducible and reversible resistance changes in the ammonia in the 5-100 ppm range. The response time is quite short, in the range 30-110 s depending on the ammonia concentration. The thin polyaniline sensors and MWCNTs composite sensors could be used as freshness indicator for food packaging for seafood and meats.

## REFERENCES

1. Wang, J. X.; Zhou, Z. B.; Wang, Z.; Zhang, F. B., Self-assembly of polyaniline nanowires into polyaniline microspheres. *Mater Lett* 2011, 65 (14), 2311-2314.
2. Arenas, C.; Sanchez, G., Optical, electrical and morphological properties of transparent binary doped polyaniline thin films synthesized by in situ chemical bath deposition. *Polym Int* 2011, 60 (7), 1123-1128.
3. Jia, C. Y.; Tu, L. L.; Weng, X. L.; Deng, L. J.; Tang, W., Electrochromic Materials Based on Conducting Polymers. *Prog Chem* 2010, 22 (10), 2053-2059.
4. Sarac, A. S.; Ates, M., Conducting polymer coated carbon surfaces and biosensor applications. *Prog Org Coat* 2009, 66 (4), 337-358.
5. Rahman, F.; Greer, A. I. M., Fabrication and properties of a polymer capacitor made entirely from polyaniline. *Appl Phys a-Mater* 2011, 103 (4), 1093-1097.
6. Xie, J. Y.; Guo, W. F.; Wang, J. Z., Sol-gel-derived Hybrid Conductive Films for Electromagnetic Interference (EMI) Shielding. *J Wuhan Univ Technol* 2011, 26 (2), 217-222.
7. Canales, M.; Curco, D.; Aleman, C., Modeling of Amorphous Polyaniline Emeraldine Base. *J Phys Chem B* 2010, 114 (30), 9771-9777.
8. Farag, A. A. M.; Ashery, A.; Rafea, M. A., Optical dispersion and electronic transition characterizations of spin coated polyaniline thin films. *Synthetic Met* 2010, 160 (1-2), 156-161.

9. Hong, J. W.; Kim, Y. B.; Park, S., Fabrication of flexible polymer dispersed liquid crystal films using conducting polymer thin films as the driving electrodes. *Thin Solid Films* 2009, *517* (10), 3066-3069.
10. Shirakawa, H., The discovery of polyacetylene film: The dawning of an era of conducting polymers (Nobel lecture). *Angew Chem Int Edit* 2001, *40* (14), 2575-2580.
11. <http://nobel.sdsc.edu/announcement/2000/chemreading.html>.
12. Soares, B. G.; Marins, J. A.; Dahmouche, K.; Ribeiro, S. J. L.; Barud, H.; Bonemer, D., Structure and properties of conducting bacterial cellulose-polyaniline nanocomposites. *Cellulose* 2011, *18* (5), 1285-1294.
13. Mu, S. L., Synthesis of poly(aniline-co-5-aminosalicylic acid) and its properties. *Synthetic Met* 2011, *161* (13-14), 1306-1312.
14. Lee, R. H.; Lai, H. H.; Wang, J. J.; Jeng, R. J.; Lin, J. J., Self-doping effects on the morphology, electrochemical and conductivity properties of self-assembled polyanilines. *Thin Solid Films* 2008, *517* (2), 500-505.
15. Qiu, J. H.; Shao, L.; Liu, M. Z.; Feng, H. X.; Lei, L.; Zhang, G. H.; Zhao, Y.; Gao, C. M.; Qin, L. J., Synthesis and characterization of water-soluble polyaniline films. *Synthetic Met* 2011, *161* (9-10), 806-811.
16. Haghi, A. K., Conducting Polymers. *J Balk Tribol Assoc* 2009, *15* (2), 141-155.
17. Stejskal, J.; Blinova, N. V.; Trchova, M.; Ciric-Marjanovic, G.; Sapurina, I., Polymerization of aniline on polyaniline membranes. *J Phys Chem B* 2007, *111* (10), 2440-2448.

18. Malinauskas, A.; Lapin, E.; Jureviciute, I.; Mazeikiene, R.; Niaura, G., A study of electropolymerization of N,N-dimethylaniline. *Synthetic Met* 2010, *160* (17-18), 1843-1847.
19. Liu, P.; Chen, F., Conducting Polyaniline Nanoparticles and Their Dispersion for Waterborne Corrosion Protection Coatings. *Acs Appl Mater Inter* 2011, *3* (7), 2694-2702.
20. Bekri-Abbes, I.; Srasra, E., Investigation of structure and conductivity properties of polyaniline synthesized by solid-solid reaction. *J Polym Res* 2011, *18* (4), 659-665.
21. Mattoso, L. H. C., Polyanilines: Synthesis, structure and properties. *Quim Nova* 1996, *19* (4), 388-399.
22. Samuelson, L.; Liu, W.; Kumar, J.; Tripathy, S.; Senecal, K. J., Enzymatically synthesized conducting polyaniline. *J Am Chem Soc* 1999, *121* (1), 71-78.
23. Schmidt, C. E.; Guimard, N. K.; Gomez, N., Conducting polymers in biomedical engineering. *Prog Polym Sci* 2007, *32* (8-9), 876-921.
24. Channu, V. S. R.; Holze, R.; Yeo, I. H.; Mho, S. I.; Kalluru, R. R., Electrochemical properties of polyaniline-modified sodium vanadate nanomaterials. *Appl Phys a-Mater* 2011, *104* (2), 707-711.
25. Tu, L. L.; Jia, C. Y.; Weng, X. L.; Deng, L. J., Preparation and Physical Properties of Electrochromic Thin Films Based on Polyaniline Derivatives. *Acta Chim Sinica* 2010, *68* (24), 2590-2594.
26. Rao, C. R. K.; Radhakrishnan, S.; Muthukannan, R.; Kamatchi, U.; Vijayan, M., Performance of phosphoric acid doped polyaniline as electrode material for aqueous redox supercapacitor. *Indian J Chem A* 2011, *50* (7), 970-978.

27. Huang, S. S.; Bo, Y.; Yang, H. Y.; Hu, Y.; Yao, T. M., A novel electrochemical DNA biosensor based on graphene and polyaniline nanowires. *Electrochim Acta* 2011, *56* (6), 2676-2681.
28. Wu, W.; Lu, X. W.; Chen, J. F.; Zhang, P. Y.; Zhao, Y. B., Preparation of Polyaniline Nanofibers by High Gravity Chemical Oxidative Polymerization. *Ind Eng Chem Res* 2011, *50* (9), 5589-5595.
29. He, D. L.; Zhou, Z.; Guo, Y. N.; Cui, Z. D.; Zeng, L. P.; Li, G. X.; Yang, R. H., Photo-induced polymerization in ionic liquid medium: 1. Preparation of polyaniline nanoparticles. *Polym Bull* 2009, *62* (5), 573-580.
30. Guo, Z. W.; Ruegger, H.; Kissner, R.; Ishikawa, T.; Willeke, M.; Walde, P., Vesicles as Soft Templates for the Enzymatic Polymerization of Aniline (vol 25, pg 11390, 2009). *Langmuir* 2010, *26* (10), 7650-7650.
31. Lee, J. H.; Bhadra, S.; Kim, N. H., Synthesis of Water Soluble Sulfonated Polyaniline and Determination of Crystal Structure. *J Appl Polym Sci* 2010, *117* (4), 2025-2035.
32. Chan, H. S. O.; Ho, P. K. H.; Ng, S. C.; Tan, B. T. G.; Tan, K. L., A New Water-Soluble, Self-Doping Conducting Polyaniline from Poly(O-Aminobenzylphosphonic Acid) and Its Sodium-Salts - Synthesis and Characterization. *J Am Chem Soc* 1995, *117* (33), 8517-8523.
33. Nguyen, M. T.; Kasai, P.; Miller, J. L.; Diaz, A. F., Synthesis and Properties of Novel Water-Soluble Conducting Polyaniline Copolymers. *Macromolecules* 1994, *27* (13), 3625-3631.
34. Nguyen, M. T.; Diaz, A. F., Water-Soluble Poly(Aniline-Co-O-Anthranilic Acid) Copolymers. *Macromolecules* 1995, *28* (9), 3411-3415.

35. Wen, T. C.; Kuo, C. W., Dispersible polyaniline nanoparticles in aqueous poly(styrenesulfonic acid) via the interfacial polymerization route. *Eur Polym J* 2008, *44* (11), 3393-3401.
36. do Nascimento, G. M.; Kobata, P. Y. G.; Temperini, M. L. A., Structural and vibrational characterization of polyaniline nanofibers prepared from interfacial polymerization. *J Phys Chem B* 2008, *112* (37), 11551-11557.
37. Manohar, S. K.; Surwade, S. P.; Agnihotra, S. R.; Dua, V.; Manohar, N.; Jain, S.; Ammu, S., Catalyst-Free Synthesis of Oligoanilines and Polyaniline Nanofibers Using H<sub>2</sub>O<sub>2</sub>. *J Am Chem Soc* 2009, *131* (35), 12528-+.
38. Cortes, M. T.; Sierra, E. V., Effect of synthesis parameters in polyaniline: influence on yield and thermal behavior. *Polym Bull* 2006, *56* (1), 37-45.
39. Kellenberger, A.; Plesu, N.; Mihali, M.; Vaszilcsin, N., Effect of temperature on the electrochemical synthesis and properties of polyaniline films. *J Non-Cryst Solids* 2010, *356* (20-22), 1081-1088.
40. Mahajan, A. M.; Shrivastava, A. G., Effect of variation in preparation temperature on the conductivity of PANI. *Optoelectron Adv Mat* 2008, *2* (12), 859-862.
41. Dearmitt, C.; Armes, S. P.; Winter, J.; Uribe, F. A.; Gottesfeld, S.; Mombourquette, C., A Novel N-Substituted Polyaniline Derivative. *Polymer* 1993, *34* (1), 158-162.
42. de Albuquerque, J. E.; Mattoso, L. H. C.; Faria, R. M.; Masters, J. G.; MacDiarmid, A. G., Study of the interconversion of polyaniline oxidation states by optical absorption spectroscopy. *Synthetic Met* 2004, *146* (1), 1-10.
43. Palaty, S.; Mary, K. J.; Honey, J.; Devi, P. V., Effect of Dopants and Preparation Conditions on the Conductivity of Polyaniline. *Prog Rubber Plast Re* 2010, *26* (3), 141-154.

44. Balkus, K. J.; Yang, Z. W.; Coutinho, D. H.; Sulfstede, R.; Ferraris, J. R., Proton conductivity of acid-doped meta-polyaniline. *J Membrane Sci* 2008, *313* (1-2), 86-90.
45. Stejskal, J.; Kratochvil, P.; Jenkins, A. D., The formation of polyaniline and the nature of its structures. *Polymer* 1996, *37* (2), 367-369.
46. Chiu, K. C.; Tang, S. J.; Wang, A. T.; Lin, S. Y.; Huang, K. Y.; Yang, C. C.; Yeh, J. M., Polymerization of aniline under various concentrations of APS and HCl. *Polym J* 2011, *43* (8), 667-675.
47. Liu, E. H.; Huang, Z. Z.; Shen, H. J.; Xiang, X. X.; Tian, Y. Y.; Xiao, C. Y.; Mao, Z. H., Preparation of polyaniline nanotubes by a template-free self-assembly method. *Mater Lett* 2011, *65* (13), 2015-2018.
48. Grummt, U. W.; Pron, A.; Zagorska, M.; Lefrant, S., Polyaniline based optical pH sensor. *Anal Chim Acta* 1997, *357* (3), 253-259.
49. Mav, I.; Zigon, M., Synthesis and NMR characterization of a novel polyaniline derivative - The copolymer of 2-methoxyaniline and 3-aminobenzenesulfonic acid. *Polym Bull* 2000, *45* (1), 61-68.
50. Osterholm, J. E.; Cao, Y.; Klavetter, F.; Smith, P., Emulsion Polymerization of Aniline. *Polymer* 1994, *35* (13), 2902-2906.
51. Iijima, S.; Yudasaka, M.; Nihey, F., Carbon nanotube technology. *Nec Tech J* 2007, *2* (1), 52-56.
52. Iijima, S., Growth of Carbon Nanotubes. *Mat Sci Eng B-Solid* 1993, *19* (1-2), 172-180.
53. Blinc, R.; Arcon, D.; Umek, P.; Apih, T.; Milia, F.; Rode, A. V., Carbon nanofoam as a potential hydrogen storage material. *Phys Status Solidi B* 2007, *244* (11), 4308-4310.

54. Horrillo, M. C.; Marti, J.; Matatagui, D.; Santos, A.; Sayago, I.; Gutierrez, J.; Martin-Fernandez, I.; Ivanov, P.; Gracia, I.; Cane, C., Single-walled carbon nanotube microsensors for nerve agent simulant detection. *Sensor Actuat B-Chem* 2011, *157* (1), 253-259.
55. Sundararaj, U.; Breuer, O., Big returns from small fibers: A review of polymer/carbon nanotube composites. *Polym Composite* 2004, *25* (6), 630-645.
56. Coll, B. F.; Dean, K. A.; Howard, E.; Johnson, S. V.; Johnson, M. R.; Jaskie, J. E., Nano-emissive display technology for large-area HDTV. *J Soc Inf Display* 2006, *14* (5), 477-485.
57. Iijima, S.; Ichihashi, T., Single-Shell Carbon Nanotubes of 1-Nm Diameter. *Nature* 1993, *363* (6430), 603-605.
58. Dervishi, E.; Li, Z. R.; Xu, Y.; Saini, V.; Biris, A. R.; Lupu, D.; Biris, A. S., Carbon Nanotubes: Synthesis, Properties, and Applications. *Particul Sci Technol* 2009, *27* (2), 107-125.
59. <http://www.isampe.org/arti2.htm>.
60. [http://sces.phys.utk.edu/~dagotto/condensed/HW1\\_2010/AoTeng\\_Report\\_CarbonNanotubes.pdf](http://sces.phys.utk.edu/~dagotto/condensed/HW1_2010/AoTeng_Report_CarbonNanotubes.pdf).
61. Hirsch, A., Functionalization of single-walled carbon nanotubes. *Angew Chem Int Edit* 2002, *41* (11), 1853-1859.
62. Chen, Q.; Wang, Y. Y.; Wang, X. S.; Wu, B. Y.; Zhao, Z.; Yin, F.; Li, S.; Qin, X., Dispersion of single-walled carbon nanotubes in poly(diallyldimethylammonium chloride) for preparation of a glucose biosensor. *Sensor Actuat B-Chem* 2008, *130* (2), 809-815.



63. Xie, X. M.; Liu, Y. T.; Zhao, W.; Huang, Z. Y.; Gao, Y. F.; Wang, X. H.; Ye, X. Y., Noncovalent surface modification of carbon nanotubes for solubility in organic solvents. *Carbon* 2006, 44 (8), 1613-1616.
64. Smalley, R. E.; Moore, V. C.; Strano, M. S.; Haroz, E. H.; Hauge, R. H.; Schmidt, J.; Talmon, Y., Individually suspended single-walled carbon nanotubes in various surfactants. *Nano Lett* 2003, 3 (10), 1379-1382.
65. [http://www.chem.zju.edu.cn/linxf/redirect.php?catalog\\_id=3805](http://www.chem.zju.edu.cn/linxf/redirect.php?catalog_id=3805)
66. Tsukruk, V. V.; Bliznyuk, V. N.; Visser, D.; Campbell, A. L.; Bunning, T. J.; Adams, W. W., Electrostatic deposition of polyionic monolayers on charged surfaces. *Macromolecules* 1997, 30 (21), 6615-6625.
67. Li, J. B.; Fei, J. B.; Cui, Y.; Yan, X. H.; Yang, Y.; Wang, K. W., Controlled Fabrication of Polyaniline Spherical and Cubic Shells with Hierarchical Nanostructures. *ACS Nano* 2009, 3 (11), 3714-3718.
68. Wang, X. J.; Hu, L. F.; Yang, F. X.; Liu, P.; Zhu, F. K., Preparation and Gas Sensitivity Properties of Polyaniline/Carbon Nanotubes Composite. *Asian J Chem* 2011, 23 (8), 3325-3328.
69. Narkis, M.; Suckeveriene, R. Y.; Zelikman, E.; Mechrez, G.; Tzur, A.; Frisman, I.; Cohen, Y., Synthesis of Hybrid Polyaniline/Carbon Nanotube Nanocomposites by Dynamic Interfacial Inverse Emulsion Polymerization Under Sonication. *J Appl Polym Sci* 2011, 120 (2), 676-682.
70. [http://www.faculty.ait.ac.th/joy/new/index.php?option=com\\_content&view=artic&id=364:layer-by-layer-dip-coating-technique&catid=75:protocol-front-page&Itemid=72](http://www.faculty.ait.ac.th/joy/new/index.php?option=com_content&view=artic&id=364:layer-by-layer-dip-coating-technique&catid=75:protocol-front-page&Itemid=72).

71. Xing, S. X.; Zheng, H. W.; Zhao, G. K., Preparation of polyaniline nanofibers via a novel interfacial polymerization method. *Synthetic Met* 2008, *158* (1-2), 59-63.
72. Wen, T. C.; Kuo, C. W., Dispersible polyaniline nanoparticles in aqueous poly(styrenesulfonic acid) via the interfacial polymerization route. *Eur Polym J* 2008, *44* (11), 3393-3401.
73. Tadjer, A. V.; Petrova, J. N.; Romanova, J. R.; Madjarova, G. K.; Ivanova, A. N., Fully Doped Oligomers of Emeraldine Salt: Polaronic versus Bipolaronic Configuration. *J Phys Chem B* 2011, *115* (14), 3765-3776.
74. Canales, M.; Curco, D.; Aleman, C., Modeling of Amorphous Polyaniline Emeraldine Base. *J Phys Chem B* 2010, *114* (30), 9771-9777.
75. Stejskal, J.; Sapurina, I.; Trchova, M., Polyaniline nanostructures and the role of aniline oligomers in their formation. *Prog Polym Sci* 2010, *35* (12), 1420-1481.
76. Matsui, H.; Nuraje, N.; Su, K.; Yang, N. L., Liquid/liquid interfacial polymerization to grow single crystalline nanoneedles of various conducting polymers. *ACS Nano* 2008, *2* (3), 502-506.
77. Deng, Y. L.; Park, M. C.; Sun, Q. H., Polyaniline microspheres consisting of highly crystallized nanorods. *Macromol Rapid Comm* 2007, *28* (11), 1237-1242.
78. Lu, Q. F.; Cheng, X. S., Preparation of high-yield polyaniline nanofibers via an unstirred polymerization. *E-Polymers* 2009.
79. Sapurina, I. Y.; Stejskal, J., The effect of pH on the oxidative polymerization of aniline and the morphology and properties of products. *Russ Chem Rev+* 2010, *79* (12), 1123-1143.

- 80 Ren, L.; Zhang, X. F., Preparation and characterization of polyaniline micro/nanotubes with dopant acid mordant dark yellow GG. *Synthetic Met* 2010, *160* (7-8), 783-787.
- 81 Wang, J. Q.; Liu, S.; Ou, J. F.; Zhou, J. F.; Chen, Y. F.; Yang, S. R., Fabrication of One Dimensional Polyaniline Nanofibers by UV-Assisted Polymerization in the Aqueous Phase. *J Nanosci Nanotechno* 2010, *10* (2), 933-940.
82. Lu, Q. F.; Cheng, X. S., Preparation of high-yield polyaniline nanofibers via an unstirred polymerization. *E-Polymers* 2009.
- 83 Liu, Y., J. Tang, and J.H. Xin, Fabrication of nanowires with polymer shells using treated carbon nanotube bundles as macro-initiators. *Chemical Communications*, 2004. (24),2828-2829.
- 84 Liu, Y., D.-C. Wu, W.-D. Zhang, X. Jiang, C.-B. He, T.S. Chung, S.H. Goh, and K.W. Leong, Polyethylenimine-grafted multiwalled carbon nanotubes for secure noncovalent immobilization and efficient delivery of DNA. *Angewandte Chemie*, 2005. *44*(30), 4782-4785.
85. Hu, H., Y. Ni, S.K. Mandal, V. Montana, B. Zhao, R.C. Haddon, and V. Parpura, Polyethyleneimine Functionalized Single-Walled Carbon Nanotubes as a Substrate for Neuronal Growth. *Journal of Physical Chemistry B*, 2005. *109*(10): p. 4285-4289.
86. Choi, J.-Y., D.H. Wang, L.-S. Tan, and J.-B. Baek, Grafting of hyperbranched polyetherketones onto multi-walled carbon nanotubes via A3 + B2 approach. *Polymer Preprints*, 2005. *46*(2), 753-754.
87. Oh, S.-J., H.-J. Lee, J.-Y. Choi, L.-S. Tan, and J.-B. Baek, In-situ grafting of poly(ether-ketones) from ab monomers with varying multi-walled carbon nanotube loads. *Polymer Preprints* (American Chemical Society,

- Division of Polymer Chemistry), 2006. 47(1), 399-400.
88. Hong, C.-Y., Y.-Z. You, and C.-Y. Pan, Synthesis of Water-Soluble Multiwalled Carbon Nanotubes with Grafted Temperature-Responsive Shells by Surface RAFT Polymerization. *Chemistry of Materials*, 2005. 17(9), 2247-2254.
  89. Cui, J., W. Wang, Y. You, C. Liu, and P. Wang, Functionalization of multiwalled carbon nanotubes by reversible addition fragmentation chain-transfer polymerization. *Polymer*, 2004. 45(26), 8717-8721.
  90. Baskaran, D., J.W. Mays, and M.S. Bratcher, Polymer-grafted multiwalled carbon nanotubes through surface-initiated polymerization. *Angewandte Chemie*, 2004. 43(16), 2138-2142.
  91. Choi, J.H., S.B. Oh, J. Chang, I. Kim, C.-S. Ha, B.G. Kim, J.H. Han, S.-W. Joo, G.-H. Kim, and H.-j. Paik, Graft Polymerization of Styrene from Single-Walled Carbon Nanotube using Atom Transfer Radical Polymerization. *Polymer Bulletin*, 2005. 55(3), 173-179.
  92. Qin, S., D. Qin, W.T. Ford, D.E. Resasco, and J.E. Herrera, Functionalization of Single-Walled Carbon Nanotubes with Polystyrene via Grafting to and Grafting from Methods. *Macromolecules*, 2004. 37(3), 752-757.
  93. Fragneaud, B., K. Masenelli-Varlot, A. Gonzalez-Montiel, M. Terrones, and J.-Y. Cavailh, Efficient coating of N-doped carbon nanotubes with polystyrene using atomic transfer radical polymerization. *Chemical Physics Letters*, 2006. 419(4-6), 567-573.
  94. Gao, C., C.D. Vo, Y.Z. Jin, W. Li, and S.P. Armes, Multihydroxy Polymer-Functionalized Carbon Nanotubes: Synthesis, Derivatization, and Metal

- Loading. *Macromolecules*, 2005. 38(21), 8634-8648.
95. Li, L. and C.M. Lukehart, Synthesis of Hydrophobic and Hydrophilic Graphitic Carbon Nanofiber Polymer Brushes. *Chemistry of Materials*, 2006. 18(1), 94-99.
  96. Tsarevsky, N.V., W. Wu, J.L. Hudson, T. Kowalewski, J.M. Tour, and K. Matyjaszewski, Grafting of well-defined polymers from the surface of functionalized single-walled carbon nanotubes via atom transfer radical polymerization and visualization of the polymer-nanotube hybrids by atomic force microscopy. *Polymer Preprints*, 2005. 46(1), 203-204.
  97. Hong, C.-Y., Y.-Z. You, D. Wu, Y. Liu, and C.-Y. Pan, Multiwalled Carbon Nanotubes Grafted with Hyperbranched Polymer Shell via SCVP. *Macromolecules*, 2005. 38(7), 2606-2611.
  98. Kong, H., W. Li, C. Gao, D. Yan, Y. Jin, D.R.M. Walton, and H.W. Kroto, Poly(N-isopropylacrylamide)-Coated Carbon Nanotubes: Temperature-Sensitive Molecular Nanohybrids in Water. *Macromolecules*, 2004. 37(18), 6683-6686.
  99. Tasis, D., N. Tagmatarchis, A. Bianco, and M. Prato, Chemistry of Carbon Nanotubes. *Chemical Reviews*, 2006. 106(3), 1105-1136.
  100. Schmidt, G. and M.M. Malwitz, Properties of polymer-nanoparticle composites. *Current Opinion in Colloid and Interface Science*, 2003. 8, 103-108.
  101. Matyjaszewski, K., P.J. Miller, N. Shukla, B. Immaraporn, A. Gelman, B.B. Luokala, T.M. Siclovan, G. Kickelbick, T. Vallant, H. Hoffmann, and T. Pakula, Polymers at Interfaces: Using Atom Transfer Radical Polymerization in the Controlled Growth of Homopolymers and block

- Copolymers from Silicon Surfaces in the Absence of Untethered Sacrificial Initiator. *Macromolecules*, 1999. 32, 8716-8724.
102. Cao, A., V.P. Veedu, X. Li, Z. Yao, M.N. Ghasemi-Nejhad, and P.M. Ajayan, Multifunctional brushes made from carbon nanotubes. *Nature Materials*, 2005. 4(7), 540-545.
  103. Niyogi, S., M.A. Hamon, H. Hu, B. Zhao, P. Bhowmik, R. Sen, M.E. Itkis, and R.C. Haddon, Chemistry of single-walled carbon nanotubes. *Accounts of Chemical Research*, 2002. 35, 1105-1113.
  104. Ausman, K.D., H.W. Rohrs, M. Yu, and R.S. Ruoff, Nanostressing and mechanochemistry. *Nanotechnology*, 1999. 10, 258-262.
  105. Srivastana, D., D.W. Brenner, J.D. Schall, K.D. Ausman, M. Yu, and R.S. Ruoff, Predictions of Enhanced Chemical Reactivity at Regions of Local Conformational Strain on Carbon Nanotubes: Kinky Chemistry. *Journal of Physical Chemistry B*, 1999. 103, 4330-4337.
  106. Gulseren, O., T. Yildirim, and S. Ciraci, Adsorption on Carbon Nanotubes. *Physical Review Letters*, 2001. 87, 116802-116806.
  107. Park, S., D. Srivastana, and K. Cho, Generalized Chemical Reactivity of Curved Surfaces: Carbon Nanotubes. *Nanoletters*, 2003. 3(9), 1273-1277.

# BIOGRAPHY

## PERSONAL DATA

**Name** : Ekarat Detsri

**Nationality** : Thai

**Date of birth** : July 4<sup>th</sup>, 1979

## EDUCATION

**1998-2002** Bachelor of Science

Department of Chemistry, Faculty of Science,  
Khon Kaen University, Bangkok, Thailand

**2002-2004** Master of Science

Department of Chemistry, Faculty of Science,  
Chiang Mai University, Bangkok, Thailand  
Major : Analytical Chemistry

**2006-1011** Doctor of Philosophy

Doctor od Philosopy Program in Nanoscience and Technology,  
Graduate School, Chulalongkorn University, Bangkok, Thailand